ABSTRACT

STATES IN ^{116}Sb FROM ^{116}Te DECAY

AND ^{116}Sn(p,nγ)^{116}Sb

by

Clare Ben Morgan

The ^{116}Te beta decay and the ^{116}Sn(p,nγ)^{116}Sb reaction with proton beam energies between 5.95 and 11.75 MeV have been used with Ge(Li) spectrometers to study properties of γ rays from states of ^{116}Sb below 1.48 MeV of excitation. The beta decay of ^{116}Te is observed to directly feed four excited levels in ^{116}Sb. The de-excitation of these levels produce 21 γ rays allowing the placement of four additional levels. These eight states and 25 others were observed in the (p,nγ) experiments. Using the predictions of the statistical compound nuclear model, spin and some parity assignments have been made based upon in-beam gamma-ray angular distributions and excitation functions in conjuction with the beta decay. These states and spin-parity are 0.0 (3^+), 93.7 (1^+), 103.0 (2^+), 410.9 (4^+), 455.2 (3), 466.0 (3), 503.1 (5), 517.9 (2^+), 550.9 (2), 574.4 (2^+), 612.5 (4), 654.1 (3), 731.6 (1^+) 815.1 (3), 820.6 (5), 841.1 (6), 881.5 (3), 917.7 (1^+), 948.0 (4), 1127.2 (2), 1158.3 (1^+), 1222.9 (2) keV.

Branching ratios for 42 γ rays are presented along with all measurements of the multipole mixing ratio. Pulsed beam experiments have been performed to measure the half-lives of the excited states. The lifetime of the 455.2 keV state is discussed. The shell model structure of low lying states is also discussed.

STATES IN ^{116}Sb FROM ^{116}Te DECAY AND ^{116}Sn(p,nγ)^{116}Sb

By

Clare Ben Morgan

A THESIS

Submitted to
Michigan State University
in paritial fulfullment of the requirements
for the degree of

DOCTOR OF PHILOSOPHY

Department of Physics

1975

ACKNOWLEDGMENTS

I wish to thank Dr. W.H. Kelly for his encouragement and interest during the experimental work and for his patience and guidance during the preparation of this thesis.

I also wish to extend special thanks to Drs. L.E. Samuelson and R.A. Warner for their invaluable assistance and encouragement during the data acquision and analysis of this work. Many of their ideas led to solutions to apparently insurmountable problems.

Dr. H.G. Blosser, Dr. P. Miller and Mr. Hilbert have assisted with the operation of the Michigan State University sector-focused cyclotron.

I wish to thank also Dr. W.C. McHarris and Mr. R. Au for their contributions to many of my various projects.

Dr. E.M. Bernstein, Dr. R. Shamu and the staff at the Western Michigan University tandem Van de Graaff Laboratory were extremely generous with their time and facilities.

Dr. T.L. Khoo, Dr. F.M. Bernthal, Mr. W. Chaffee, Ms. C. Dors, and Mr. B.D. Jeltema aided in data collection and interpretation.

Mrs. Peri-Anne Warstler aided greatly by typing the final version of this manuscript.

Much of the financial assistance for this research has been provided by the National Science Foundataion, The U.S. Atomic Energy Commission, and Michigan State University.

TABLE OF CONTENTS

LIST OF TABLES

LIST OF FIGURES

I. INTRODUCTION AND PREVIOUS WORK

Understanding of the residual n-p interaction (that part of the mutual interaction which is not accounted for by the central potential) is essential for full understanding of the structure of nuclei. Nuclear spectroscopy of odd-odd nuclei is a convenient method of examining this interaction. States are available at much lower energies in odd-odd nuclei than in even-even nuclei, making them more readily available. Little is known of these nuclei other than they are very tightly packed with levels presenting serious experimental problems. It is felt that near a closed shell there may be some simplifications, therefore a series of investigations has been initiated near the Z = 50 closed shell where many stable targets are available so that the systematics may become more evident.

Little previous work has been done on the odd-odd antimonies below A = 122 with the (p,nγ) reaction. Elliot et al. have studied low lying states in ^{122}Sb[1] and Chaffee et al.[2] have studied states in ^{118}Sb below 1200 keV via the (p,nγ) reaction. The beta decay of ^{116}Te has been studied by B. G. Kiselev et al.[3], O. Rahmouni[4], and Fink et al.[5].

Fink established the half life of the ^{116}Te ground state as 2.50±0.02 hours and the existence of a 93.9 keV γ ray.

Rahmouni established the existence of two additional γ rays and made tentative identifications of several others. He placed excited levels at 93.5, 196.5, and 723.5 keV, depopulated by γ rays of energies 93.5, 103. and 630. keV respectively. More recently the spins and parities of the 3^+ ground and the 8^- isomer states in

^{116}Sb were measured by atomic beam studies by C. Ekstrom et al.[6].

The ^{116}Sn(p,nγ)^{116}Sb reaction was chosen for this study because the reaction should be well described by the statistical compound nuclear theories of Hauser and Feshbach[7] as used in the computer codes of Sheldon and Van Patter[8-11]. It is expected that at the energies used in these experiments (E_p = 5.5 to 7.5 MeV) the dominant part of the reaction should be compound nucleus as opposed to direct reaction. All states for which the incoming energy and angular momentum are sufficient should be excited in this type of reaction. The statistical model as applied to the excitation function data and angular distribution data is an excellent method of making many unambiguous spin assignments as was done here. In addition, γ-ray multipole mixing ratios, precise level energies, and γ-ray branching ratios were obtained.

In addition to the (p,nγ) work, the γ-ray spectrum accompanying the ^{116}Te electron capture decay was investigated. These experiments corroborated and complemented the in-beam experiments and were able to resolve several discrepancies encountered in the in-beam studies. Several gamma rays that were not observed by the previous investigators were found.

The (p,3nγ) and (α,3nγ) reactions were also briefly investigated to study the ^{116}Sb nucleus.

II. THEORETICAL CONSIDERATIONS

A. Statistical Compound Nucleus Theory

The basic tool for data analysis was the program MANDY[8] written by E. Sheldon and R. M. Strang which uses the framework of statistical compound nucleus (CN) theory for the evaluation of angular distributions. Samuelson and Morgan have since modified MANDY so that it may be used with excitation function data in a more straight forward way. The program assumes incoming and outgoing particles with spins of S=1/2.

The general expression of the differential cross section written as a Legendre-Polynomial expansion of even order is

$$\frac{d\sigma}{d\Omega} = \sum_{\nu=0,2,4\ldots} A_\nu P_\nu(\cos\theta)$$

in which the summation extends over angular momenta entering into the over-all process and over the index ν. The A_ν coefficients can be decomposed into a product of energy-dependent and of momentum-dependent terms.

$$A_\nu = 1/4\, \lambda\!\!\!^{-2}\, gB_\nu(j_1 j_1 J_0 J_1; s_1) B_\nu(j_2 j_2 J_2 J_1; s_2)\tau$$

The B_ν's are transition parameters leading to or decaying from CN states $J_1^{\pi_1}$. Two additional momentum dependent terms also appear λ, which is the rationalized wavelength of the incident particle and g which is a statistical spin factor that takes account of the probability that the incident particles of spin s have the right orientation for resonance capture,

$$g = (2J_1+1)/(2(2J_0+1)(2s_1+1)) = 1/4(2J_1+1).$$

The energy dependent term τ is the Hauser-Feshbach penetrability term where

$$\tau = T_{\ell_1}(E_1)T_{\ell_2}(E_2)/\sum_{\ell jE} T_\ell(E)$$

This term takes account of the CN barrier penetrabilities for incident particles of energy E_1 and emergent particles of energy E_2 in the center-of-mass system. The sum runs over all possible decay channels. The spin orbit interaction is included by use of generalized transmission coefficients $T_\ell^{(\pm)}$, where they are related to normal coefficients by

$$T_\ell = ((\ell+1)T^{(+)}+\ell T^{(-)}) \ / \ (2\ell+1)$$

The notation employed by MANDY is summarized in Fig. II-1.

Gamma ray angular distributions as a function of the mixing ratios, δ, of the gamma rays are computed using

$$\frac{d\sigma}{d\Omega} = A_0(1+A_2^* P_2(\cos\theta)+A_4^* P_4(\cos\theta))$$

where $A_\nu^* = A_\nu/A_0$. The series for $\frac{d\sigma}{d\Omega}$ is limited to the first three terms as higher order terms are expected to be negligible. The multipole mixing ratio δ is the intensity of the gamma transition of multipolarity L+1 (L') divided by the intensity of the gamma transition of multipolarity L. The locus of points for possible values of A_2^* and A_4^* as a function of δ form an ellipse where δ takes on all values from $-\infty$ to $+\infty$. Comparison with experimental values of A_2^* and A_4^* usually allows a determination of δ with its usually narrow error limits.

The calculated cross sections are highly dependent on energy of bombardment and angular momentum. For the range of energies (5.5 to 7.5 MeV) used in this investigation, the cross section peaks at ℓ = 1 or 2 and falls off rapidly with increasing values nearly vanishing for values greater than 5.

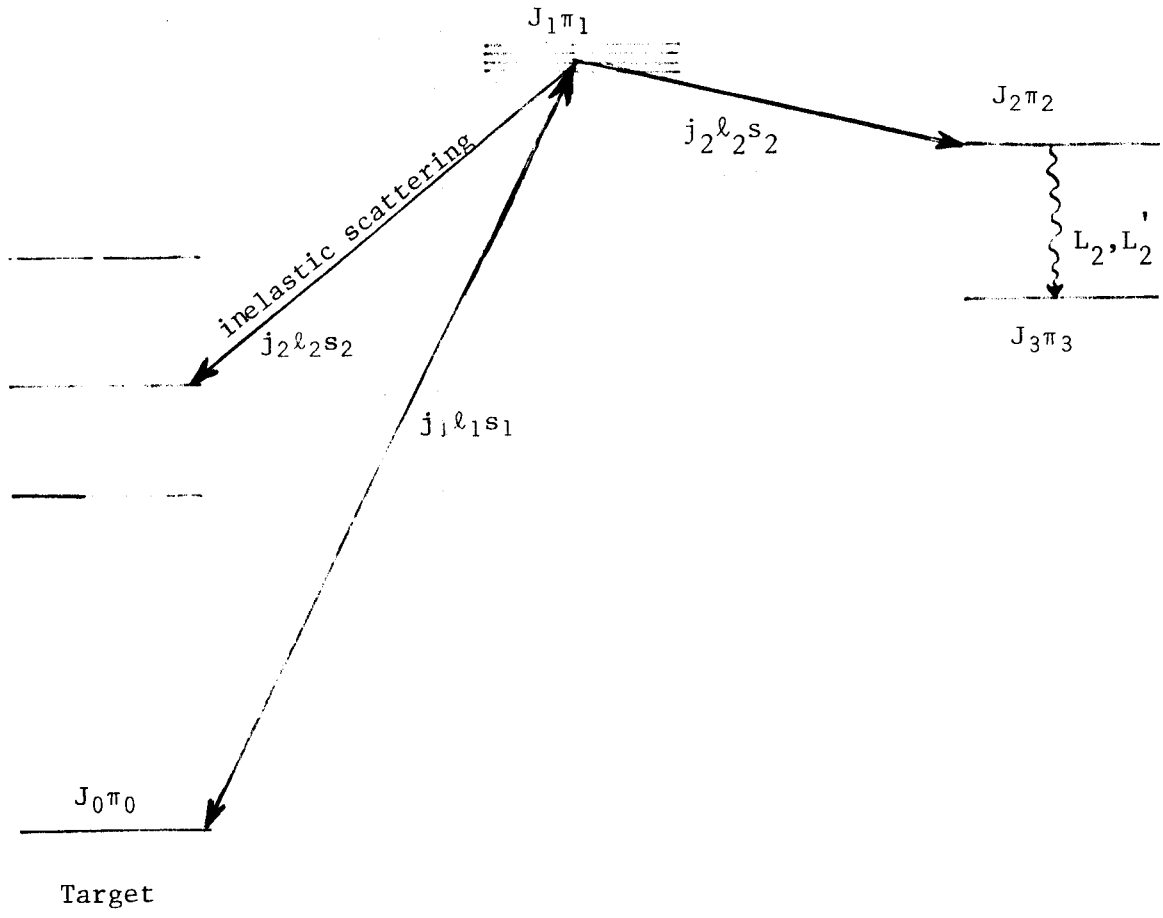

Notation used by MANDY
Figure II-1.

Therefore all total cross section calculations were limited to $0 \leq J \leq 6$.

B. Shell Model Description

Given the structure of the states, shell-model fits can be made to derive matrix elements of the residual interaction. Full knowledge of the residual interaction may help to lead to a more complete understanding of nuclear forces.

Antimony 116 with Z=51 and N=65, falls in the region between the 50 and 82 closed shells for both protons and neutrons. For low excitations (below approximately 1 MeV) the states should consist of the various couplings of the single neutron and proton orbitals plus various collective states. If we look at the neighboring even neutron Antimonies (odd proton) we find the ground states are $d_{5/2}$ with the order of the other orbitals being $g_{7/2}, s_{1/2}, d_{3/2}$ with excitation energies of 724, 771, 1072 keV respectively in ^{115}Sb and 527, 720, 924 keV, respectively, in ^{117}Sb[27,28]. The $h_{11/2}$ lies at a higher energy and has not been observed. The odd neutron in ^{117}Te and ^{115}Sn give an idea of what to expect in ^{116}Sb.[28,29] The ground state in both cases is $s_{1/2}$, followed by $d_{3/2}$ (330 and 497 keV respectively), $h_{11/2}$ (380 and 726 keV respectively), and the $g_{7/2}$ lies at a higher unknown energy.

The ground state configuration is expected to be $(\pi d_{5/2}, \nu s_{1/2})$. Nordheim coupling rules, as modified by Brennan and Bernstein[30], predict that the spin of the ground state is

$$J = |J_1 + J_2| = 5/2 + 1/2 = 3$$

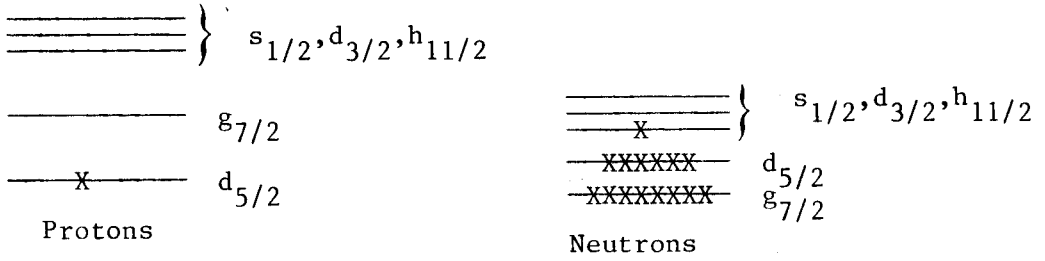

Shell Model Orbitals in ^{116}Sb.

Figure II-2.

This is in agreement with the recent atomic beam studies of C. Ekstrom et al.[6] Since the $g_{7/2}$ state lies at ≃ 600 keV in the adjacent odd antimonies, we anticipate that up the configuration of low lying excited levels probably include the proton $d_{5/2}$ up to about 600 keV, with the various neutron states. The first excited 2^+ state (see chapter 7 for discussion of spin assignments) is believed to be the spin 2 coupling of the ground state configuration.

The next lowest neutron orbital is the $d_{3/2}$, which coupled to the $d_{5/2}$ proton orbital will produce states with $J^\pi = 1^+, 2^+, 3^+, 4^+$. The J = 1 state might be the 93.7 keV state and the 4^+ probably is the 410.9 keV state. It is not possible to uniquely pick out the 2^+ of 3^+ states with this configuration as there exist too many possibilities. The same is true of the $h_{11/2}$ which yields states of 3^- to 8^-.

III. THE BETA DECAY OF ^{116}Te

A. Source Preparation

Enriched ^{116}Sn was obtained from the Oak Ridge National Laboratory Isotope Division in the form of a powdered oxide. This was placed within a rabbit[12] (pneumatic target transport system) for bombardment by the MSU Cyclotron with 71 MeV ^{3}He. Since the Q-value of the (^{3}He,3n) and (^{3}He,4n) reactions are -15.66 and -26.80 MeV respectively, the cyclotron beam was degraded to 32 MeV with an 62 mil Al absorber. The 32 MeV was chosen on the basis of calculations with the computer code CS8N[13], which predicted that the cross-section for the (^{3}He,3n) reaction would peak at that energy. After bombardment for periods of 30 to 60 minutes, the sources were allowed to sit for approximately 30 minutes to allow undesired shorter lived contaminant activities to decay. Then the activities were placed within fresh aluminum foil envelopes for counting.

B. Singles

The samples were counted with an 18% efficient (the full energy detection efficiency for the 1332 keV gamma of ^{60}Co relative to that of a 3 in × 3 in NaI(Tl) scintillator detector with a source to detector distance of 25 cm) Ge(Li) detector that has a resolution of 2.0 keV FWHM and a peak to Compton background ratio of 45:1 for the 1332 keV gamma of ^{60}Co. The singles gamma-ray spectra data were taken at time intervals of 2.0 hours over a period of 10.0 hours. Those γ rays with the correct lifetime of 2.5 hours were assumed to be

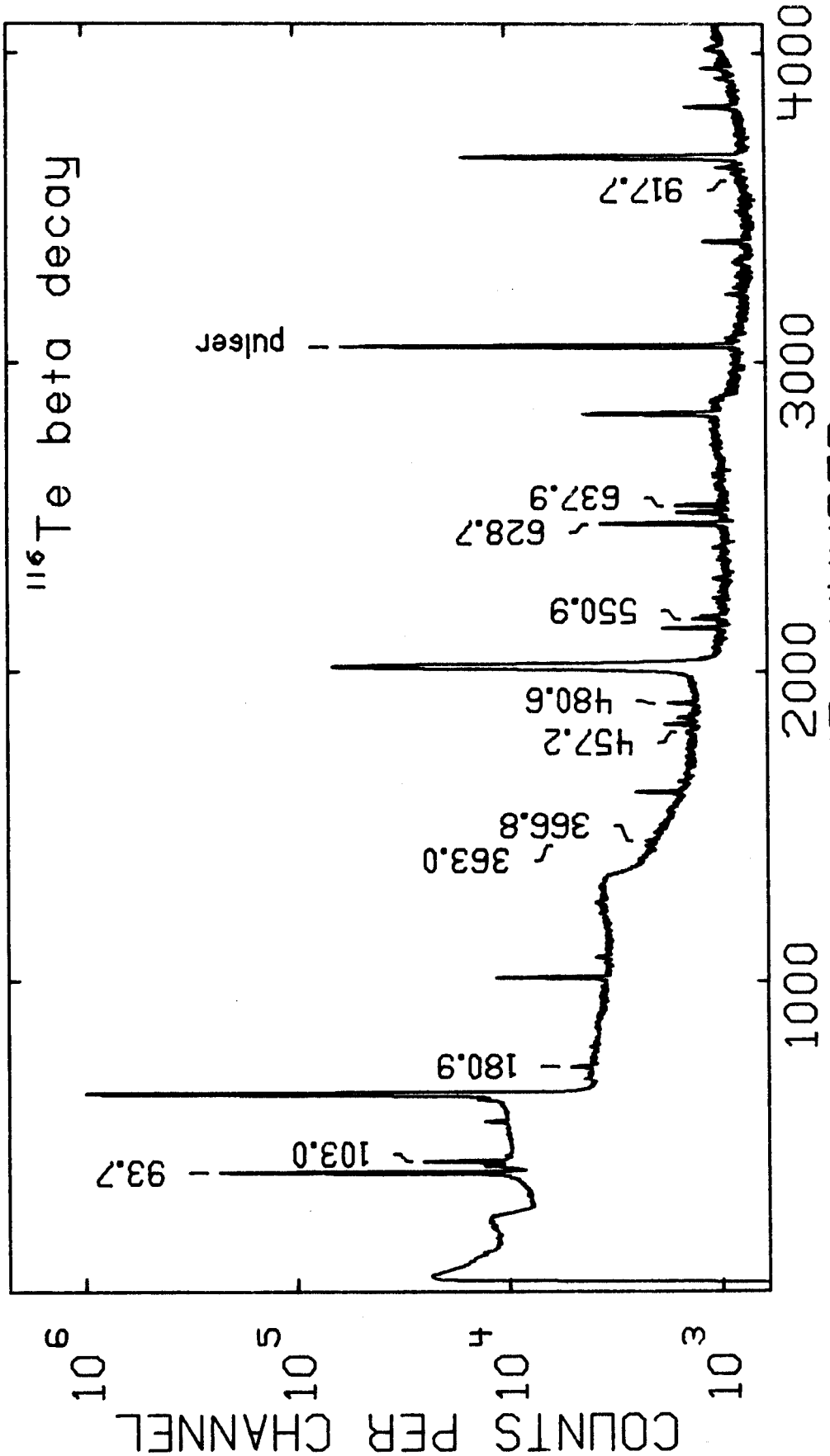

Gamma-ray spectrum from ^{116}Te decay.

Figure III-1

candidates for placement in the decay of ^{116}Te. In all sixteen γ rays were found with the proper lifetime.

C. Gamma-Gamma Coincidence

The detectors used were the 18% Ge(Li) detector, previously described, and an 8% Ge(Li) with 1.95 keV FWHM at 1332 keV and a peak to Compton ratio of 33:1. The detectors were placed with a half inch of lead between them to reduce Compton scattering from one detector to the other. The source was placed at the end of the sheet of lead (which lacked about a quarter of an inch of going to the edge of the detectors) as is shown in Figure III-2. A singles counting rate of about 2×10^4 cps was maintained in the 18% detector which gave a coincidence rate of approximately 300 cps. About 7×10^6 events were stored on magnetic tape using the MSU on-line PDP-9 computer. The data were recovered using weighted background subtraction with the MSU Xerox SIGMA-7 computer. The results of this measurement are found in Table III-1.

D. Level Scheme and Spin and Parity Assignments

The level scheme constructed (Figure III-3) consists of eight excited states, four of which are fed directly by electron capture decay. These four states are the 1158.3, 917.7, 731.6, and 93.7 keV states which have beta transitions with log ft's of 5.4, 6.3, 5.5, and 4.7 respectively. Since these log ft's are low enough that the beta decay is probably allowed, spin and parity assignments of either 1^+ or 0^+ can be made to these four levels. The log ft of the beta

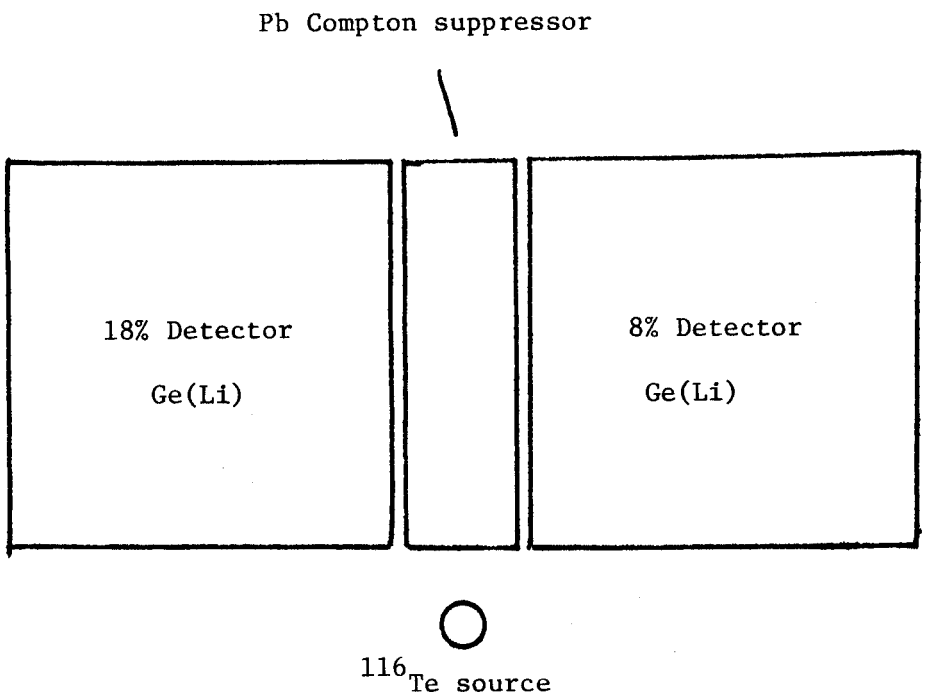

Detector arrangement for γ-γ coincidence.

Figure III-2

Table III-1. Results of two parameter γ-γ coincidence experiments from ^{116}Te beta decay.

Gated γ ray (keV)	Coincident γ rays (keV)
103.0	628.7, 1055.3
180.9	550.9
363.0	103.0, 108.5
366.8	457.2, 550.9
447.8	180.9
457.2	180.9, 366.8
480.6	93.7, 157.2
550.9	180.9, 366.8
574.4	157.2
628.7	103.0
1055.3	103.0

Table III-2. Gamma rays per 1000 decays of ^{116}Te

Gamma ray (keV)	Intensity (γ's/1000 decays)
93.7	958.21
103.0	29.46
108.5	.47
157.2	4.08[a]
180.9	2.12
363.0	.59
366.8	1.31
447.8	.52
457.2	1.01
466.0	b
471.4	.42
480.6	3.7
550.9	2.90
574.5	.36
583.8	.87
628.7	30.29
637.9	7.14
824.0	1.08
917.7	1.38
1055.3	6.46[c]
1064.6	2.32[c]

[a]The intensity for the 157.2 keV γ ray was computed from the sum of the γ ray depopulating the 574.4 keV level.

[b]The 466.0 keV γ ray was not observed in the beta decay but is known to account for 11% of the deexcitation of the 466.0 keV level.

[c]These intensities were computed using the branching ratios obtained from in-beam experiments.

transition to the 917.7 keV level may indicate a first forbidden transition, but this is considered unlikely as no such shell model configurations should exist at this low an excitation. Gamma-ray angular distribution data (described in Chapter IV) eliminates the 0^+ possibility for all but the 93.7 keV level (which is isotropic due to its long lifetime) as they are anisotropic. Electron internal conversion work by Fink et al.[5] show that the 93.7 keV γ ray is an E2 transition to the 3^+ ground state. Therefore, all four levels fed by beta decay are assigned a spin and parity of 1^+. The 103.0 keV level is assigned a spin and parity of 2^+, as described in Chapter VII.

The spin 2 states are not expected to have any observed feeding by beta decay of ^{116}Te as this would require a second forbidden transition. The spins of the spin 2 and the excited spin 3 levels were based upon in-beam gamma-ray angular distribution and excitation function data (described in Chapter VII).

An additional gamma ray of 466.0 keV (shown depopulating the 466.0 keV level) is known to exist from the in-beam studies, but was not seen in the beta decay of ^{116}Te. This is not surprising in view of the fact that this gamma ray is very weak. Since the 157.2 keV γ ray is obscured by the large 158 keV decay peak from ^{117}Sb, its intensity was computed from the depopulation of the 574.4 keV level, as there should be no direct beta feeding to this level. The three γ rays de-exciting the 1158.3 keV level were observed in the coincidence data, but only the 583.8 keV γ ray was observed in the singles (due to a low amplifier gain setting). The intensities were inferred using the branching ratios obtained from the in-beam measurements discussed in Chapter IV.

^{116}Sb levels from ^{116}Te ε decay.

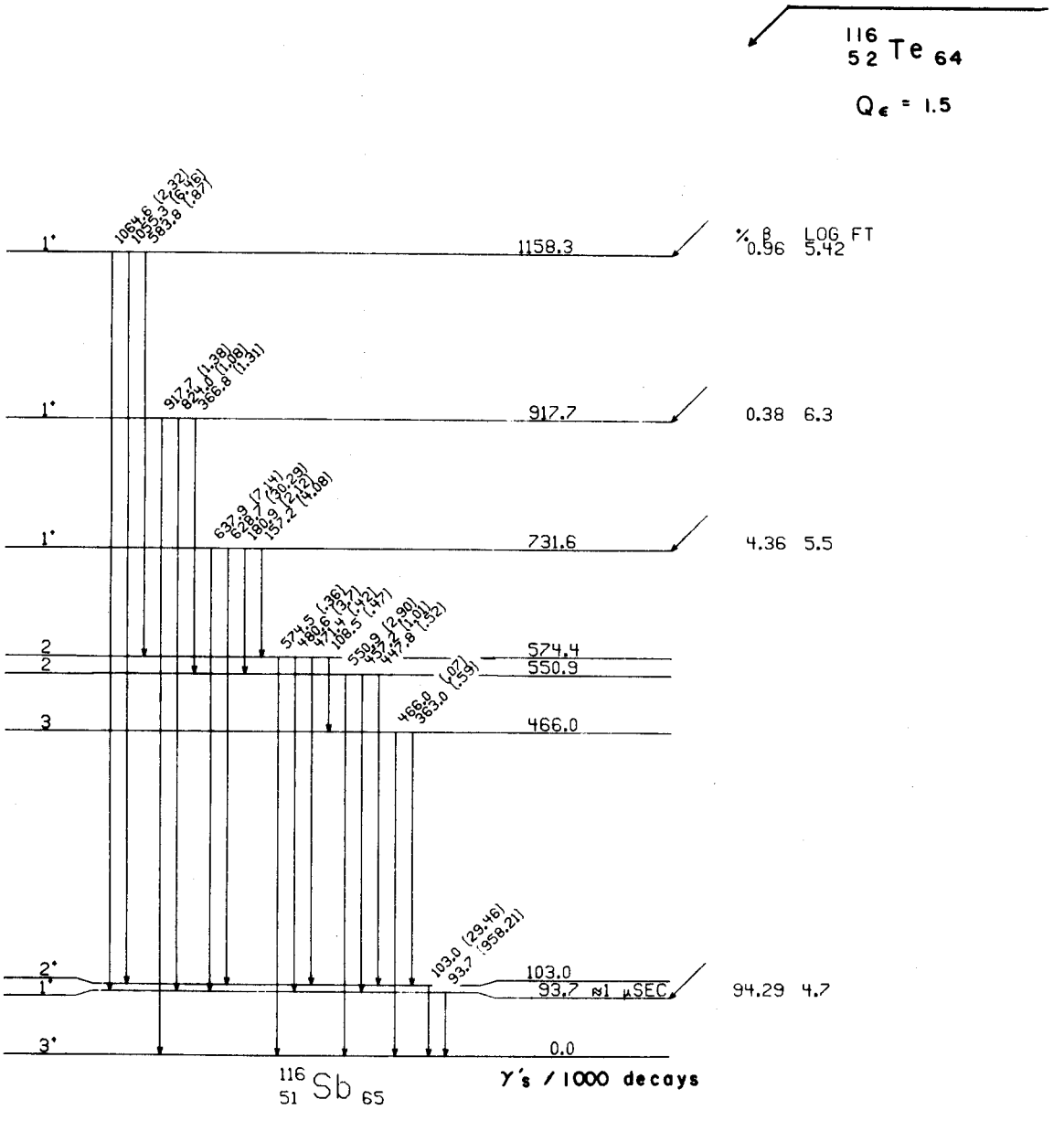

Figure III-3.

IV. THE $^{116}Sn(p,n\gamma)^{116}Sb$ REACTION

Although the Q-value for the $^{116}Sn(p,n\gamma)^{116}Sb$ reaction is not accurately known, it is near the value (-5.37 MeV) calculated from the 1972 mass compilation[14].

Four different types of gamma-ray experiments were performed using the $^{116}Sn(p,n\gamma)^{116}Sb$ reaction: excitation function measurements, gamma-gamma coincidences, lifetime measurements and angular distributions.

In the first type of experiment, excitation function data were taken from below threshold up to approximately 1.78 MeV of excitation. The excitation functions provided threshold information which greatly aided in the placement of the gamma rays within the excited level scheme. Also these provided information on relative cross sections as a function of proton energy. The cross sections can be related to the spins of the levels producing a method of making these assignments which complements the angular distribution method. Gamma-ray branching ratios were derived from the individual spectra.

In the second type of experiment, gamma-gamma coincidences were measured with a Ge(Li)-Ge(Li) spectrometer for excitation energies of 1.0, 2.5, 2.8, and 6.2 MeV. Except for the case of ground state transitions (or to the delayed 93.7 keV state) involving no coincidences, this method is an excellent way to identify those gamma rays which belong to the de-excitation of ^{116}Sb and is a great asset in placing them within the level scheme.

The third type of experiment was a lifetime measurement using a beam sweeping system. These measurements indicated that there are

two delayed states, the 93.7 keV state with a lifetime of greater than approximately 0.2 microseconds (not measured) and the 455.2 keV state with a lifetime of 1.85 0.06 nanoseconds. This method is a very good way to identify those contaminant gamma rays which are from beta decay as they will appear with very long lifetimes.

The fourth experiment is angular distributions of the various ^{116}Sb gamma rays for excitation energies of 400, 750, 1150, and 1830 keV. Where possible, the beam energies were chosen such that the particular states in question were not fed from above by gamma-ray transitions. The gamma-ray angular distributions provided information on spins, gamma-ray multipole mixing ratios, and gamma-ray branching ratios.

A. Gamma-Ray Thresholds and Excitation Functions

Gamma-ray excitation data were taken from approximately 75 keV to 1.0 MeV of excitation in 50 keV steps, and from there to 1.5 meV in 100 keV steps. The proton beam energies ranged from 5.64 to 7.15 MeV. These data were taken with the Western Michigan University Tandem Van de Graaff. The target was a ^{116}Sn foil of about 95% purity and a thickness of approximately 1 mg/cm^2 which contributed 33 keV to the energy spread of the proton beam for a beam energy of 5.5 MeV and 27 keV for a beam energy of 7.5 MeV. The gamma rays from the ^{116}Sn(p,nγ)^{116}Sb reaction were detected with a 10.4% efficient Ge(Li) detector (with a peak to Compton of 35:1 and a resolution of 2.0 keV FWHM) at approximately 55 degress (which is close to a zero of $P_2(\cos\theta)$) from the beam direction at a distance of 5.5 cm. This

acts to minimize angular distribution effects and allows one to more directly use intensities to calculate branching ratios for the various gamma rays. The charge was collected and integrated in an electrically shielded piece of lead-lined aluminum beam pipe. The integrated current was used to trigger a tailpulse generator which was fed into detectors preamplifier giving dead-time and amplifier pile-up corrections. The pulser peak was placed so as not to interfere with γ-ray peaks and was used as a run to run normalization. The γ-ray spectra were stored in the WMU on-line PDP-15 computer as 4096 channel spectra with about 0.3 keV per channel. Run times were typically 1 hour with typical counting rates of 4000 cps to 8000 cps.

Gamma-ray spectra that show the growth of the ^{116}Sb γ rays with increasing proton beam energy are shown in Figure IV-1. The threshold information and gamma-ray intensities obtained from these data were crucial to the placement of several levels and their associated gamma rays.

For neutron cross sections the neutron population of each state was determined by subtacting the total intensities of all electromagnetic transitions to a particular state from the sum of the intensities of all electromagnetic transitions de-exciting that state. Internal conversion coefficients were used as in Table IV-1[15]. Where the multipolarity of a transition was unknown, for this calculation it was assumed to be M1. Other conversion coefficient corrections were determined to be less than 1% and were ignored. The gamma intensities were determined by the peak fitting program SAMPO[21] and the detectors' relative efficiency curves. All intensities were normalized to the pulser peak. These relative cross sections

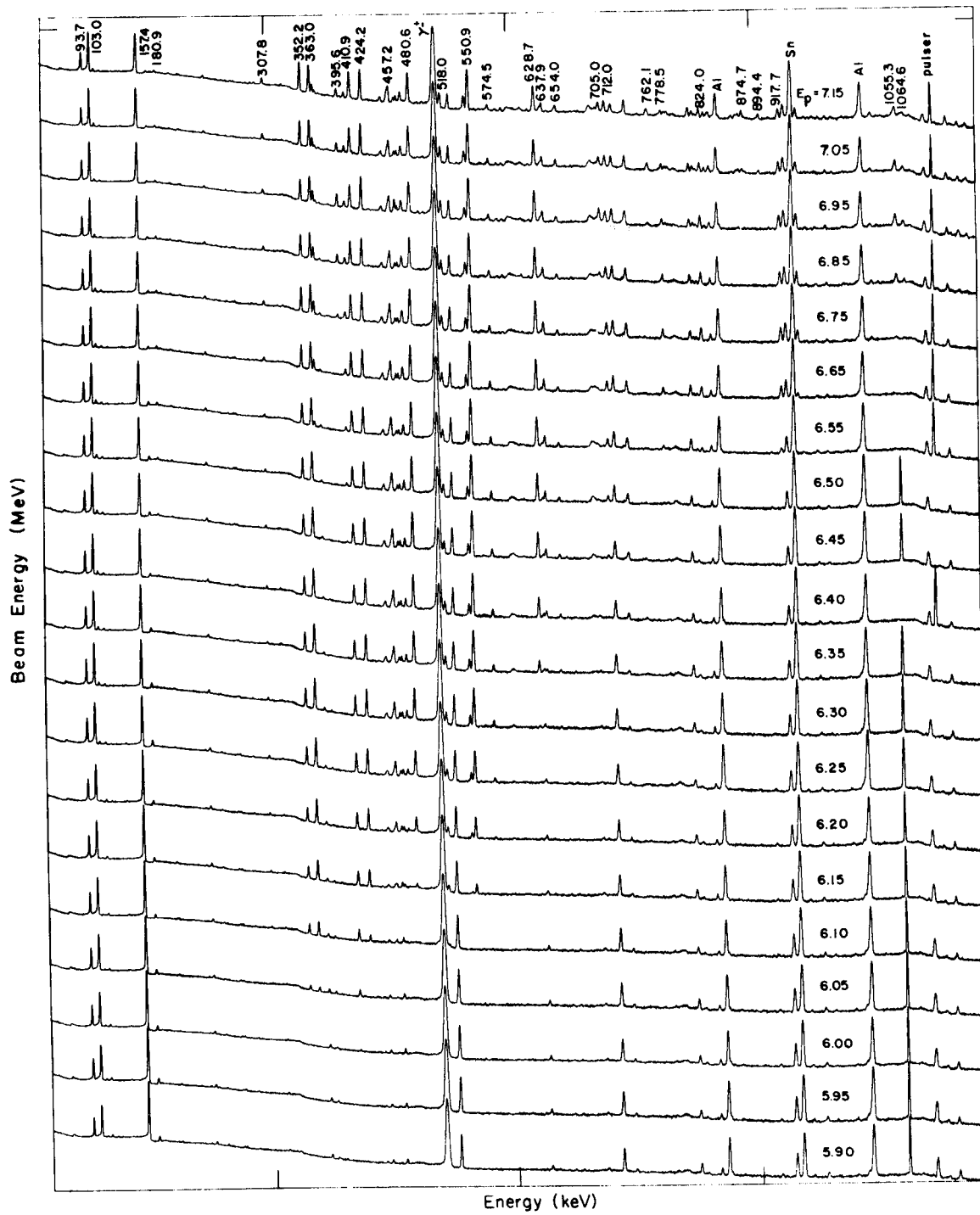

Gamma-ray spectra as a function of beam energy.

Figure IV-1.

Table IV-1. Internal conversion coefficients[a] used in the excitation function calculations.

Gamma ray (keV)	α_K	α_L	total (K+1.33*L)
92.2	0.6518	0.0821	0.7609
93.7	1.6176	0.5088	2.2943
103.0	0.5030	0.0613	0.5845
108.5	0.4015	0.0516	0.4702
157.4	0.1429	0.0179	0.1666
180.9	0.0954	0.0137	0.1136
208.1	0.0730	0.0091	0.0851
307.7	0.0313	0.0042	0.0369

[a]These values were obtained from Reference 15.

are shown in Chapter VII where they are used as an aid to the spin assignments.

The data were analyzed using a modified version of the computer code MANDY[10] containing ABACUS II[16] as a subroutine. The simplified program input consists of masses of target and resultant nuclei, Q-value, beam energy, and for each level in the target (for inelastic scattering) and the resultant nucleus, the energy, spin and parity were included. The program calculates all transmission coefficients for all ℓ values having coefficients greater than 10^{-6} for all levels energetically possible. MANDY then produces cross sections for $0^{+} \leq J^{\pi} \leq 6^{+}$ and $0^{-} \leq J^{\pi} \leq 6^{-}$ for each level, using all other levels as extra exit channels. Spins higher than 6 have cross sections that are vanishingly small at the proton energies used here and were deemed not necessary for the present data. Since the cross sections are dependent upon the extra exit channels (which are also the results of the calculation) the process must be an iterative one, until the results match the input. The placement of γ rays within the level scheme and all of the spin assignments must be correct to obtain completely correct results from MANDY for the excitation fuction data.

MANDY uses a general statistical model approach[8] to calculate the total cross sections for each level within ^{116}Sb as a function of beam energy. The program assumes that a compound nucleus is formed with no fluctuations in level density or of the density of the states with specific spins and parities. The probability of forming the compound nucleus is that obtained from the transmission coefficients produced by the program ABACUS II[16] using optical model parameters

from Perey and Buck[17] (Table IV-2).

The general expression for the differential cross section is

$$\frac{d\sigma}{d\Omega} = \sum_{\nu=0,2,4\ldots} A_\nu P_\nu(\cos\theta)$$

where for the excitation functions we are interested only in the A_0 term, which gives the total cross section. The expression for A_0 obtained from Chapter II and simplified is

$$A_0 = \frac{\lambda\!\!\!^{-2} g\tau}{4} = \frac{(2J_1+1)\tau\lambda\!\!\!^{-2}}{4(2J_0+1)(2S_1+1)}$$

where g is the statistical spin factor and $\lambda\!\!\!^{-}$ is the rationalized wavelength for the incident particle. This gives the relationship for σ the total interaction cross section used by MANDY[10].

$$\sigma = \Sigma 4\pi A_0 = \pi\lambda\Sigma\ \tau(2J_1+1)(2J_0+1)^{-1}(2S_1+1)^{-1}$$

The J_1's are the nuclear spins of the compound nucleus (CN) levels, S_1 is the spin of the incoming proton and J_0 is the targets ground state nuclear spin (0 for our case). The penetrability term τ is a measure of the relative probability of barrier penetration by particles and is a function of transmission coefficients $T_{\ell j}(E)$.

$$\tau = T_{\ell j}(E_1)\ T_{\ell j}(E_2)\ /\Sigma\ T_{\ell J}(E)$$

Table IV-2. Form of the optical-model potential and parameters used in the calculations of transmission coefficients. The Coulomb potential, $V_c(r)$, is that due to a uniformly charged sphere of radius $1.25A^{1/3}$ [F]. The parameter E is the center-of-mass energy of the nucleon in MeV.

Nucleon	V_0 (MeV)	W_D (MeV)	r_0 (F)	r_0' (F)	a (F)	a' (F)	V_{so} (MeV)
Proton[a]	$46.7-0.32E + ZA^{-1/3}$	11	1.25	1.25	0.65	0.47	7.5
Neutron[b]	48.0 - 0.29E	10	1.25	1.25	0.65	0.47	7.5

$$V = V_c(r) - V_0 \frac{1}{1 + e^{(r-R)/a}} + i W_D \frac{d}{dr} \frac{4a'}{1 + e^{(r-R')/a'}} + \left(\frac{h}{m_\pi c}\right)^2 \frac{V_{so}}{r} \ell\cdot\sigma \frac{d}{dr} \frac{1}{1 + e^{(r-R)/a}} ;$$

$$R = r_0 A^{1/3}, \; R' = r_0' A^{1/3}$$

[a]The proton parameters, except V_{so}, are from Ref. 22.

[b]The neutron parameters and the proton V_{so} are from Ref. 17.

The sum extends over all open channels, including inelastic scattering, by which the CN state can decay. The transmission coefficients depend upon the particles' center of mass energy, and orbital and total angular momenta ℓ and j, respectively.

The sum in the total cross section expression is made over all possible values of j_1 and j_2, which are the total angular momenta of the incoming protons and outgoing neutrons. Since this sum involves the spins of the intermediate compound-nuclear states, parity conservation and the angular momentum coupling rules require a different sum over the penetrability term for each final excited-state spin and parity. Since the target has $J^{\pi} = 0^{+}$ and the outgoing neutrons are mostly $\ell = 0$, the spin of the final state is determined predominately by the angular momenta of the incident protons. At these energies the incoming protons are mostly $\ell = 2$. Therefore the cross sections are expected to be largest for J values of 1 and 2.

The proton transmission coefficients were calculated using the local optical model parameters listed in Table IV-2. The neutron transmission coefficients were calculated using the local equivalent optical model parameters of Perey and Buck[17]. It was assumed that the energy dependence would allow the use of the proton parameters at proton energies as low as 5.5 MeV and the neutron parameters as high as neutron energies of 2 MeV, i.e. within the energy range used in these experiments.

All known inelastic proton channels (12) below 2.9 MeV were used along with all known open neutron channels in each MANDY calculation.

To eliminate possible systematic errors introduced by optical

model parameters, the cross sections, both experimental and calculated, were normalized to a level having a known J^{π} (in this case the 93.7 keV level). Internal consistency of the present experimental results indicate that these possible errors are minimal. It is believed that a high density of unobserved states above approximately 1 MeV of excitation was responsible for the observed disagreement (the experimental values were much lower than theory) for states in that energy region. Comparisons of these cross-section ratios are made later in Chapter VII.

B. In-Beam Gamma-Gamma Coincidence Measurements

Proton beams of 6.54, 7.28, 7.99, 8.4, and 11.75 MeV (lab) were obtained from the MSU Cyclotron for the different in-beam coincidence measurements. The target used was a 15 mg/cm^2 ^{116}Sn foil enriched to approximately 95%, and rolled from the metal powder which was obtained from the Isotopes Division of Oak Ridge National Laboratory. The detectors used are briefly described in Table IV-3.

The detectors were positioned as shown in Figure IV-2. The lead block between the detectors has a 1.3 cm diameter hole drilled almost through it and serves as a shielded beam stop as well as an attenuator for Compton photons scattered from one detector into the other.

Two experiments consisted of a typical two parameter, fast-slow coincidence arrangement with constant-fraction timing discrimination. The single-channel analyzer window set on the output from a time-to-amplitude converter was slightly smaller than the approximately

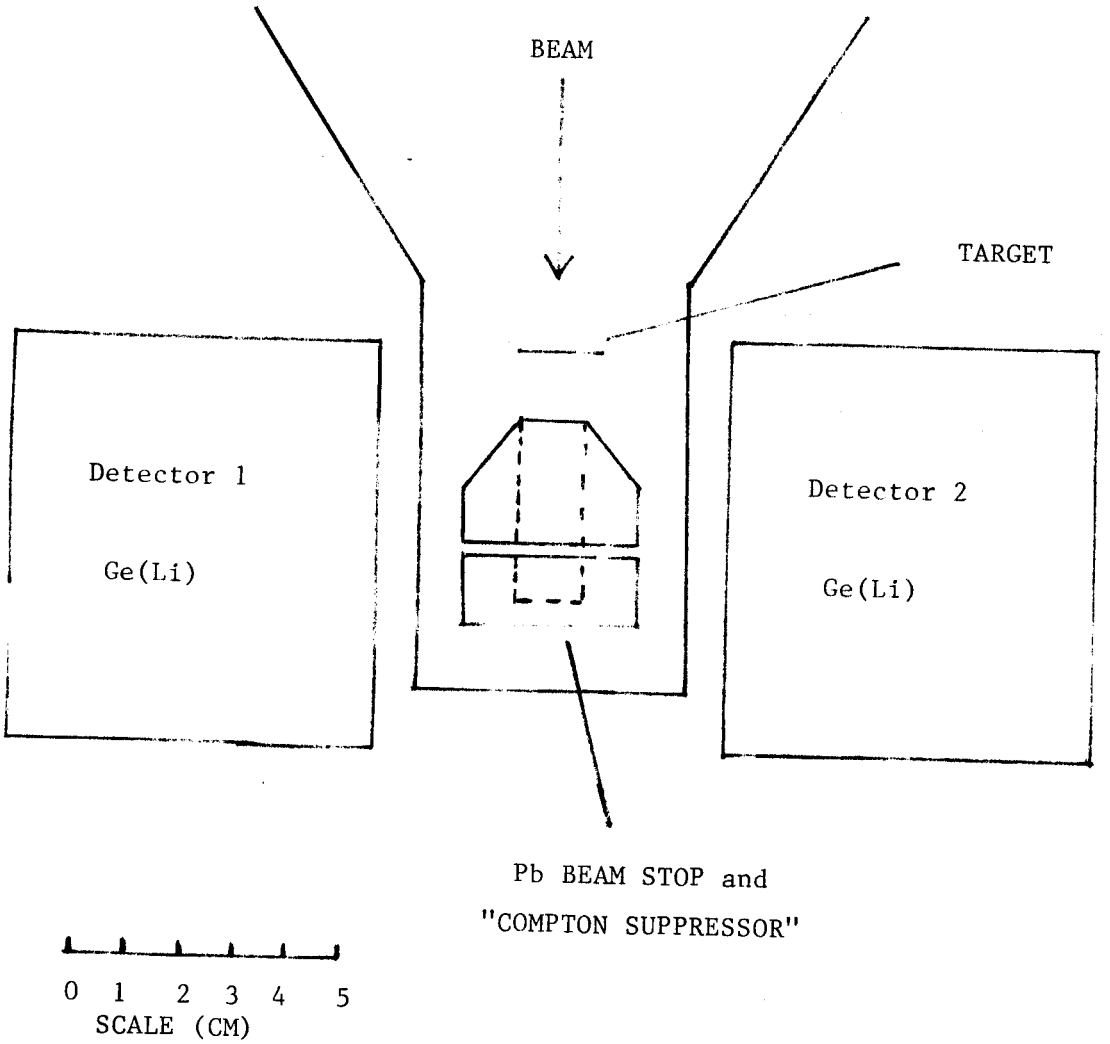

Arrangement for in-beam γ-γ coincidence.

Figure IV-2

Table IV-3. Ge(Li) detectors used in in-beam γ-γ measurements.

E_p(MeV)	Detector 1	Detector 2
6.54	4.5%	7.0%
7.28	4.5%	7.0%
7.99	4.5%	7.8%
8.30	4.5%	7.8%
11.75	10.0%	7.0%

The detectors are listed by their efficiency for the full energy detection for the 1332 keV gamma of ^{60}Co relative to that of a 3 in × 3 in NaI(Tl) scintillator detector with a source to detector distance of 25 cm. The energy resolution for these detectors ranges from 1.9 keV to 2.2 keV FWHM for the 1332 keV gamma of ^{60}Co.

70 nanoseconds between the beam bursts.

The last three experiments were performed as three parameter gamma-gamma-time experiments. The TAC output was preserved, along with the energy information, for later analysis.

Coincident events were stored on magnetic tape as pairs or triplets of channel numbers, and sorted off-line using weighted background subtraction.

The short half life of the ground state (15 min) resulted in a large radioactive build up of beta decay within the target. At equilibrium nearly half of the detected activity could be attributed to the beta decay.

The spectra produced by the 6.54 MeV protons contained about 5×10^6 events taken during a 2 day period. The 7.28 MeV spectra contained close to 8×10^6 events and the 11.75 MeV spectra more than 55×10^6 in the same time duration. Typical singles counting rates ranged from 1.5×10^4 to 2.0×10^4 counts per second in the detectors with up to 700 cps of coincidence events. The beam current required was typically about 2 nanoamps.

Numerous programs were used to recover the data from the magnetic tapes. The first program (used for the E_p = 6.54 MeV data) allowed 10 gates to be recovered simultaneously from tapes containing up to 1.8×10^6 events of 2 parameter data. Three parameter data (approximately 3.5×10^6 events per tape) were initially recovered with a similar program. Finally our most recent program (Chapter VI) will recover up to 120 gates of 2 or 3 parameter data, simultaneously. Execution time is only slightly longer than the original program thus giving a savings of an order of magnitude in computer time for cases

where large numbers of gates need to be recovered.

The integral spectra, along with some representative gated spectra from the coincidence experiment with E_p = 11.75 MeV, are shown in Figure IV-3. Fifty-nine γ rays were definitely identified by fast coincidences to be from ^{116}Sb. The energies of the ^{116}Sb γ rays are listed in Table IV-4, and the coincidences observed between these γ rays are listed in Tables IV-5 through IV-9. All the gated spectra can be found in the Appendix.

The positions of the levels within the level scheme shown in Figure IV-4 are consistent with the coincidence and excitation function data. Dots denote observed coincidence relationships between γ-ray transitions entering and leaving a state. The spin assignments (except that of the ground state) are based upon the present work and will be discussed in detail in Chapter VII.

All levels built upon the state with a measurable lifetime (the 455.2 keV state) have no transitions to other levels indicating that they may be negative parity states which M1 decay until they reach the lowest possible negative parity state where they must undergo an ℓ-forbidden E1 transition.

Because of high Compton background and the large number of transitions present, it is possible that some ground state and isomeric transitions have not been identified. Several difficulties were encountered during the construction of the level scheme from problems with unresolvable doublets in the spectra. Two of these are the 480.6 keV γ's and the 550.9 keV γ's which were determined to be doublets after great effort. Difficulties were also encountered with the large 158.5 keV γ ray from the beta decay of ^{117}Sb. Two of the ^{116}Sb γ

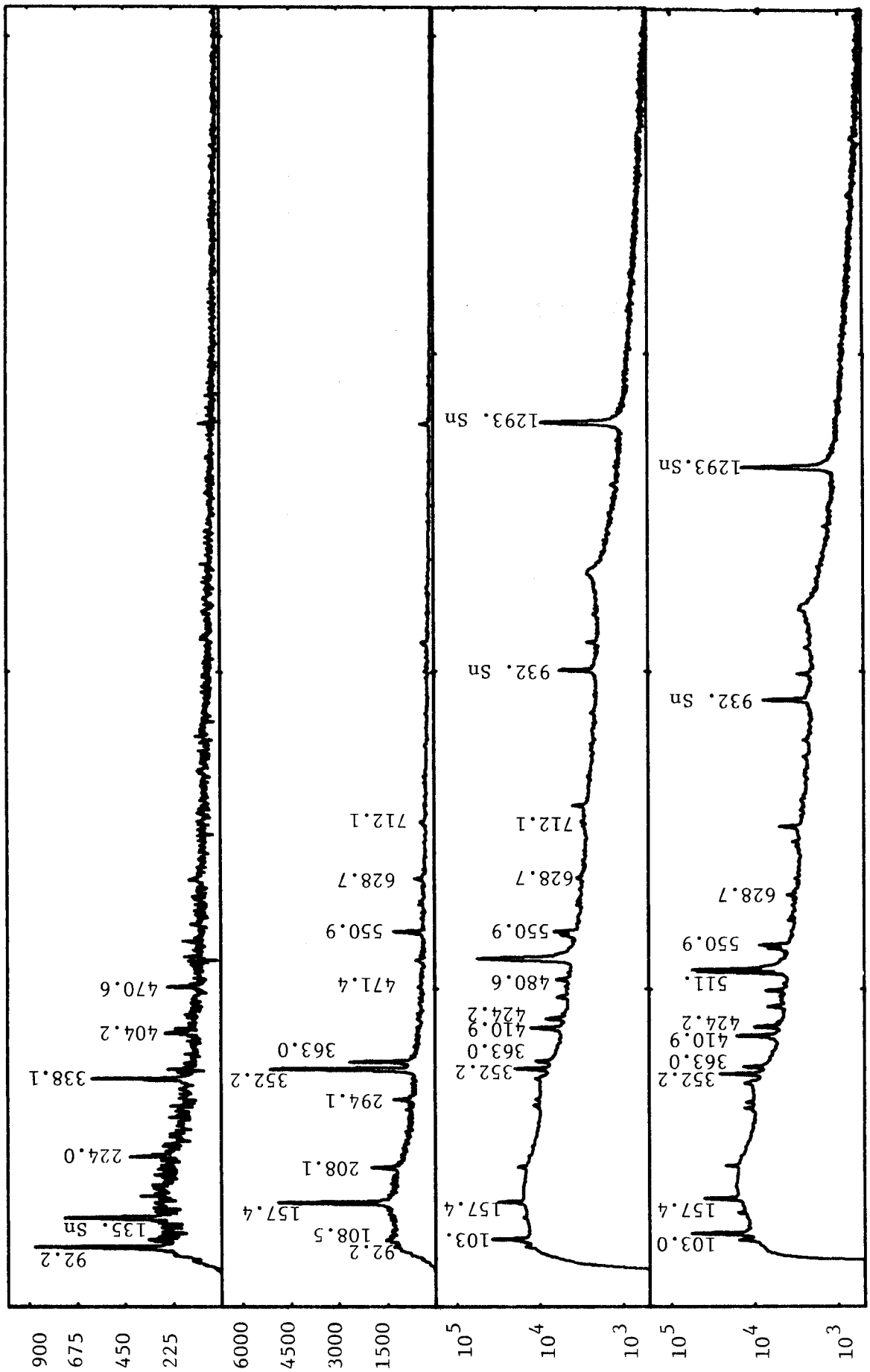

Figure IV-3 Integral and representative gated spectra from the 11.75 MeV coincidence experiment.

Table IV-4. Gamma-ray energies[a] from ^{116}Sb.

1	92.2	410.9	653.9
2	93.7	424.2	705.0
3	103.0	432.6	712.0
4	108.5	447.8	762.1
5	157.2	455.2	778.5
6	157.4	457.2	785.6
7	176.7	466.0	815.1[b]
8	180.9	470.6	824.0
9	208.1	471.4	867.5
10	224.0	480.6[b]	868.6
11	294.1	518.0	870.3
12	307.8	550.9[b]	874.7
13	338.1	574.5	894.4
14	352.2	583.8	907.7
15	363.0	590.1	917.7
16	366.8	596.1	948.4
17	380.	612.5	1025.9
18	388.9	621.5	1055.3
19	395.6	628.7	1064.6
20	404.2	637.9	1129.2

[a]Errors are approximately 0.1 keV for energies less than 600 keV and range from 0.2 to 0.5 for energies above 600 keV.

[b]These γ rays have been determined to be doublets.

Table IV-4a. Gamma-ray calibration energies used to determine energies in ^{116}Sb.

E_γ(keV)	Source	Ref.
88.036±0.008	^{109}Cd	23
122.061±0.010	^{57}Co	23
136.471±0.010	^{57}Co	23
165.853±0.007	^{139}Ce	23
279.189±0.006	^{203}Hg	23
391.688±0.010	^{113}Sn	23
513.996±0.016	^{85}Sr	24
661.638±0.019	^{137}Cs	24
846.790±0.030	^{56}Co	25
898.021±0.019	^{88}Y	24
931.800±0.050	^{116}Sn	26
1173.208±0.025	^{60}Co	24
1238.300±0.020	^{56}Co	25
1293.538±0.040	^{116}Sn	26
1332.491±0.041	^{60}Co	24
1771.410±0.030	^{56}Co	25
1836.130±0.040	^{88}Y	25
2015.360±0.030	^{56}Co	25

Table IV-5. Results of two parameter γ-γ coincidence with E_p = 6.54 MeV

Gated γ ray (keV)	Coincidence γ rays (keV)
103.0	108.5, 352.2, 363.0, 471.4, 550.9, 628.7
108.5	103.0, 363.0
157.2 & 157.4	103.0, 352.2, 480.6
352.2	103.0, 157.4
363.0	103.0, 108.5
480.6	157.2
550.9	103.0
628.7	103.0

Table IV-6. Results of two parameter γ-γ coincidence with E_p = 7.28 MeV

Gated γ ray (keV)	Coincidence γ rays (keV)
92.2	103.0
103.0	92.2, 157.4, 208.1, 307.8, 352.2, 363.0, 471.4, 550.9, 628.7, 712.0, 778.5, 1055.3
108.5	103.0, 363.0
157.2 & 157.4	103.0, 208.1, 352.2, 455.2, 480.6, 388.9
208.1	103.0, 157.4, 352.2
294.1	550.9
307.8	103.0
352.2	103.0, 157.4, 208.1, 388.9, 590.1, 880.[a] 960.[a], 1025.9
363.0	103.0, 108.5, 621.5, 762.1, 870.3
366.8	103.0, 457.2, 550.9
395.6	103.0, 628.7, 638.9
404.2	307.7, 410.9
410.9	92.2, 404.2, 470.6
424.2	93.7, 480.6, 705.0, 815.1, 867.5, 907.7
447.8	103.0
455.2 & 457.2	366.8, 785.6, 874.7
466.0	103.0, 307.7, 410.9, 629.[a]
470.6 & 471.4	103.0, 410.9
480.6	157.2, 424.2, 653.9, 762.1

Table IV-6. Continued

Gated γ ray (keV)	Coincidence γ rays (keV)
546.2[a]	103.0, 550.9, 457.2
550.9	103.0, 180.9, 294.1, 366.8, 546.2[a], 829.[a]
	874.7
612.5	550.9
628.7	103.0, 395.6, 363.0, 550.9, 653.9, 735.[a]
653.9	480.6
705.0	424.2, 518.0
712.0	103.0
762.1	103.0, 363.0, 480.6, 471.4, 574.5
815.1	424.2
870.3	363.0
874.7	457.2, 550.9
880.[a]	352.2
907.7	424.2, 518.0
1055.3	103.0

[a]These gamma rays seem to be in coincidence with ^{116}Sb γ rays but were not placed within the present level scheme.

Table IV-7. Results of three parameter γ-γ coincidence with E_p = 7.99 MeV

Gated γ ray (keV)	Coincident γ rays (keV)
103.0	157.4, 307.8, 352.2, 363.0, 471.4, 550.9, 628.7, 712.0
108.5	363.0
157.2 & 157.4	103.0, 208.1, 352.2, 455.2, 480.6
208.1	157.4, 352.2
307.8	103.0
352.2	103.0, 157.4, 208.1
363.0	103.0, 108.5
404.2	410.9
410.9	404.2
424.2	480.6, 705.0
455.2 & 457.2	157.4
470.6	410.9
480.6	157.2, 424.2
550.9	103.0, 366.8
628.7	103.0
705.0	424.2

Table IV-8. Results of three parameter γ-γ coincidence with E_p = 8.4 MeV

Gated γ ray (keV)	Coincident γ rays (keV)
103.0	157.4, 352.2, 363.0, 550.9, 628.7
157.4	103.0, 208.1, 352.2
208.1	103.0, 157.4, 352.2
307.8	103.0
352.2	103.0, 157.4, 208.1
363.0	103.0
410.9	92.2, 404.2
480.6	424.2
550.9	103.0

Table IV-9. Results of three parameter γ-γ coincidence with E_p = 11.75 MeV

Gated γ ray (keV)	Coincident γ rays (keV)
92.2	307.8, 338.1, 410.9
103.0	92.2, 108.5, 157.4, 208.1, 294.1, 307.8, 352.2, 363.0, 471.4, 550.9, 570.7[a], 590.1, 628.7, 712.1, 778.5, 868.6, 1055.3
108.5	363.0
157.2 & 157.4	103.0, 208.1, 352.2, 380., 388.9, 432.6, 455.2, 480.6, 868.6
178.6	380.
208.1	103.0, 157.4, 352.2, 455.2, 388.9
224.0	103.0, 338.1, 410.9, 708.[a]
294.1	103.0, 550.9
307.8	92.2, 103.0
338.1	92.2, 103.0, 224.0, 307.8, 410.9, 682.[a]
341.3[a]	735.7[a]
352.2	103.0, 157.4, 208.1, 380., 388.9, 590.1 868.6
363.0	103.0, 108.5, 621.5, 629.[a]
366.8	457.2, 550.9
388.9	103.0, 157.4, 208.1, 352.2
404.2	410.9
410.9	92.2, 224.0, 338.1, 404.2, 470.6
424.2	480.6, 705.0, 815.1, 890.[a]

Table IV-9. Continued

Gated γ ray (keV)	Coincident γ rays (keV)
432.6	103.0, 157.4, 352.2
447.8	103.0
455.2	157.4, 208.1
470.6 & 471.4	103.0, 410.9
480.6	157.2, 424.2, 518.0, 762.1
482.[a]	338.1
546.2[a]	550.9
550.9	103.0, 294.1, 366.8, 570.7[a], 635.[a]
570.7[a]	103.0, 550.9
590.1	103.0, 352.2
621.5	363.0
628.7	103.0
705.0	424.2
712.0	103.0
778.5	103.0
868.6	103.0, 157.4, 352.2
894.4	103.0

[a]These gamma rays seem to be in coincidence with ^{116}Sb γ rays but were not placed within the present level scheme.

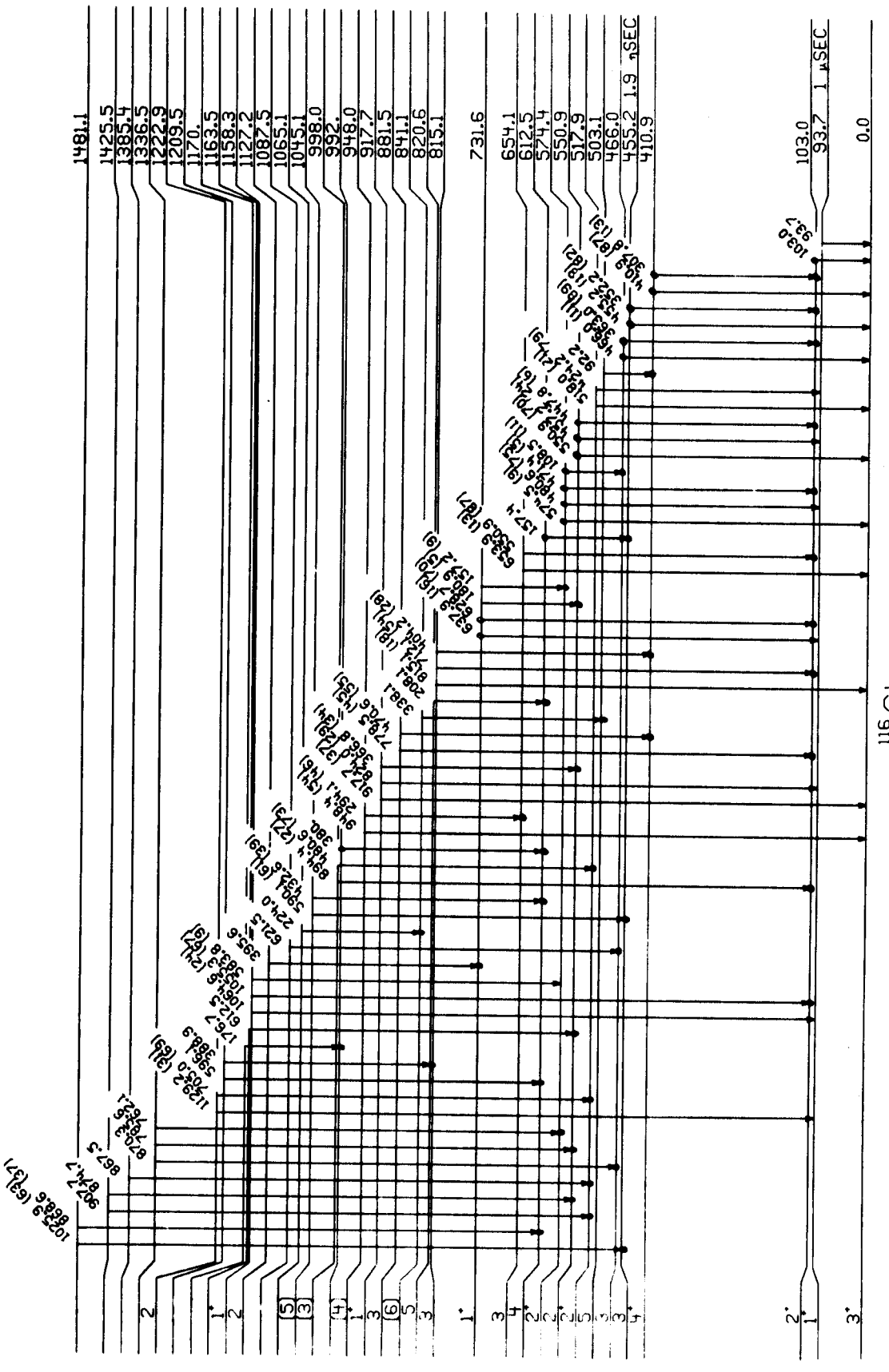

Figure IV-4 Level scheme for ^{116}Sb.

rays lie very close in energy (157.2 and 157.4 keV) to this huge decay peak, causing problems with the resolution of these peaks. The 157.4 keV peak can be resolved at higher energies where the intensity becomes comparable to that of the 158.5 keV γ ray. However, the 157.2 keV γ ray cannot be resolved as it is too weak and too close to the 157.4 keV γ ray. It's existence has been indicated by the coincidence data, both from the beta decay of ^{116}Te and the in-beam gamma-ray experiments.

C. Lifetime Measurements

A proton beam of 7.3 MeV (excitation of 1.93 MeV) was obtained from the MSU Cyclotron for the in-beam lifetime measurement. The target used was the thick target described in the γ-γ section. The detector used was a Low Energy Photon Spectrometer (LEPS) which has very good timing characteristics in the few nanoseconds region.

The detector was positioned at 90° with respect to the beam direction. Preamplifier pulses from the detector were used to start a time-to-amplitude converter which was stopped by a pulse from the cyclotron R.F. unit.

The data was collected by the MSU Sigma 7 computer as two parameter (energy vs time) events. Ten windows of equal width (4.052 ns) were set upon the time axis. The data were then sorted into ten single parameter spectra using these windows.

Analysis of the data was done using the time centroid shift of the delayed peak relative to that from a prompt peak. Two ^{116}Sb γ rays (352.2 and 455.2 keV) were found to have measurable lifetimes

Figure IV-5.

Comparison of a prompt γ ray to a delayed.

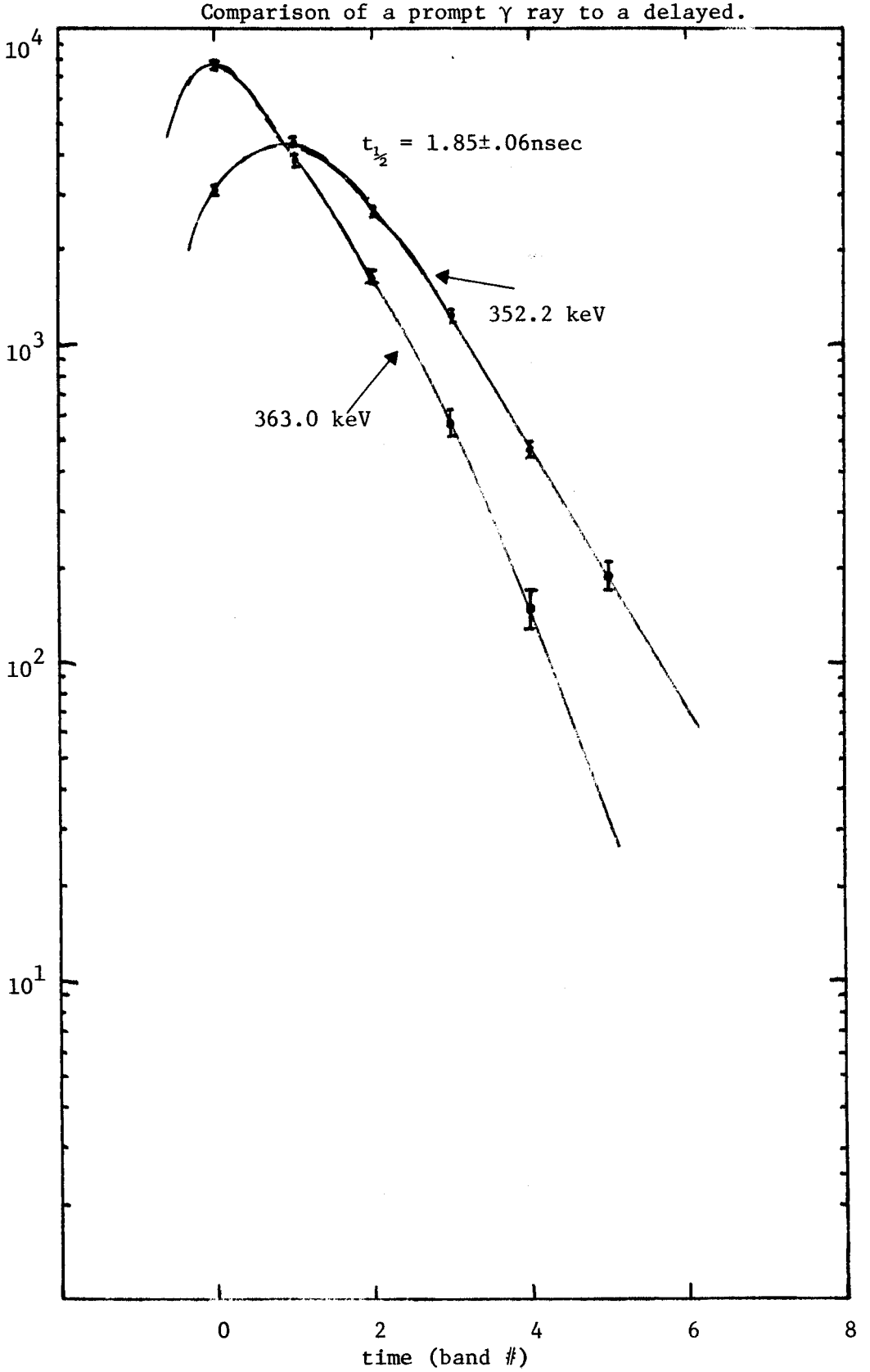

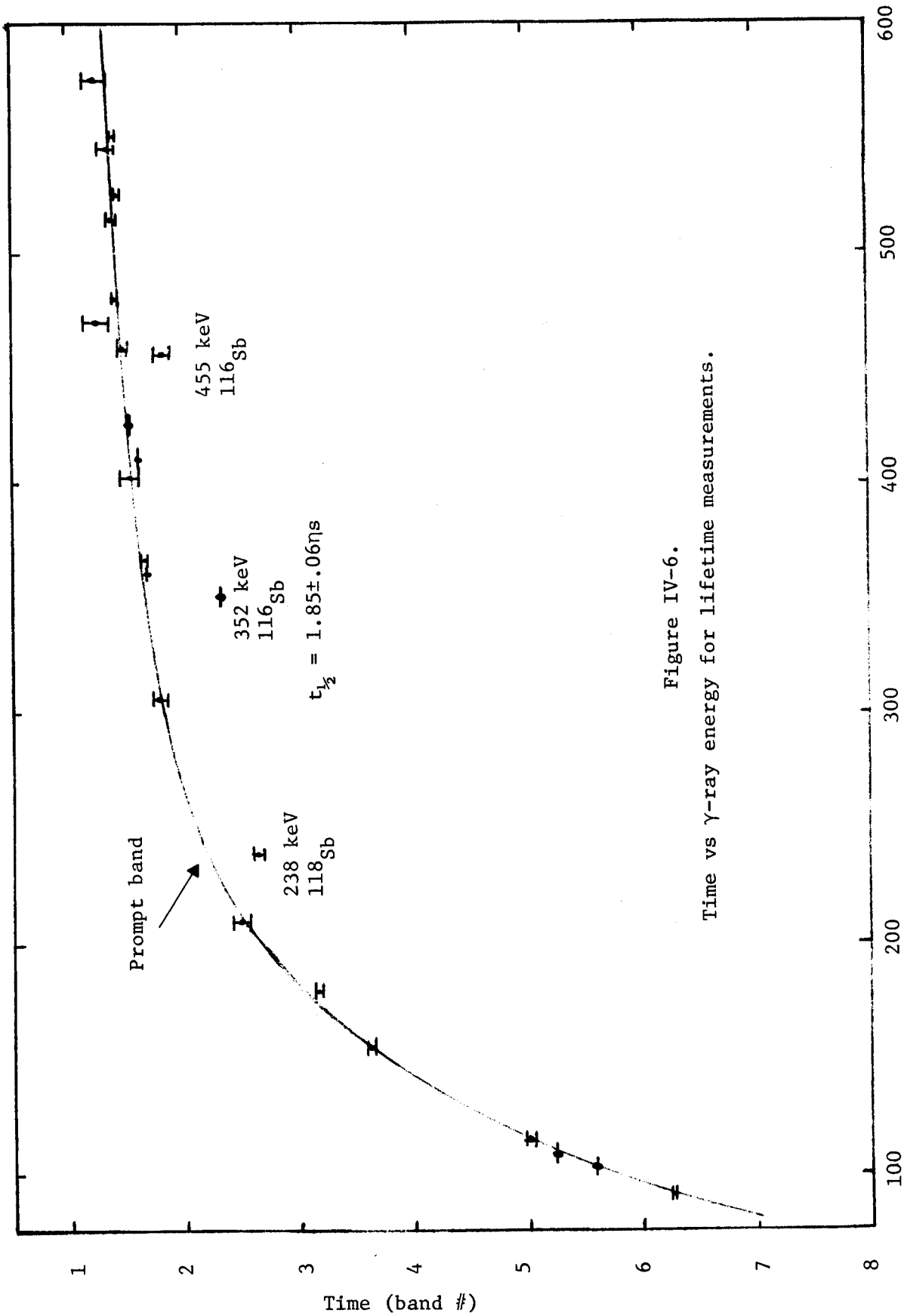

Figure IV-6.

Time vs γ-ray energy for lifetime measurements.

(only the 93.7 keV γ ray has a longer lifetime). The centroid shift found (mean life) was 2.66±0.08 nsec which gives a halflife of 1.85±0.06 nsec.

The multipolarity, L = 1, for the 352.2 keV transition, as obtained from the angular distribution experiments described in Chapter IV Section D, indicates that the transition must be hindered by a factor of 3500 if it is E1 and by 100 if it is M1. Electric and magnetic dipole transitions in odd A nuclei in this region are known to be hindered by these amounts.

The neutron single particle for negative parity states must be $h_{11/2}$, assuming that negative parity states produced by protons lie considerably higher in energy. Since the lowest lying states are either ($\pi d_{5/2}$, $\nu d_{3/2}$) or ($\pi d_{5/2}$,$\nu s_{1/2}$) the resultant E1 transitions would involve changing the neutron from a J of 11/2 to 3/2 which would be a ℓ-forbidden transition and therefore probably hindered.

D. Gamma-Ray Angular Distributions

Proton beam energies of 5.95, 6.25, 6.65, and 7.32 MeV were obtained from the MSU Cyclotron for in-beam measurements of gamma-ray angular distributions. The target used was the same target as used in the excitation function measurements. The detector used was an 8% efficient EDAX Ge(Li) detector.

The detector was positioned as shown in Figure IV-7, with angles from approximately 15 degrees to 90 degrees available for use. The beam was stopped in a small lead cup placed at zero degrees. Those γ rays which were produced from the beam hitting the beam stop had

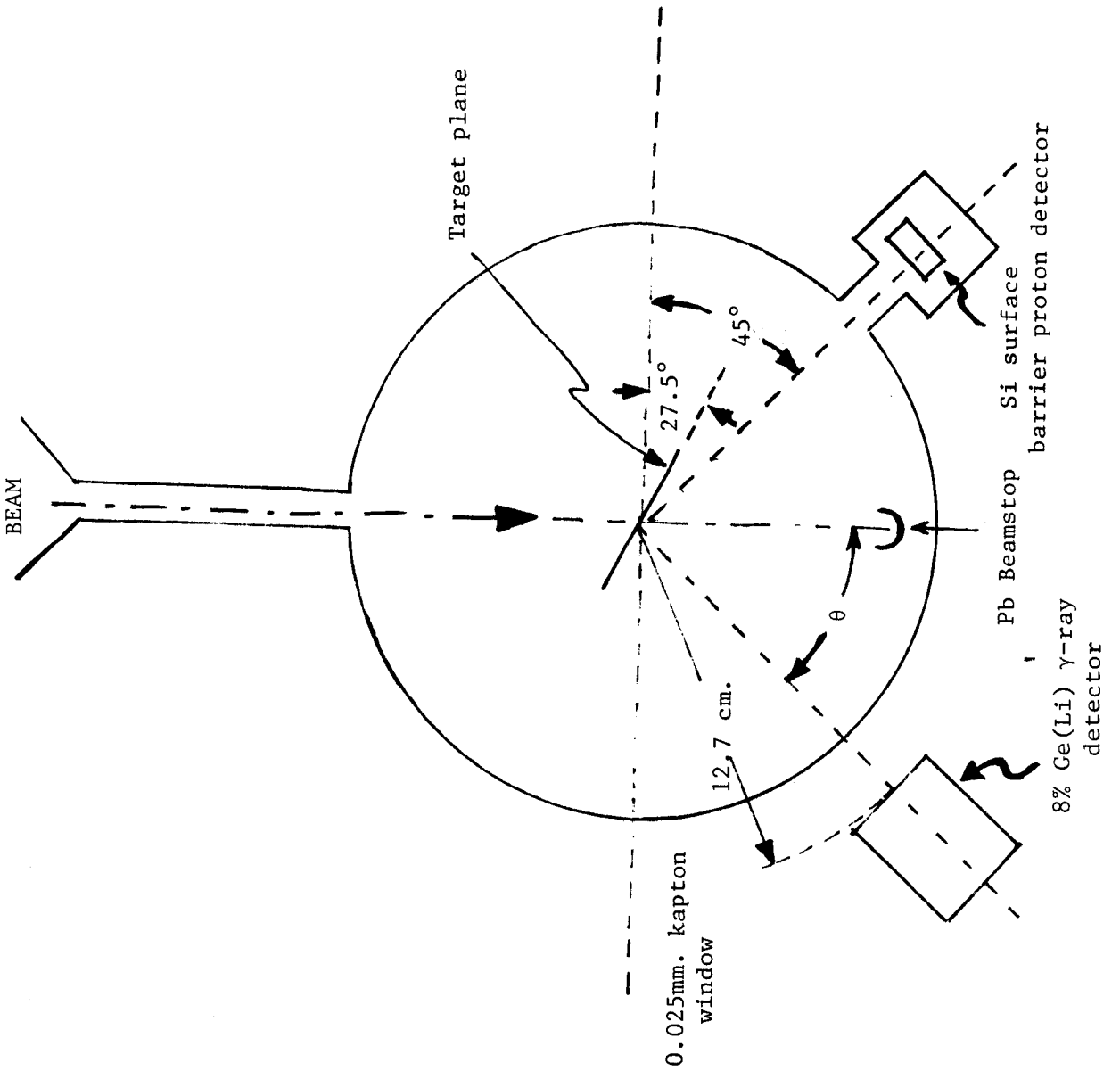

Arrangement used for γ-ray angular distributions.

Figure IV-7.

a definitely unique angular distribution, which gave 5 to 8 times greater intensity at small angles, allowing them to be disposed of easily.

The data were stored in the MSU Cyclotron Laboratory's Sigma 7 computer using the Northern Scientific 50 MHz analog to digital converters (ADC's). Data were collected in a random order of angles from 15 to 90 degrees to minimize possible systematic errors. As many points as possible were duplicated to check reproducibility and to increase confidence in the data. Typically, data were accumulated for 2 hours at each angle.

The first experiment at 5.95 MeV produced only the 93.7 and 103.0 keV γ rays. The normalization was produced by detecting the elastic protons with a silicon detector at an angle of 45 degrees (on the side opposite the Ge(Li) detector). A single channel analyzer window was set upon the elastic events. Every tenth pulse from the elastic events was used to trigger a tailpulse generator which was then fed into the detectors preamplifier making possible dead-time and amplifier pile up correction. The pulser peak was placed so as to not interfere with any γ ray peaks. The results of this first run indicated that, to within very small errors, the 93.7 keV transition is isotropic. Although the pulser normalization was included in later runs, it was found that much better consistencies were obtained by using the intensity of the 93.7 keV γ ray as the normalization.

Although the thickness of the target and the density of states above 400 keV of excitation make it difficult to selectively populate levels with an appreciable yield, it is possible to choose energies

of excitation such that very little or no γ-ray feeding from higher lying states is observed. The second angular distribution (E_p = 6.25 MeV) populated the levels up to 612.5 keV with very little feeding from higher states to this last level. No serious perturbations were produced by the three possible weak γ rays which could feed lower levels. The experiment with the third beam energy (E_p = 6.65 MeV) produced angular distributions from an additional five levels, none of which could be gamma fed from above.

The final experiment was performed at an excitation higher than the highest known state (1481 keV) in ^{116}Sb producing an additional set of levels not known to be gamma fed from above.

Peak intensities were derived from the peak fitting program SAMPO[15], and fit to the equation

$$W(\theta) = A_0(1+A_2^*P_2(\cos\theta)+A_4^*P_4(\cos\theta))$$

using the least squares fitting computer code GADFIT[20]. The parameters extracted from the fit are A_0 (the intensity integrated over all solid angles), A_2^*, and A_4^*. The A_2^* and A_4^*'s measured are found in Tables IV-10 through IV-12.

The angular distribution data were analyzed using the modified MANDY[8] program described in Section IV-A. For each γ ray, 180 values of the gamma ray multipole mixing ratio (δ) for $0 \leq J_3\text{-}2 \leq J_2 \leq J_3+2$ for both positive and negative parity were calculated. The differences obtained between the positive and negative parity values are smaller than the experimental errors. The experimental values for A_2^* and A_4^* were entered into the program which calculated the limits of δ for each δ ellipse

Table IV-10. Results of angular distribution experiments at 5.95 and 6.25 MeV.

E_p (MeV)	E (keV)	A_2^*	A_4^*	δ
5.95	93.7	-0.002±0.025	-0.015±0.038	a
	103.0	-0.065±0.013	0.003±0.020	$0.00<\delta<0.11$
6.25	103.0	-0.065±0.010	0.018±0.014	$\delta=0.07$[b]
	108.5	-0.017±0.115	0.076±0.168	$0.40<\delta<5.67$
	307.8	0.542±0.090	0.049±0.131	$0.07<\delta<0.34$
	352.2	-0.26-±0.034	0.022±0.047	$-0.03<\delta<0.07$
	363.0	-0.287±0.027	0.035±0.037	$-0.02<\delta<0.03$
	410.9	0.641±0.019	0.086±0.027	$0.67<\delta<0.78$
	424.2	-0.254±0.031	0.012±0.043	$-0.31<\delta<-0.07$
	455.2	0.300±0.066	-0.082±0.096	$-0.14<\delta<0.14$
	480.6	-0.283±0.068	0.036±0.095	$-2.36<\delta<-0.02$
	518.0	-0.176±0.030	-0.023±0.040	$0.21<\delta<0.47$
	550.9	-0.173±0.070	0.027±0.099	$0.03<\delta<0.81$
	574.5	-0.214±0.148	0.133±0.210	$-3.27<\delta<-0.11$

[a] The 93.7 keV γ ray loses its angular correlation due to its long lifetime.

[b] No error limits were computed as the ellipse did not pass through the data box. δ was assigned by the closest point on the ellipse.

Table IV-11. Results of angular distribution measurements with E_p = 6.65 MeV.

E_γ(keV)	A_2^*	A_4^*	δ
92.2	-0.373±0.054	-0.089±0.070	δ=-0.03[a]
103.0	-0.044±0.005	0.001±0.007	0.02<δ<0.09
108.5	0.013±0.030	0.028±0.043	-0.11<δ<0.02
157.2&157.4	-0.214±0.034[b]	-0.044±0.049[b]	0.02<δ<0.09[b]
208.1	-0.376±0.095	-0.086±0.125	-0.12<δ<2.05
307.8	0.458±0.016	-0.032±0.022	0.11<δ<0.18
352.2	-0.218±0.032	0.044±0.045	-0.09<δ<0.00
363.0	-0.272±0.021	0.043±0.029	δ=-0.02[a]
366.8	-0.017±0.031[c]	-0.040±0.051[c]	δ=0.23 or -9.52[a,c]
404.2	-0.046±0.029	-0.014±0.041	-0.09<δ<0.02
410.9	0.563±0.011	0.008±0.016	δ=0.73[a]
424.2	-0.178±0.004	-0.001±0.005	-0.11<δ<-0.07
455.2	0.225±0.023	-0.024±0.033	-0.02<δ<0.18
457.2	-0.230±0.014	-0.010±0.020	-0.27<δ<-0.14
466.0	0.221±0.020	-0.171±0.030	δ=-0.11 or 1.80[a]
480.6	-0.208±0.006[b]	-0.013±0.008[b]	δ=-0.14[a,b]
518.0	-0.206±0.027	-0.018±0.039	0.34<δ<0.81
550.9	-0.168±0.008[b]	0.010±0.012[b]	0.34<δ<0.42[b]
574.5	-0.074±0.020	0.050±0.029	δ=-11.43 or 0.11[a]
628.7	-0.006±0.014	-0.020±0.020	-0.23<δ<0.29
637.9	-0.065±0.024	-0.038±0.035	δ=-0.97[a]
712.0	-0.230±0.023	-0.037±0.033	0.02<δ<0.07
778.5	-0.420±0.021	-0.017±0.029	-0.12<δ<-0.05

[a]No error limits were computed as the ellipse did not pass through the data box. δ was assigned by the closest point on the ellipse.

[b]These data are a composite from an unresolved doublet.

[c]The ellipse for these J_2 values lie entirely within the data box.

Table IV-12. Results of the angular distribution at E_p = 7.32 MeV

E_γ(keV)	A_2^*	A_4^*	δ
92.2	-0.208±0.063	-0.045±0.079	-0.03<δ<0.11
103.0	-0.034±0.005	0.005±0.006	0.02<δ<0.09
108.5	-0.037±0.024	-0.003±0.035	-0.11<δ<0.19
157.2+157.4	-0.163±0.015[a]	-0.004±0.021[a]	a
180.9	-0.100±0.034	-0.054±0.044	δ=1.38[b]
208.1	-0.268±0.041	-0.117±0.059	δ=0.00[b]
294.1	-0.374±0.051	0.084±0.079	-0.14<δ<-0.03
307.7	0.194±0.019	-0.083±0.023	-0.12<δ<-0.03
338.1	0.523±0.100[a]	-0.224±0.138[a]	a
352.2	-0.182±0.016	-0.008±0.022	-0.19<δ<-0.07
363.0	-0.179±0.011	-0.009±0.014	-0.05<δ<0.02
366.8	-0.044±0.016	-0.037±0.021	δ=1.38[b]
395.6	-0.049±0.018	0.004±0.022	0.09<δ<0.21
404.2	0.072±0.109	-0.047±0.140	-0.55<δ<0.05
410.9	0.471±0.008	0.028±0.010	δ=1.00[b]
424.2	-0.109±0.007	0.002±0.008	-0.05<δ<0.02
432.6	0.489±0.084	0.315±0.106	c
455.2	0.166±0.017	-0.006±0.021	0.07<δ<1.19
457.2	-0.160±0.019	-0.017±0.024	-0.23<δ<-0.07
466.0	0.111±0.019	-0.033±0.025	δ=-0.18 or 14.30[b]
470.6+471.4	-0.234±0.178[a]	-0.460±0.218[a]	a
480.6	-0.157±0.008[a]	0.021±0.011[a]	a
550.9	-0.156±0.012[a]	0.009±0.015[a]	a
574.4	-0.177±0.070	-0.025±0.091	-14.30<δ<0.12
590.1	-0.177±0.070	-0.138±0.092	c
621.5	0.280±0.256	0.264±0.270	c
628.7	0.093±0.053	0.027±0.070	-0.38<δ<-0.31
637.9	-0.030±0.051	0.028±0.064	0.31<δ<3.73
653.9	-0.053±0.079[a]	0.157±0.102[a]	a

Table IV-12. Continued.

E_γ(keV)	A_2^*	A_4^*	δ
705.0	-0.105±0.026	0.106±0.036	$-0.02<\delta<0.05$
712.0	-0.200±0.022	0.025±0.031	$\delta=0.12$[b] or $-8.14<\delta<-5.14$
762.1	0.150±0.040	0.018±0.051	$-0.31<\delta<-0.12$
778.5	-0.458±0.062	0.067±0.075	$-2.36<\delta<-1.28$ or $-0.38<\delta<-0.16$
917.7	-0.020±0.035	-0.059±0.047	$\delta=0.60$ or -5.14[b]
1055.3	-0.110±0.034	-0.047±0.045	$\delta=-1.73$[b]

[a]These data were obtained from an unresolved doublet.

[b]No error limits were computed as the ellipse did not pass through the data box.

[c]No determination of δ could be made as the data are of poor quality and inconsistent.

(the loci of δ form an ellipse in A_2^* and A_4^* space) which passed nearer the data point than the errors assigned. Also the program calculated the point on each ellipse nearest to the data point giving the χ^2 per degree of freedom for these points. For each γ ray one plot was produced including the data box (the box formed by the error bars on the data point) and the δ ellipses for negative and positive parity cases for each value of J_2. The input included that used for the excitation function plus one card per gamma ray containing the γ's energy, the level energy, the final state spin (as described in Chapter VII), A_2^*, ΔA_2^* (the error in A_2^*), A_4^*, ΔA_4^*. The spins were chosen using the δ ellipse plots, the χ^2 plots, and the excitation data, plus overall consistency with other levels. Plots of the ellipses and χ^2 can be found in the Appendix and Chapter VII.

V. THE $^{118}Sn(p,3n\gamma)^{116}Sb$ REACTION

^{116}Sb can be studied via the $^{118}Sn(p,3n\gamma)$ reaction. This reaction is of interest because the $(p,n\gamma)$ reaction populates states to spin 3 or 4 with relatively large cross sections and has very little feeding to states with spin 5 and greater. Proton of 30 MeV energy should produce states with twice the angular momentum as the 7.5 MeV protons used in the $(p,n\gamma)$ experiments. Calculations from CS8N[13] indicate that the largest cross section exists for $\ell=6$ for the (p,3n) reaction.

A. Singles

The $^{118}Sn(p,3n\gamma)^{116}Sb$ reaction was performed with a proton beam of 30 MeV obtained from the MSU Cyclotron. The Q-value for this reaction is -21.76 MeV with the Q-value for the 4n reaction being -29.81 MeV. Neutron cross sections were calculated using the program CS8N which indicated that the maximum for the 3n reaction would be at 30 MeV. The target used was a 15 mg/cm^2 enriched foil of ^{118}Sn which was rolled from powdered metallic tin obtained from the Isotopes Division of Oak Ridge National Laboratory. Both a Low Energy Photon Spectrometer (LEPS) and a larger 10.4% Ge(Li) detector were used to accumulate data in the MSU Sigma 7 computer.

The higher spin states were enhanced, as expected, with spin 5 states being approximately 4 times as strong as spin 1 states, as can be seen in Figure V-1.

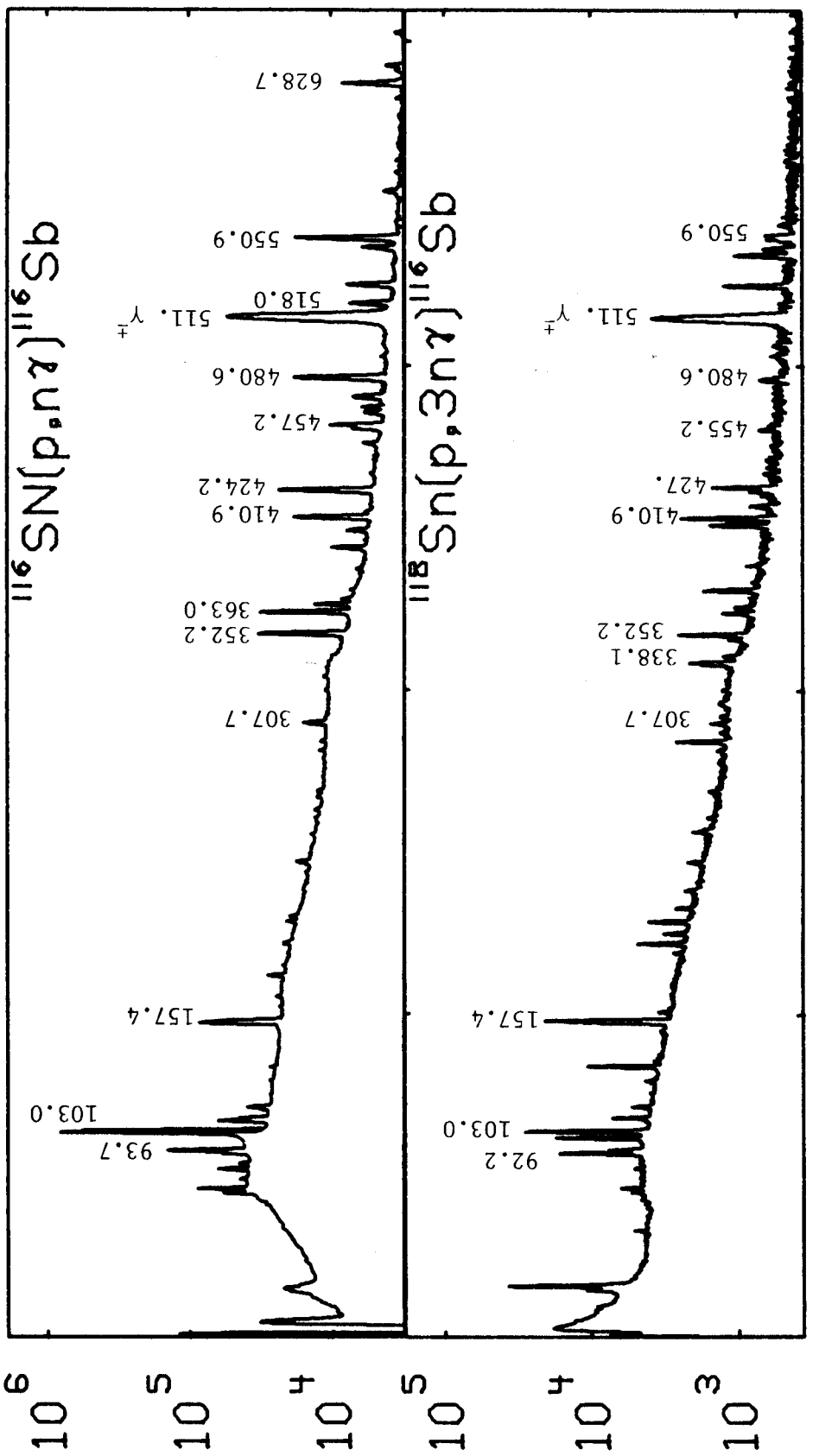

Comparison of singles from (p,nγ) and (p,3nγ) reactions.

Figure V-1

B. Gamma-Gamma Coincidence

The target used was the previously described ^{118}Sn target. The detectors used were an 8% and 9.6% efficient Ge(Li) detector. The detectors were positioned as in Figure III-2 except the beam passed through the block which acted only as a Compton suppressor. The experiment consisted of a typical three parameter fast-slow coincidence arrangement with constant-fraction timing discrimination. The TAC information was preserved along with the energy information for later analysis. Coincidence events were stored as triplets of channel numbers and sorted off-line using weighted background subtraction. Approximately 14×10^6 events were collected over a 2 day period. Although this experiment added little new information to the $(p,n\gamma)$ reaction, it was able to offer more and better information on the cascades among high spin states and corroborate the results of the existing low energy $(p,n\gamma)$ work. Observed coincidences can be found in Table V-1 and the gated spectra for the $(p,3n\gamma)$ coincidence reaction can be found in the Appendix.

Table V-1. Results of three parameter γ-γ coincidence for the $^{118}Sn(p,3n\gamma)^{116}Sb$ reaction

Gated γ ray (keV)	Coincident γ rays (keV)
92.2	224.0, 307.8, 338.1, 410.9
103.0	157.4, 208.1, 216.[a], 307.8, 352.2, 363.0, 550.9
157.2 & 157.4	103.0, 208.1, 352.2, 455.2, 457.2, 550.9
208.1	103.0, 157.4, 352.2, 380.
224.0	338.1, 410.9
307.8	103.0
338.1	92.2, 224.0, 410.9, 546.2[a]
352.2	103.0, 157.4, 208.1, 426.3[a]
363.0	103.0, 157.2
410.9	92.2, 224.0, 338.1
424.2	480.6
426.3[a]	352.2, 455.2, 546.2[a]
455.2	157.4, 208.1
550.9	103.0, 157.2, 338.1

[a]These gamma rays seem to be in coincidence with the ^{116}Sb γ rays but were not placed within the present level scheme.

VI. EVENT RECOVERY

As a part of these and other gamma-ray spectroscopy studies a large amount of gamma-gamma-time coincidence data have been taken, both two and three-dimensional. Because of large coincidence counting rates which can be obtained in experimental in-beam studies with nuclei containing rotational structure and the large number of transitions involved in odd-odd nuclei, we have, upon occasion, found the need to record and subsequently recover from 50 to 70 million events. With the present computing facilities, the limitation on recovery is the amount of core required to contain the spectra. If the core requirements become too large, it becomes necessary to store pages of core temporarily on the disk. The swap time becomes prohibitively large with a small increase in program size and consequently the data recovery was often very cumbersome and time consuming.

Since a large fraction of the time needed to recover a tape was consumed in reading, as opposed to sorting, the total time would be greatly reduced by reading the tape once and doing all the sorting at the same time. This cannot be implemented because of the finite size of core memory, so it was decided to copy from tape to disk storage and sort it from there with the limit of 12 gates per pass through the disk file. Storage of the entire tape on disk would require about 5×10^6 words of temporary storage, which is almost never available, therefore, the data needed to be reduced to the smallest possible subset as they were transferred to disk. This is accomplished in two ways. First, if the data are 3 parameter, the TAC half words are gated immediately using a TAC gate common to all energy gates. The

TAC information is reduced to one bit of information which is set to indicate background and not set to indicate a peak channel. The second method is to immediately throw away any event whose gating side does not appear within a gate. This method requires that gates be recovered from only one energy axis at a time. A rather arbitrary limit of 12 gates sorted simultaneously was imposed, making necessary multiple sorts from file. To ensure minimum time requirements the gates are sorted into ten nonoverlapping sets, making possible a maximum of 120 gates for one pass through the tape. An array corresponding to the range of channel numbers is set up such that the channels not used contain a zero and those that are used contain a number from 1 to 10 corresponding to the set which contains the gate. The data are then presorted into ten files using the set number as a file number (with zeros being thrown away). At the same time, if necessary, the half-words are swapped to insure the gated side appears first, removing the need to check again. Each file is then read in turn and sorted as in earlier programs (with weighted background subtraction for both TAC and energy gates) with the data being punched at the end of each file and the core being available for the next set of spectra. A block diagram of the program appears in Figures VI-1 and VI-2.

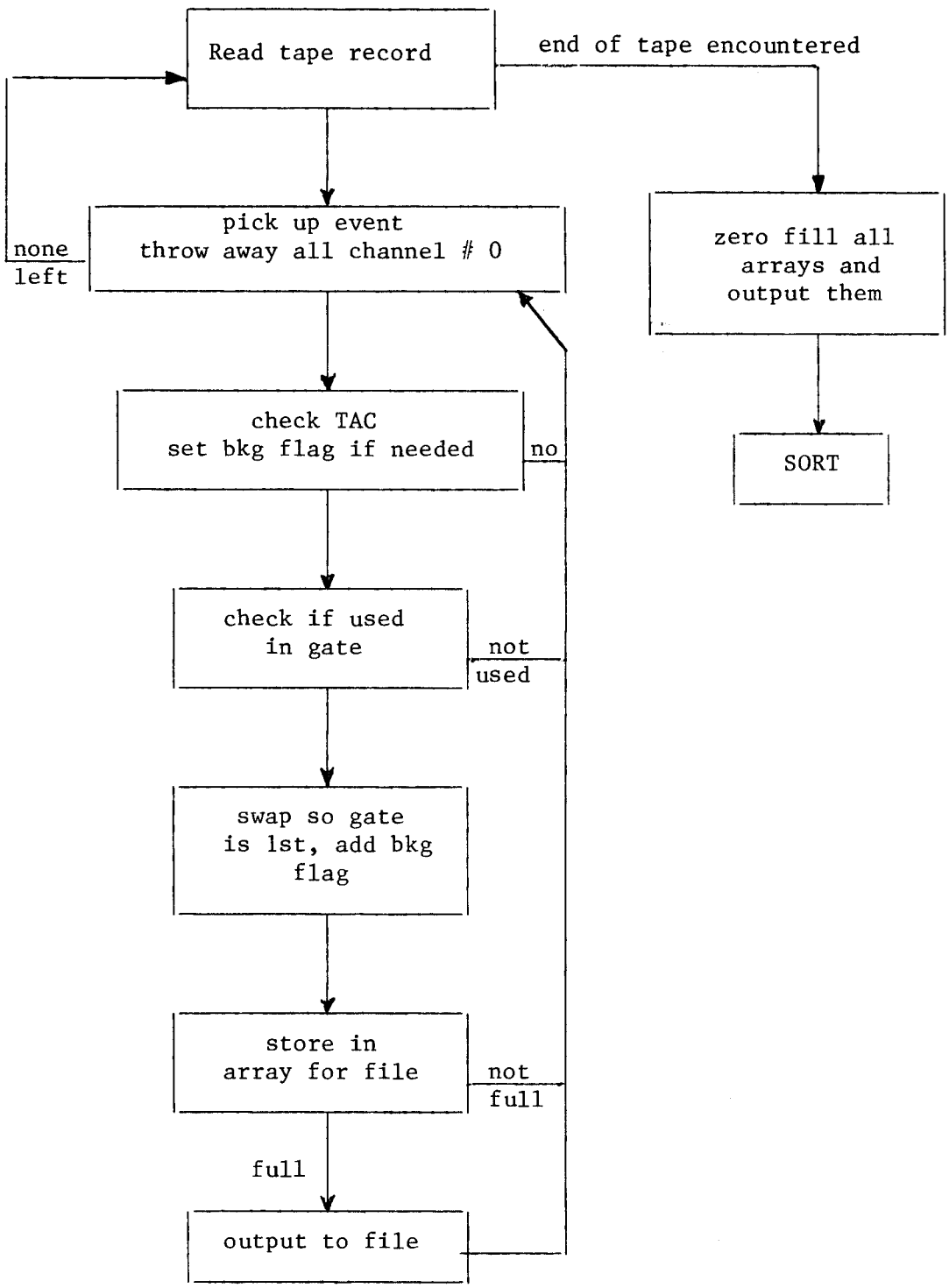

Tape reading routine in EVENT RECOVERY.

Figure VI-1.

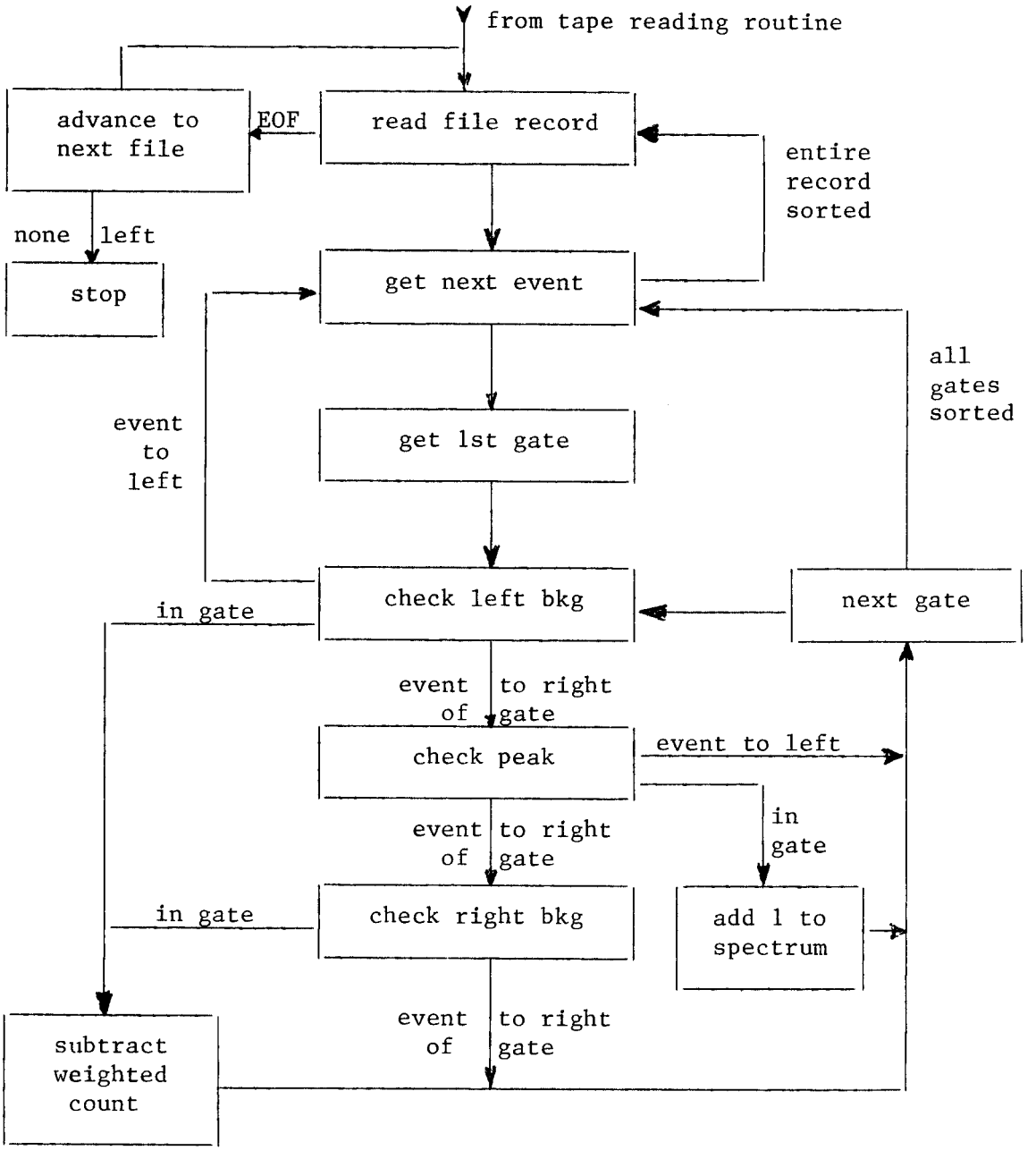

Sorting routine in EVENT RECOVERY.

Figure VI-2.

VII. DISCUSSION OF INDIVIDUAL LEVELS

Except for the ground state, all spin and parity assignments to the states of ^{116}Sb as shown in Figure IV-4 are based upon the present work. First, using the results of the electron capture decay of ^{116}Te reported in Chapter III, the spin and parity assignments were made to the 93.7, 731.6, 919.7, and 1158.3 keV levels. The assignments for the other levels were made based upon the in-beam studies. The γ-ray angular distributions were used in conjunction with theoretical predictions of MANDY to obtain the spin assignments, often giving unambiguous choices. Where an ambiguity remains, experimentally determined cross-section ratios (described in Chapter IV) were compared with theoretical predictions of MANDY. These were particularly useful when the state in question was of spin 4 or greater. In cases where more than one choice remains, the multipolarities of the γ rays are examined for reasonable and consistent values. The parities of the states are based upon the beta decay or conversion electrons.

Delta ellipse and χ^2 plots are shown for those γ rays for which angular distributions were measured. Energies for level excitation, gamma ray energy, and proton beam energy are listed along with the spin of the state produced by the gamma-ray transition. Spins shown on the different ellipses and χ^2 plots are the possible values for the particular state in question. The dotted line on the χ^2 plots corresponds to a circle which passes through the corners of the data box and is given as a reference to indicate which spin may be the better choice, but is not meant to be a stringent criterion for the

choice of a given spin. It is assumed, except for the 93.7 keV state, that all states de-excite rapidly enough that there is very little if any perturbation of the directional correlations.

A. Ground State $J^{\pi} = 3^{+}$

The ground state spin is not measured in this experiment but is important because it is a basic starting point for use as the final spin (J_3) in MANDY[11]. The ground state J^{π} has been previously determined to be 3^{+} by the atomic-beam magnetic resonance method[6], and inference from the log ft data for its electron capture decay to states in ^{116}Sn. The results of the present beta decay and in-beam gamma-ray work are consistent with this assignment.

B. $E_x = 93.7$ keV $J^{\pi} = 1^{+}$

The 93.7 keV state has a half life longer than approximately 0.2 μsec. This long lifetime causes the 93.7 keV gamma ray to have an isotropic angular distribution. A very careful measurement of the angular distribution of this γ ray at an excitation of about 400 keV confirmed that this is indeed the case as indicated in Table IV-6. The internal conversion work of Fink et al.[5] has shown the 93.7 keV γ ray to be an E2 transition ($\alpha_K = 1.52$). Log ft measurements from the beta decay of ^{116}Te also confirm that this level has $J^{\pi} = 1^{+}$.

C. E_x = 103.0 keV $J^\pi = 2^+$

Previous internal conversion electron measurements and gamma ray work by Rahmouni[18] gave a K internal conversion coefficient of 0.20±0.02 for the 103.0 keV γ ray, which suggests that the transition may be E1. When intensities derived from the current electron capture decay work are used for the 93.7 and 103.0 keV γ rays and Rahmouni's values are used for electron intensities (α_K = 1.52 for the 93.7 keV γ ray), a value for α_K (103.0) of 0.67±0.07 is calculated. Values from Hager and Seltzer[19] are 0.153 for E1 and 0.503 for M1, therefore the multipolarity must be M1 yielding possible values of 2^+ and 4^+ for the 103.0 keV state, of which the spin 4 can be eliminated by the excitation function data shown in Figure VII-1. Angular distribution data in Figure VII-2 provide us with a mixing ratio of δ = 0.05±0.06 which indicates that the 103.0 keV γ ray is nearly 100% M1.

D. E_x = 410.9 keV $J^\pi = 4^+$

The 410.9 keV level is depopulated by two transitions both of which have a large positive A_2^* (Figure VII-3). For the 307.8 keV gamma ray both the 3 and 4 values are likely. For the more intense 410.9 keV gamma ray, as shown in Figure VII-3, the values for the spin are more likely to be 4 or 5. The J = 5 value can be eliminated as that would require the 307.8 keV gamma ray to be 6% M3 and 94% E4 which is very unlikely since this transition is not delayed by the amount expected for such a high multipolarity. The positive parity can be assigned on the basis that the observed mixing (δ = 0.73)

Figure VII-1

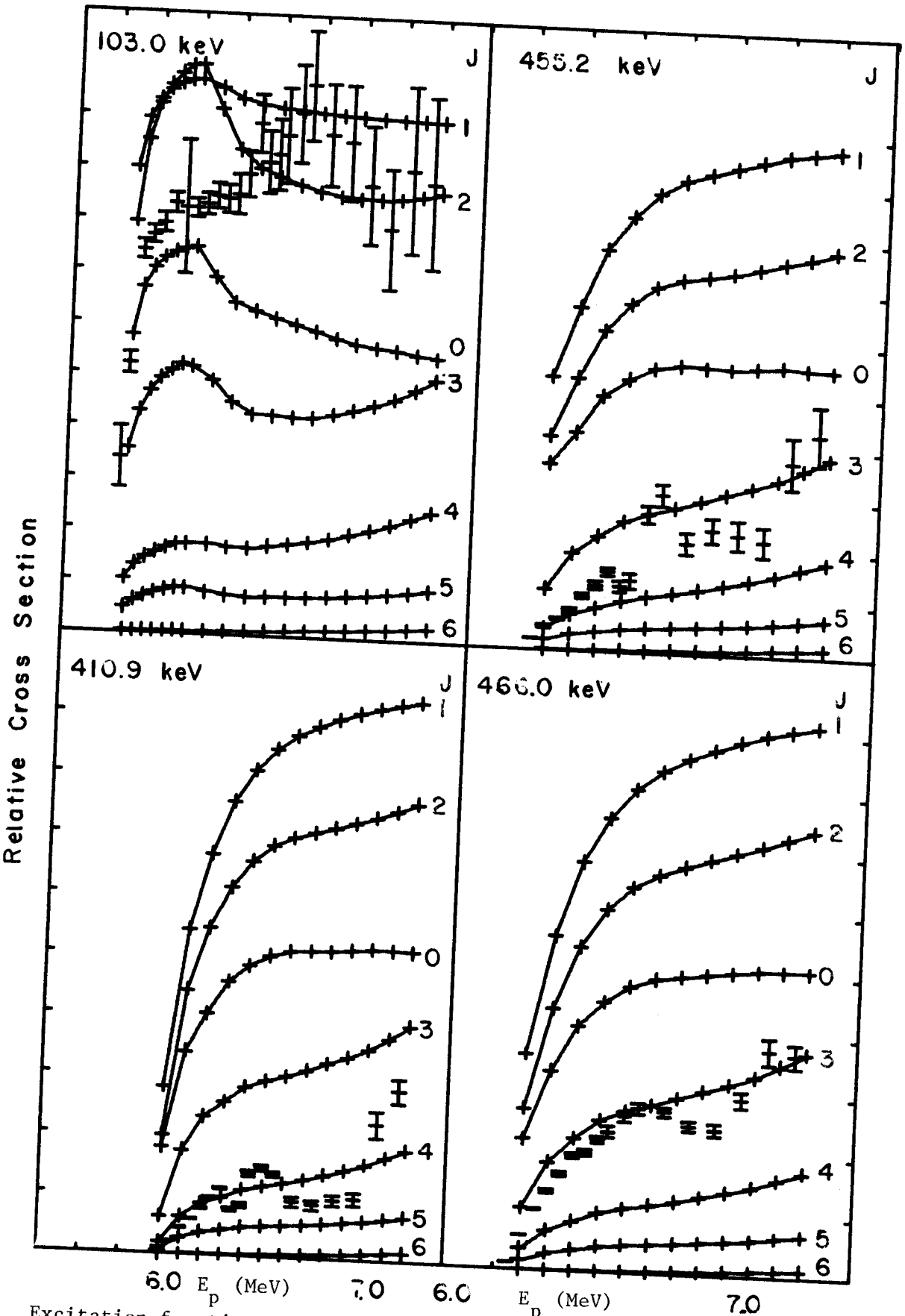

Excitation functions for 103.0, 410.9, 455.2, and 466.0 keV levels.

Figure VII-2.

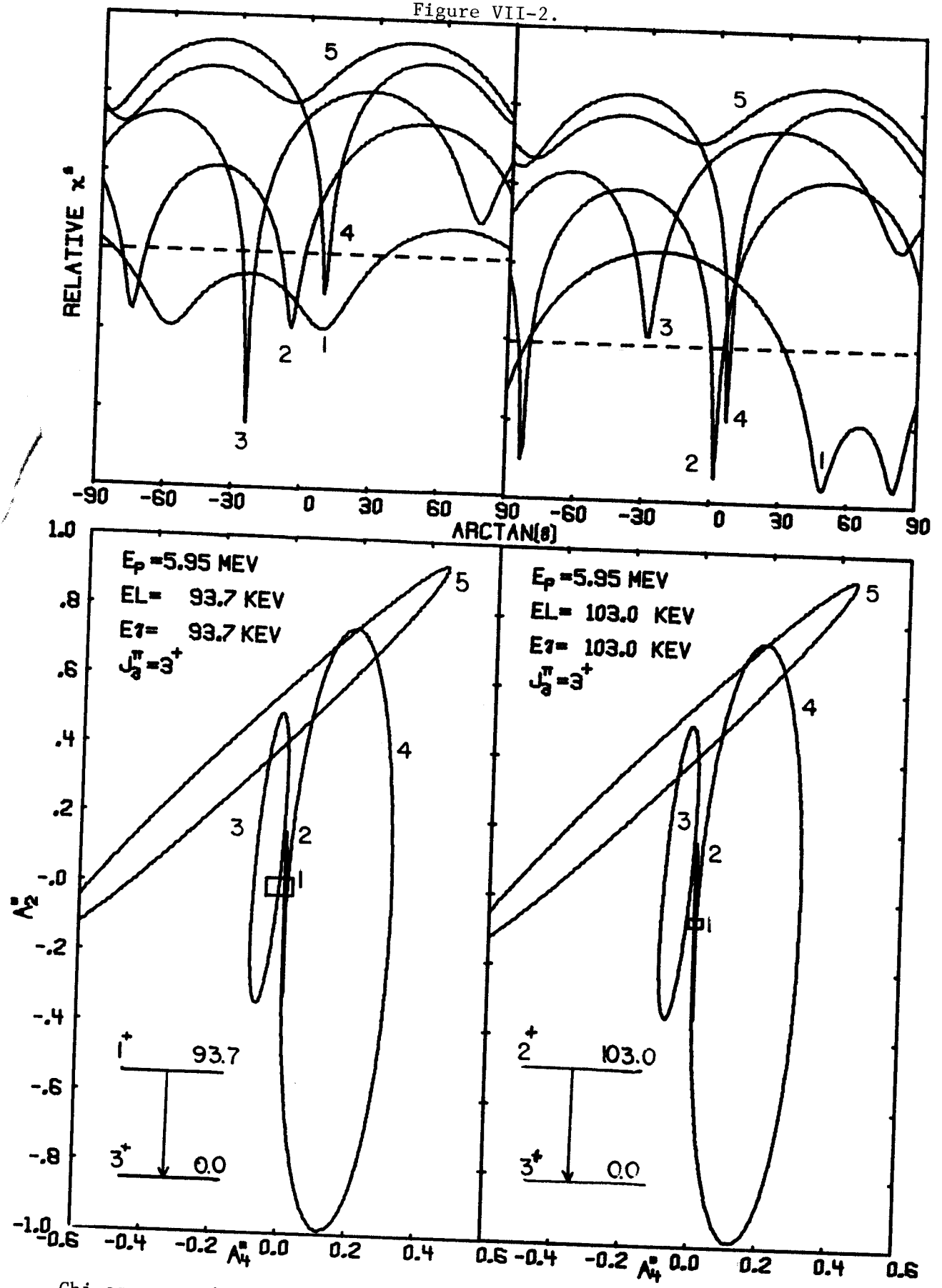

Chi square and delta ellipse plots for the 93.7 and 103.0 keV gamma rays.

Figure VII-3.

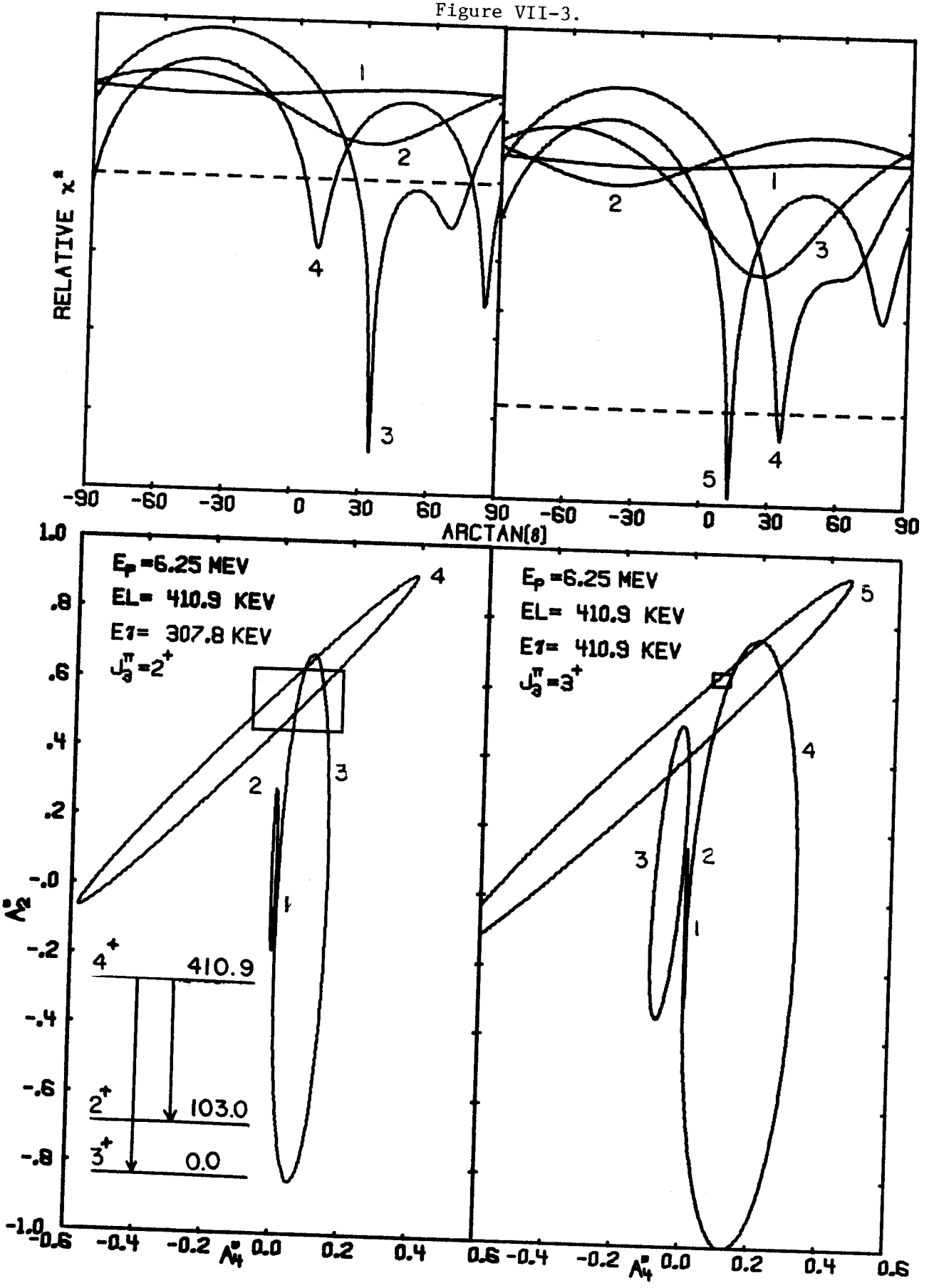

Chi square and delta ellipse plots for the 307.8 and 410.9 keV gamma rays.

for the 410.9 keV γ ray would be expected to be highly unlikely for E1 and M2 transitions, which would be required for a negative parity assignment.

Comparison with theoretical estimates of single particle transition rates for γ-ray de-excitation indicate that the M1 component of the 410.9 keV γ ray is hindered by a factor of approximately 1600 relative to that of the E2 component.

E. E_x = 455.2 keV J = 3

An unambiguous assignment can be made for J = 3 for this level. The γ-ray angular distribution for the 352.2 keV γ ray has a fairly large negative A_2^* which places it on the J = 3 ellipse (Figure VII-4) and far from the other ellipses, except for that for J = 2, however. A spin 2 can be eliminated by the excitation function data which is shown in Figure VII-1. The value for δ gives 96% E1 (M1) and 4% M2 (E2) for the 352.2 keV γ ray. The other branch (455.2 keV gamma ray) was somewhat weaker and more difficult to analyze, however, there exists a minimum in χ^2 for J = 3 giving 100% E1 (M1).

A half life of 1.85±0.06 nsec was measured for this state as described in Chapter IV Section C. This indicates either a ℓ-forbidden M1 or E1. Seven states lie above the 455.2 keV state which de-excite through cascades which terminate on the 455.2 keV state and bypass other states. This possibly indicates a difference between the character of these eight states and the other excited states. It is felt that the most plausible difference is that these states are negative parity states constructed from the neutron orbital $h_{11/2}$.

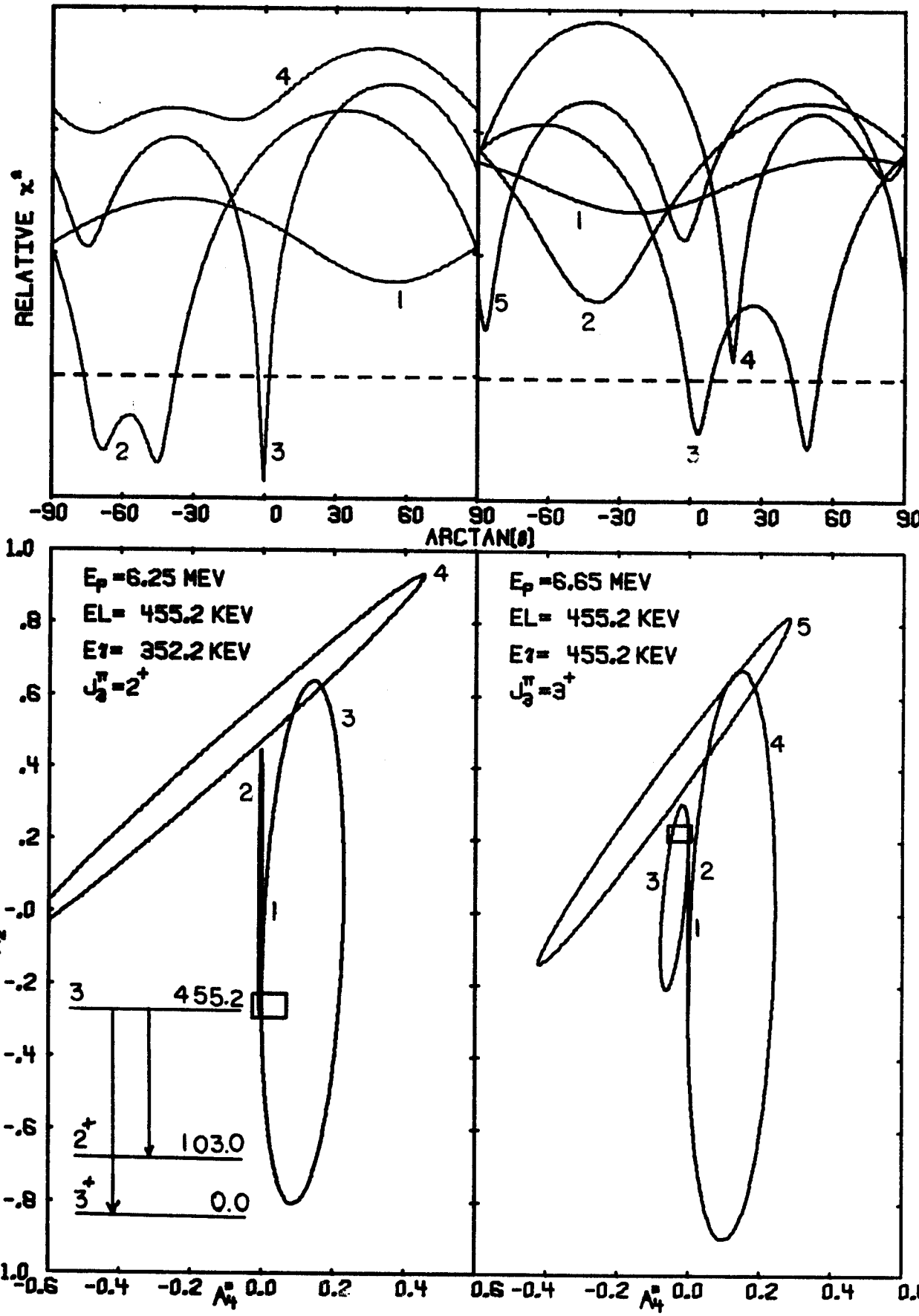

Chi square and delta ellipse plots for the 352.2 and 455.2 keV gamma rays.

Figure VII-4.

The 455.2 keV branch is hindered by a factor approximately 9.8 relative to the 352.2 keV branch compared to what would be expected from the branching ratio based upon Weisskopf single particle estimates.

F. E_x = 466.0 keV J = 3

The 466.0 keV state also exhibits the behavior of the angular distribution for the 363.0 keV γ ray, the most intense branch, having a relatively large negative A_2^* giving an unambiguous choice of J = 3 as shown in Figure VII-5. The 466.0 keV γ ray is too weak to be of any value in the determination of J from its angular distribution data. Our excitation data (Figure VII-1) give a very good fit for J = 3.

The 466.0 keV branch is hindered by a factor of 17.1 relative to the 363.0 keV branch (assuming that the 466.0 keV γ ray is 100% M1) as compared to what would be expected from Weisskopf single particle estimates.

G. E_x = 503.1 keV J = 5

The 503.1 keV level depopulates via the 92.2 keV γ ray, which cannot be resolved from the 93.7 keV γ ray at low excitations. Figure VII-5 shows that the angular distributions are inconclusive, possibly allowing values of 3, 4, and 5 for J. However the data from the excitation function give a reasonably good fit to the calculated values for J = 5 as shown in Figure VII-6.

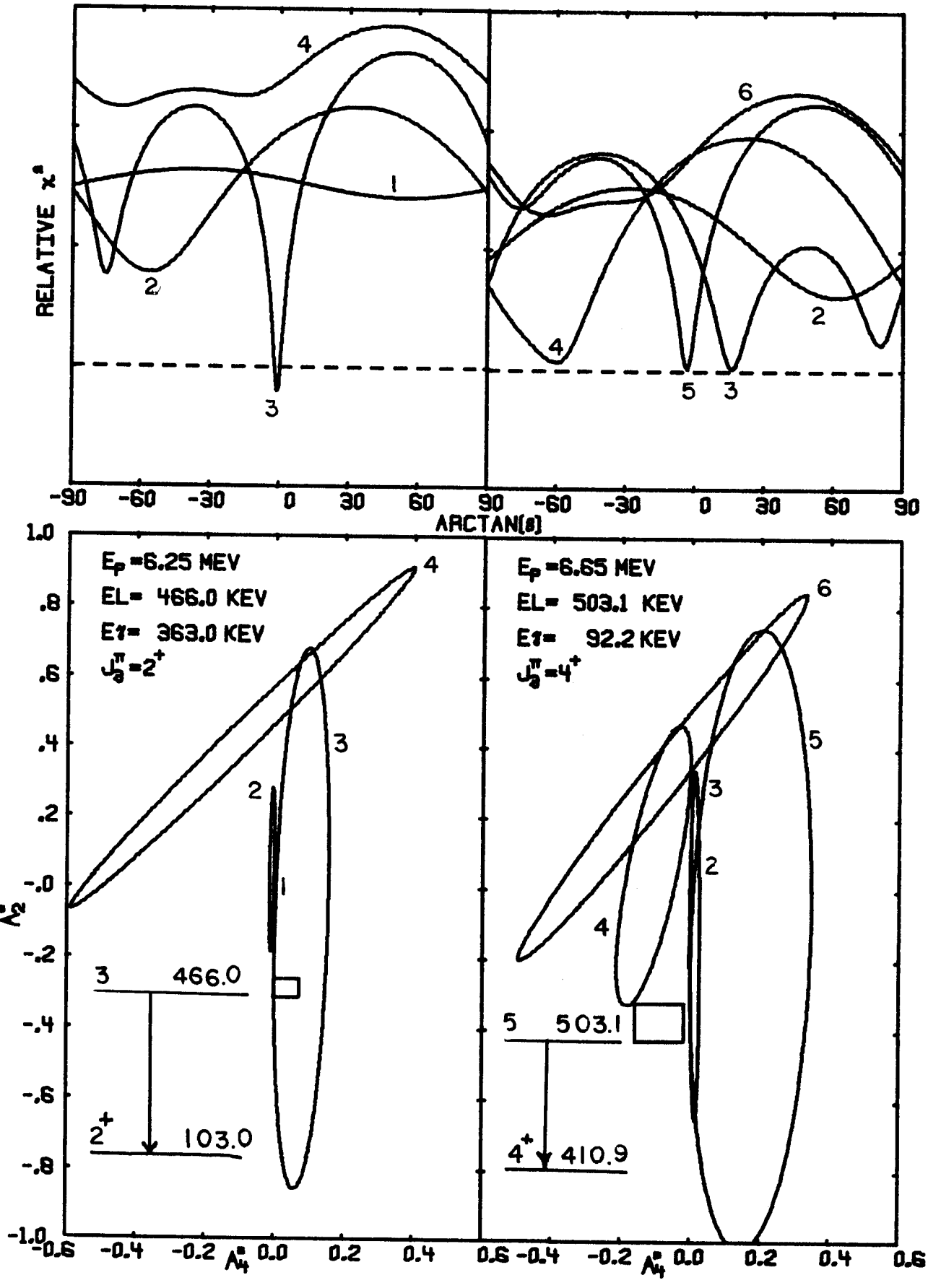

Chi square and delta ellipse plots for the 363.0 and 92.2 keV gamma rays.

Figure VII-5.

Figure VII-6

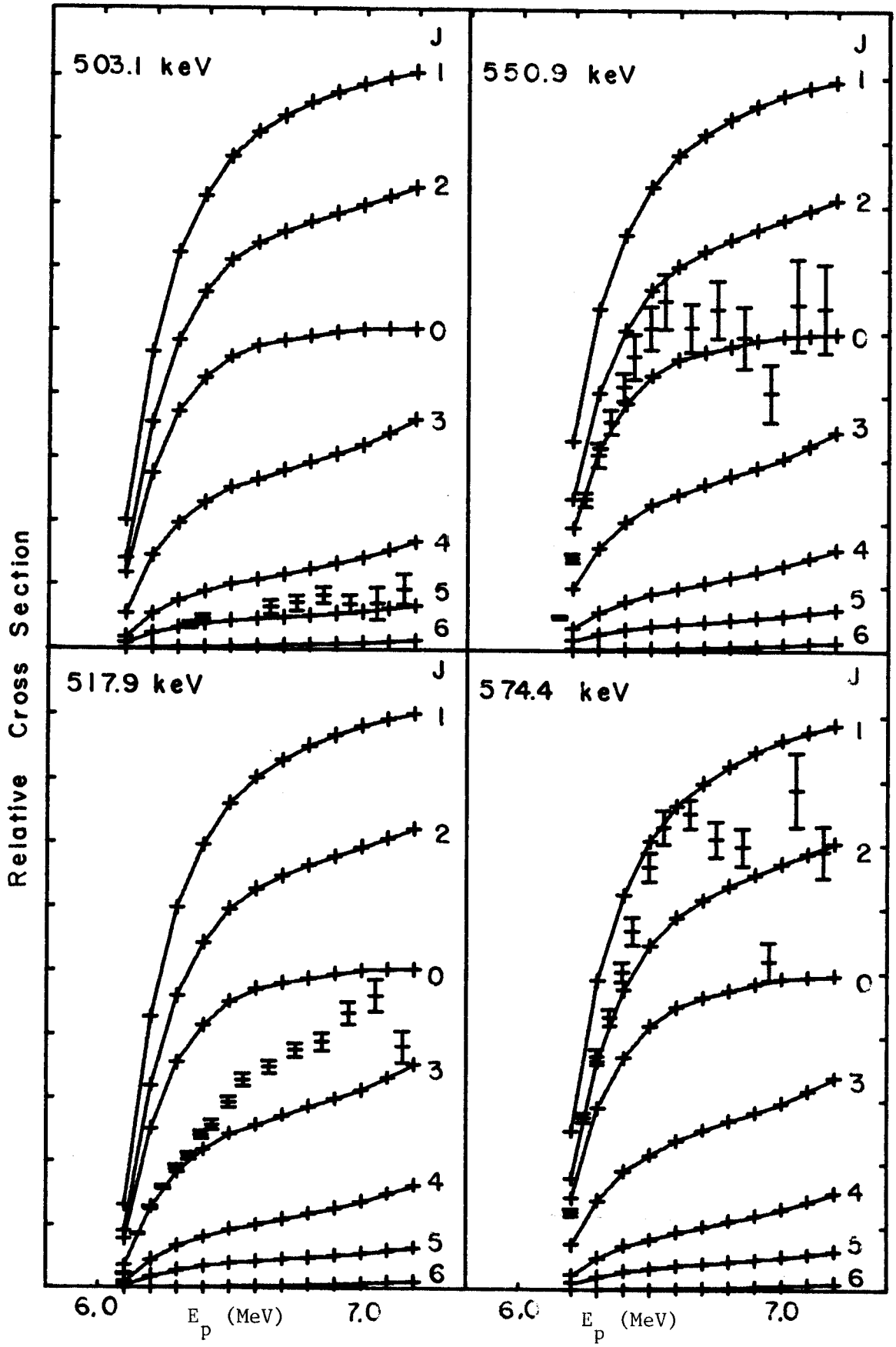

Excitation functions for the 503.1, 517.9, 550.9, and 574.4 keV levels.

H. E_x = 517.9 keV J = 2

The 424.2 keV branch from the 517.9 keV state has a large negative A_2^* (Figure VII-7) which allows an assignment of J = 2. The 518.0 keV γ ray is somewhat weaker and overlaps some with the 511 keV annihilation gamma peak. The data for this gamma ray, as shown in Figure VII-7, allows J = 2,3,4. Excitation function data (Figure VII-6) indicate that this state has a higher cross section than calculated for J = 3 or 4 but not quite enough for J = 2. It is felt that the measured values are, however, a good indication of J = 2. Thus, a spin assignment of 2 for the 517.9 keV level can be justified.

I. E_x = 550.9 keV J = 2

Three transitions depopulate the 550.9 keV state, of which two (457.2 and 550.9 keV) give useful angular distributions. The 550.9 keV γ ray at an excitation of approximately 700 keV is relatively free of contamination by a γ ray of the same energy from a level at 654.1 keV. The fit to theory indicates possible values of J = 2, 3, and 4 (Figure VII-8). The 457.2 keV γ ray is too weak for analysis at this excitation but an an excitation of approximately 1.1 MeV it has an excellent fit to J = 2 as shown in Figure VII-8. Excitation function data, Figure VII-6, show that this level is characteristic of J = 2. Also the depopulation of this state is to three different states having J values of 1, 2, and 3. Therefore, it is felt that J = 2 is the best choice for the spin for the 550.9 keV state.

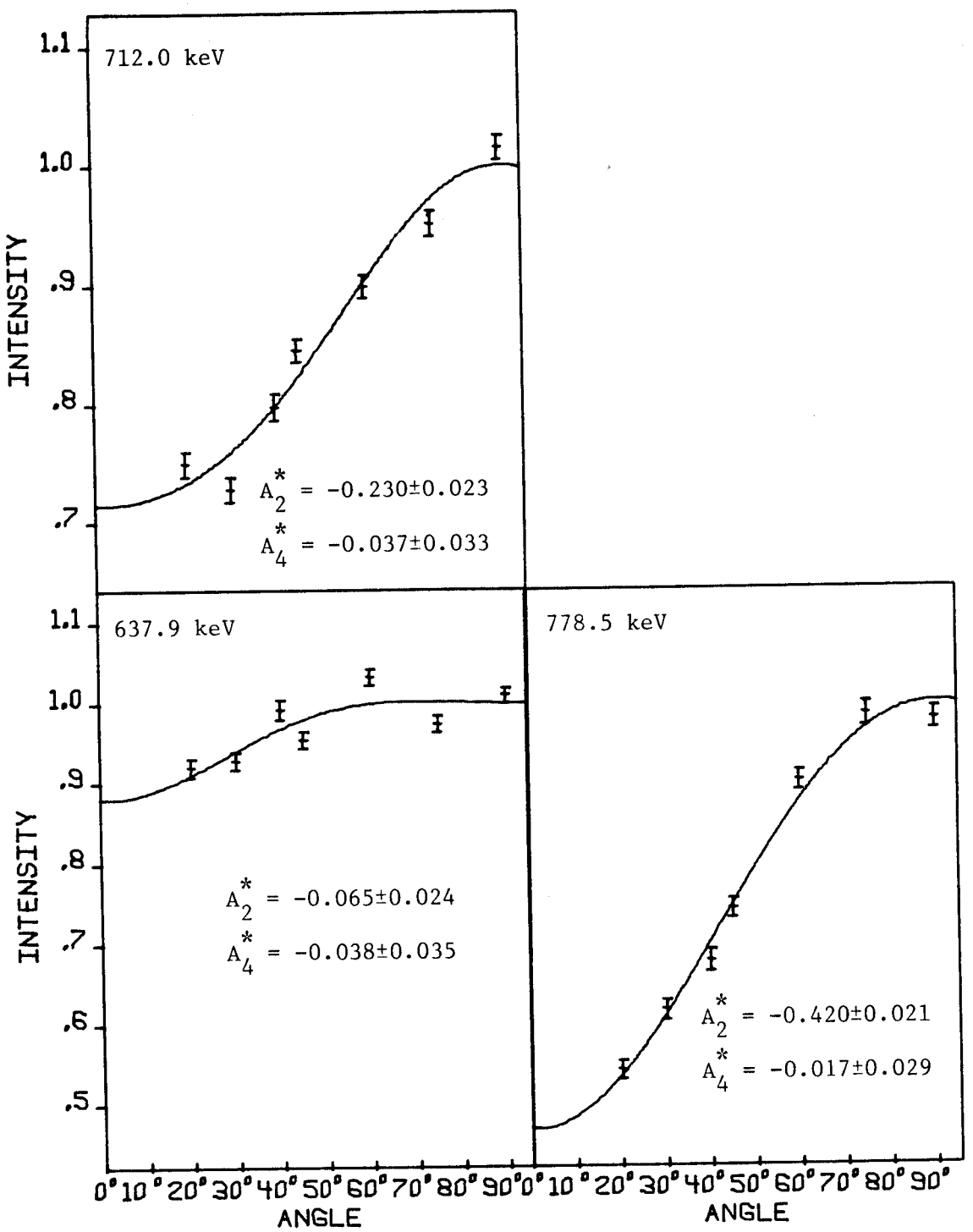

Figure C-3 continued.

Figure C-4. Gamma-ray angular distributions from the $^{116}Sn(p,n\gamma)^{116}Sb$ reaction at 7.32 MeV. The data are normalized to the isotropic 93.7 keV γ ray.

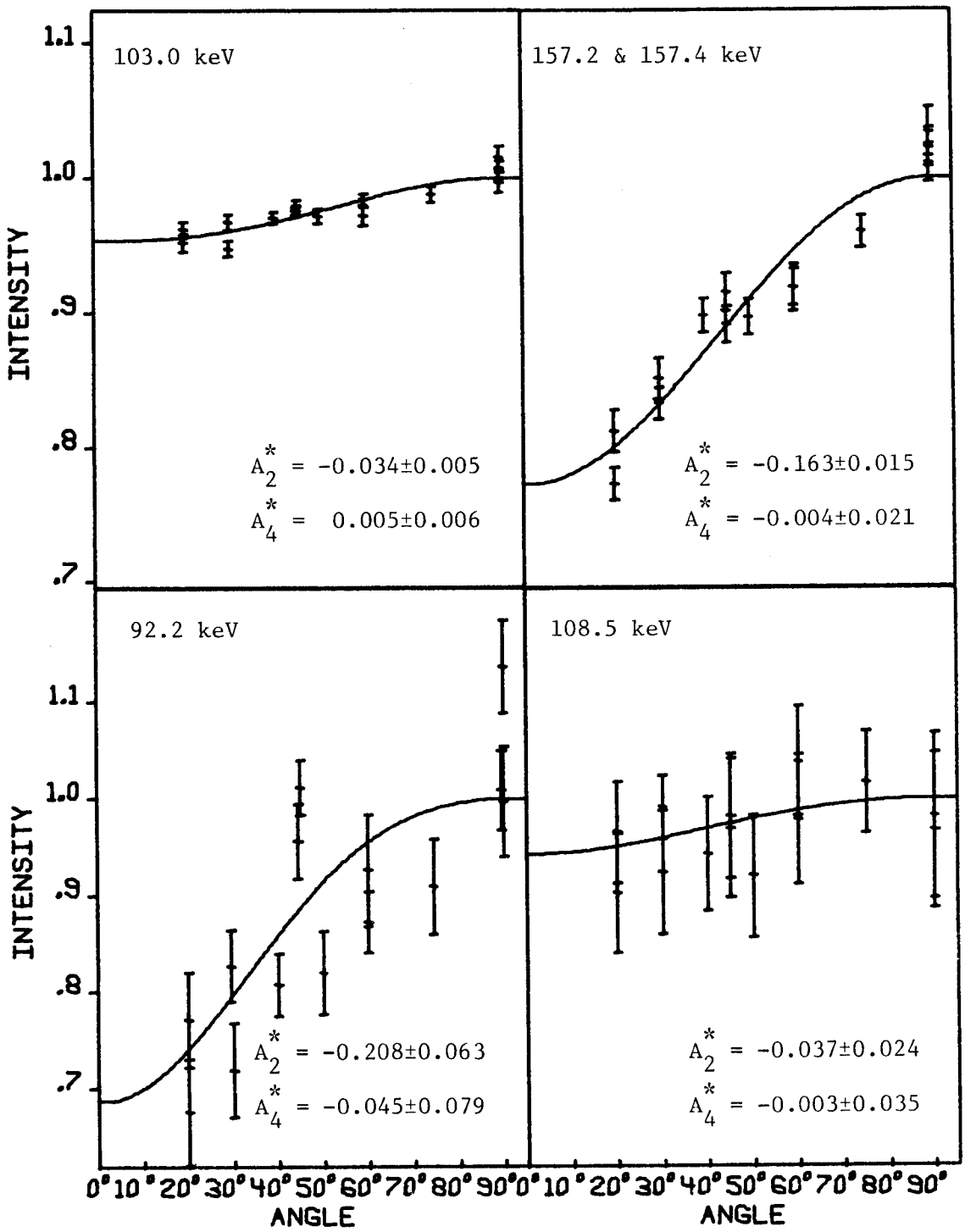
103.0 keV
157.2 & 157.4 keV
92.2 keV
108.5 keV
$A_2^* = -0.034 \pm 0.005$
$A_4^* = 0.005 \pm 0.006$
$A_2^* = -0.163 \pm 0.015$
$A_4^* = -0.004 \pm 0.021$
$A_2^* = -0.208 \pm 0.063$
$A_4^* = -0.045 \pm 0.079$
$A_2^* = -0.037 \pm 0.024$
$A_4^* = -0.003 \pm 0.035$
INTENSITY
INTENSITY
1.1
1.0
.9
.8
.7
0° 10° 20° 30° 40° 50° 60° 70° 80° 90°
0° 10° 20° 30° 40° 50° 60° 70° 80° 90°
ANGLE
ANGLE

Figure C-4.

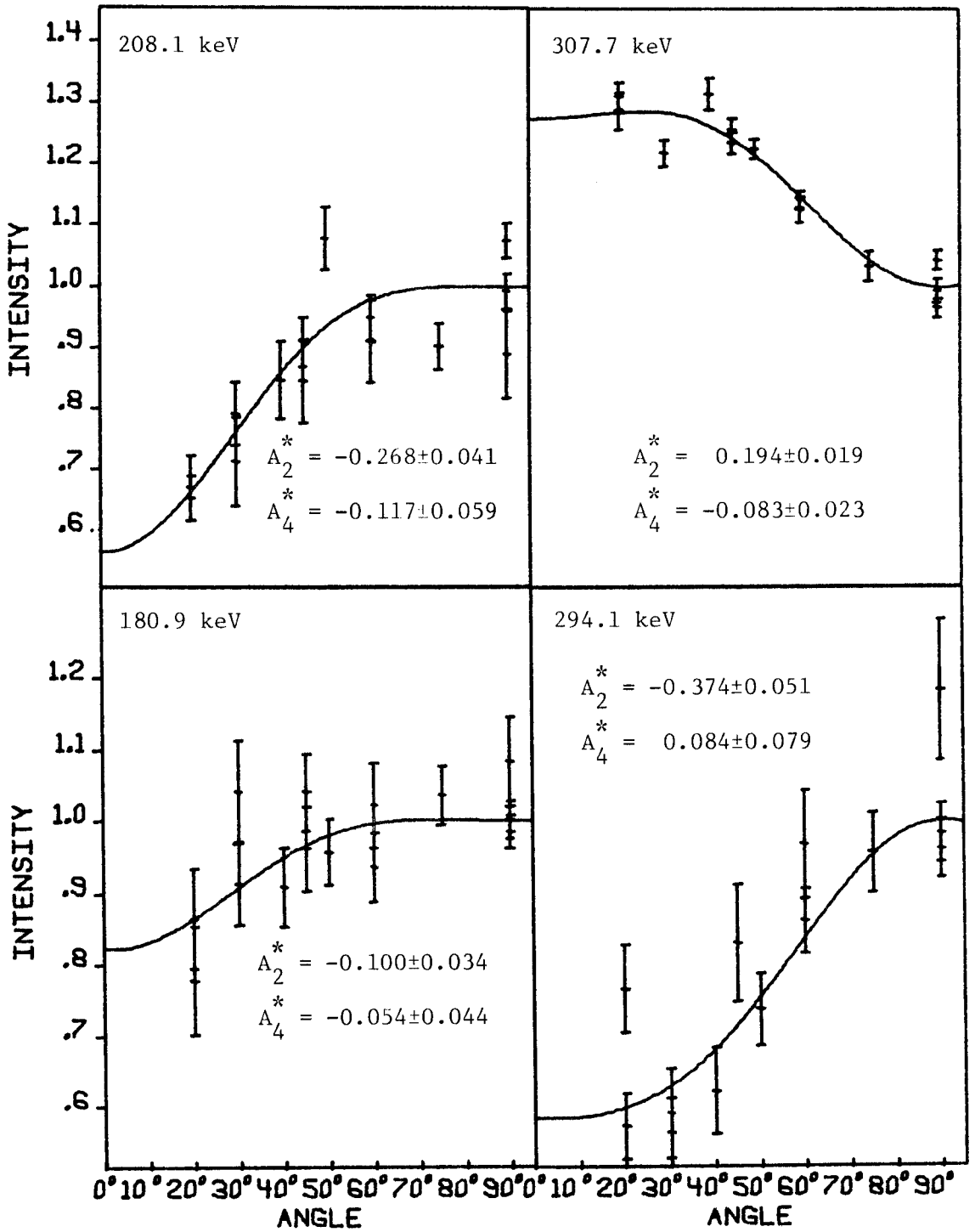

Figure C-4 continued.

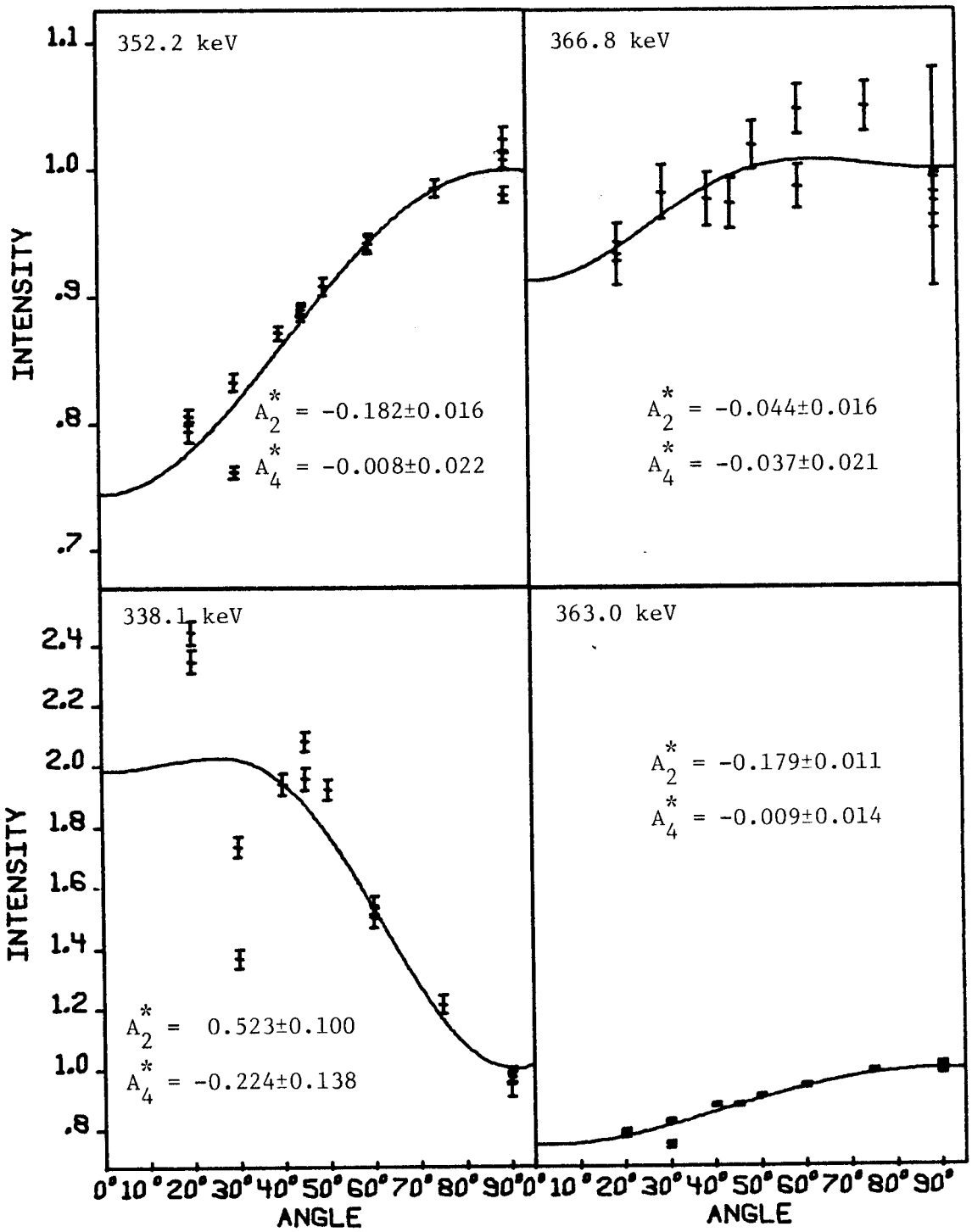

Figure C-4 continued.

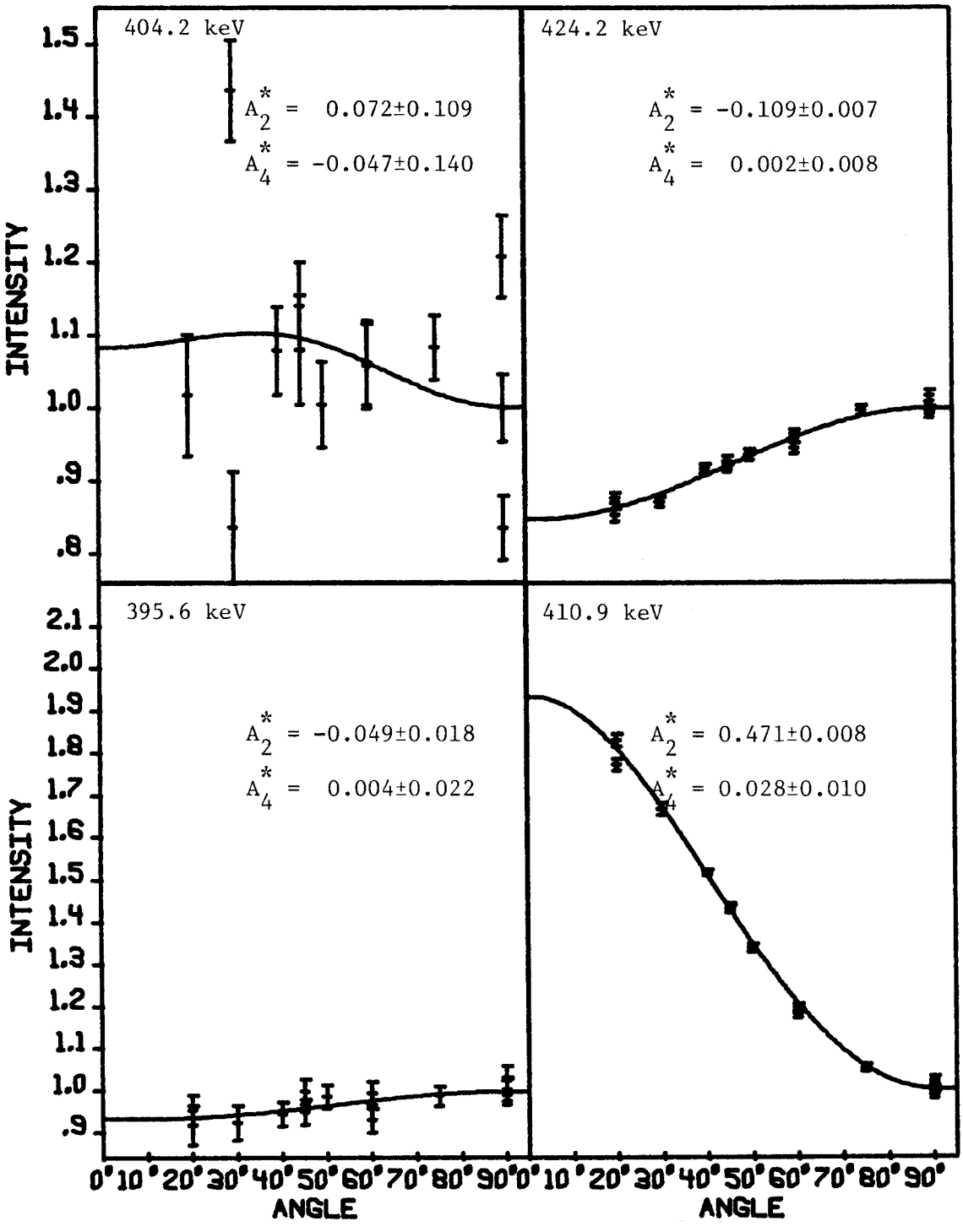

Figure C-4 continued.

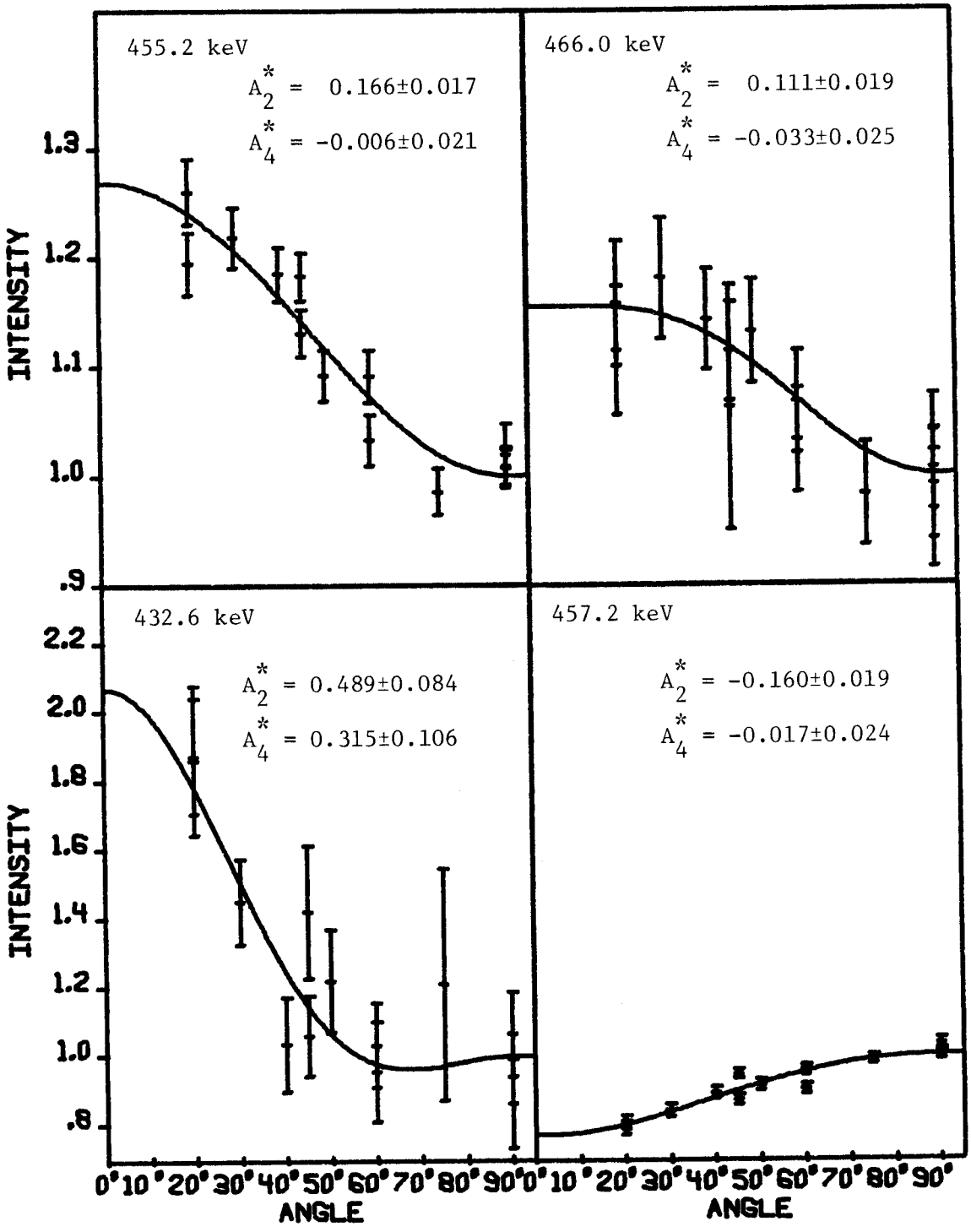

Figure C-4 continued.

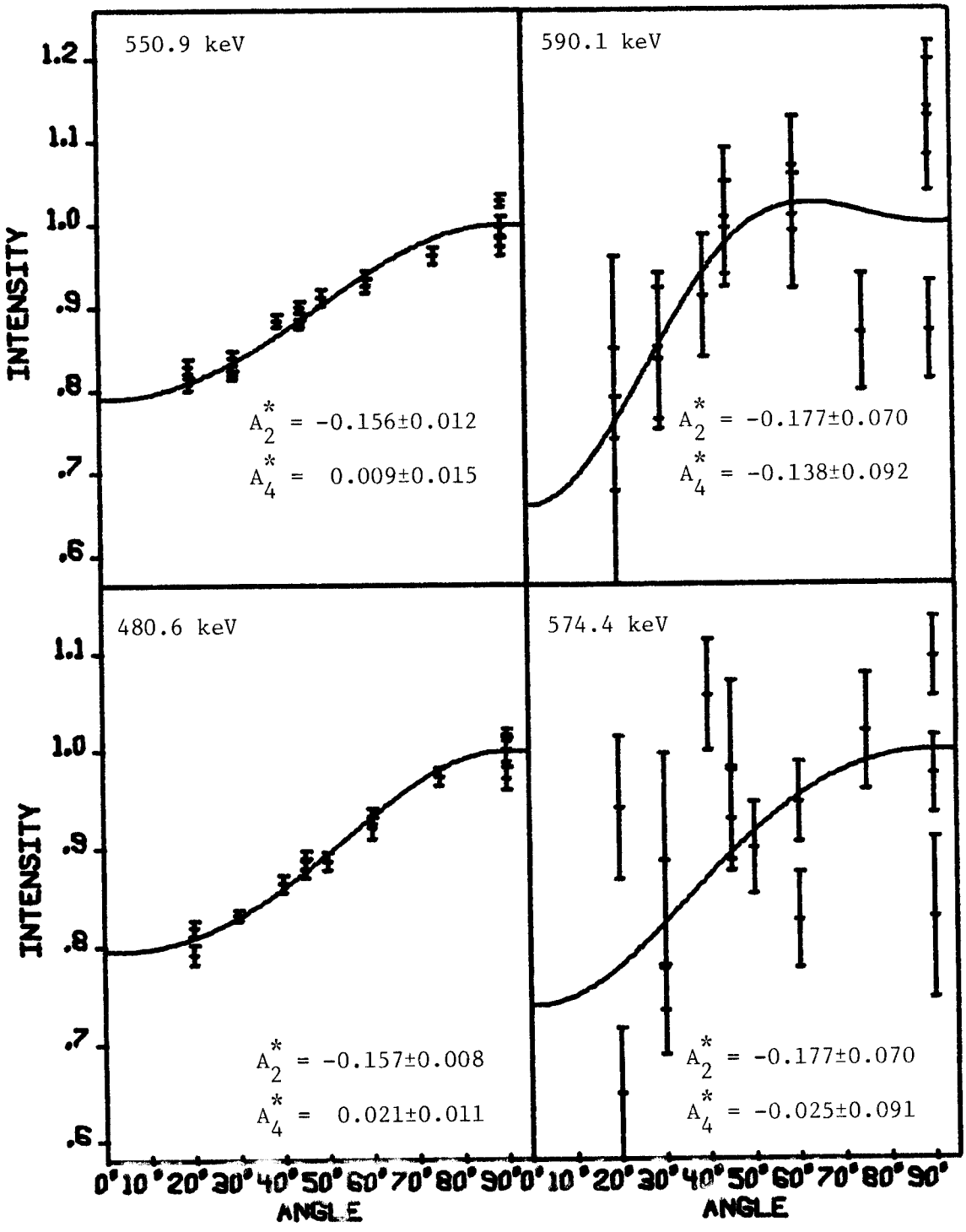

Figure C-4 continued.

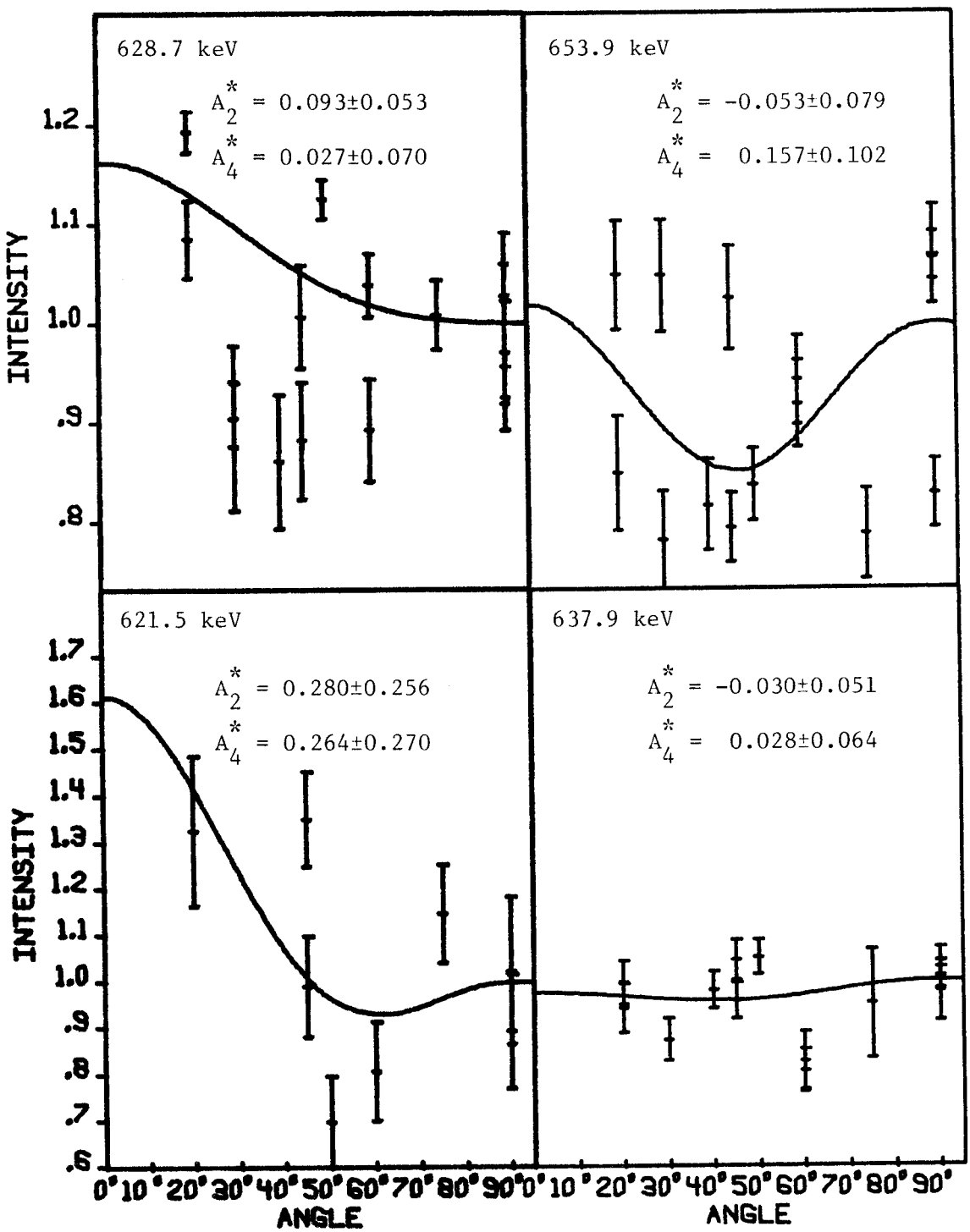

Figure C-4 continued.

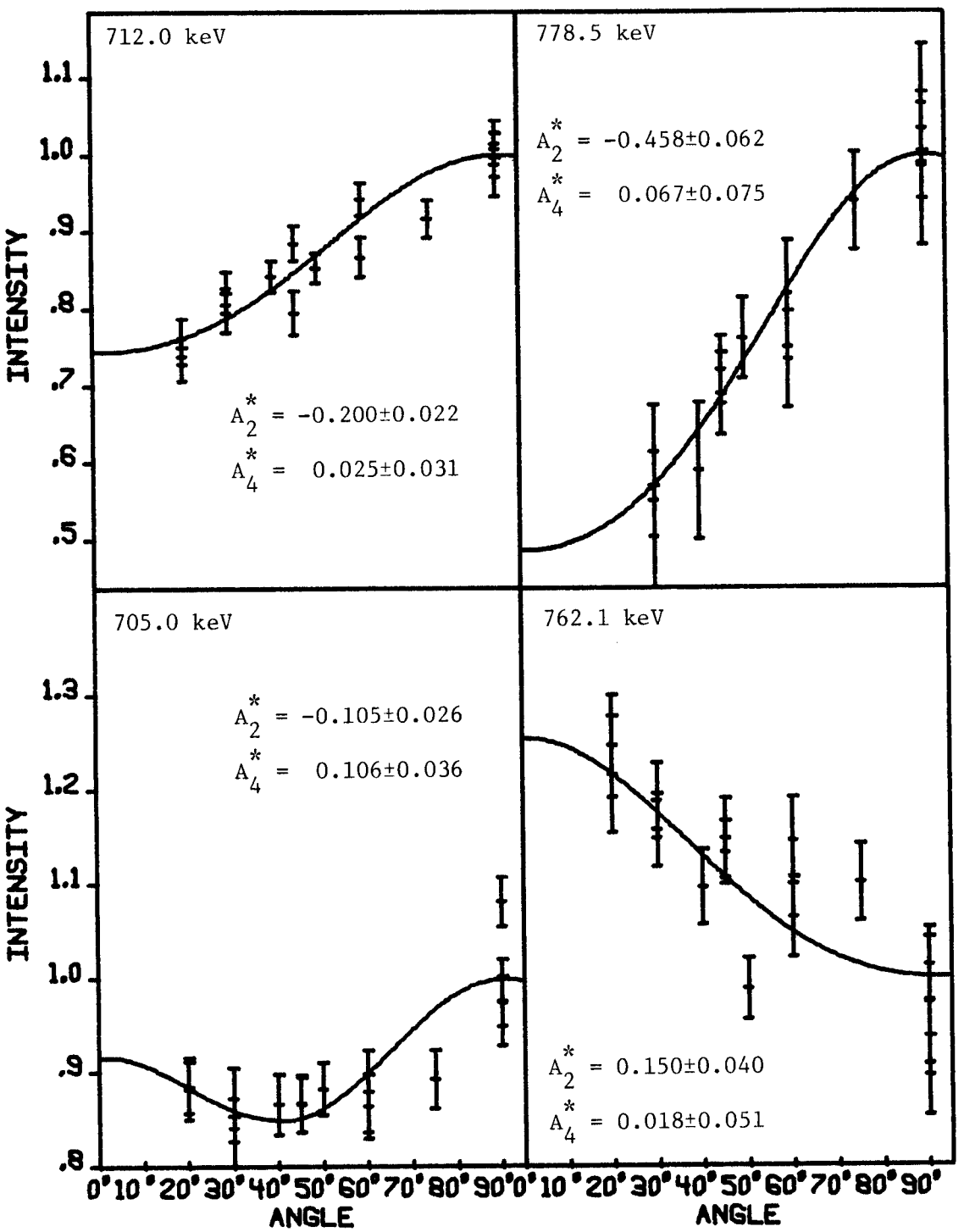

Figure C-4 continued.

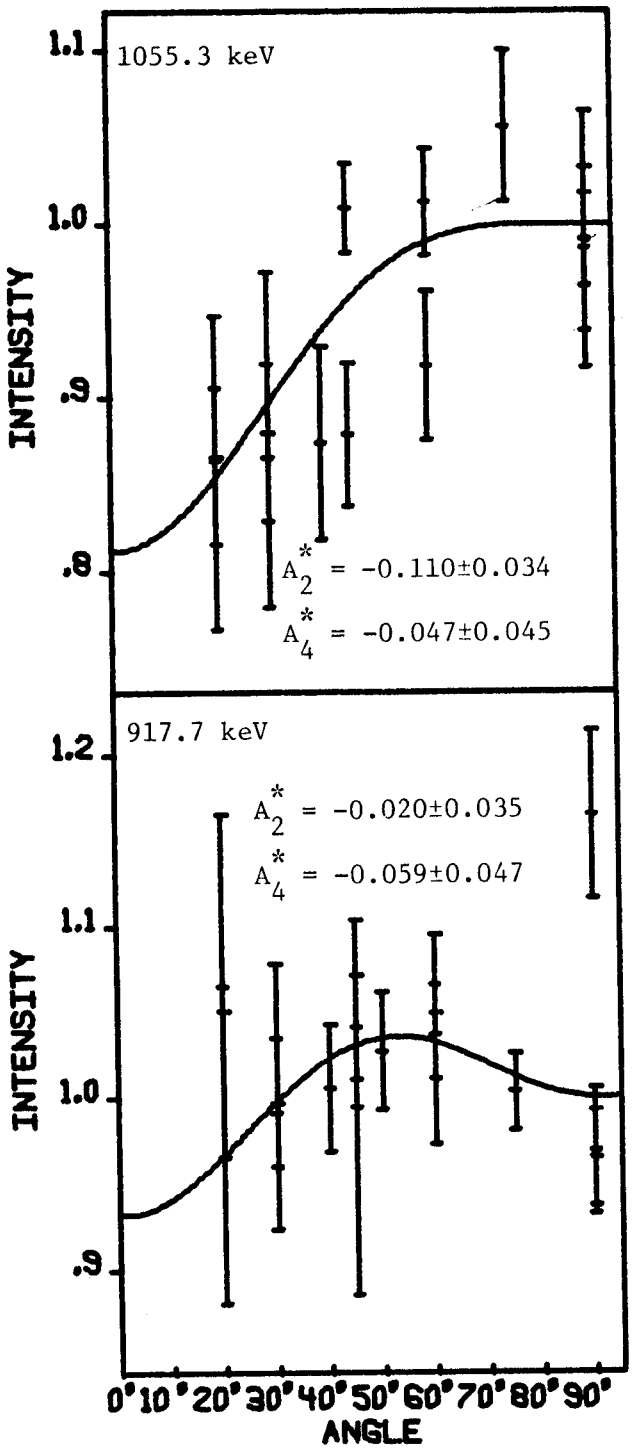

Figure C-4 continued.

APPENDIX C

Angular Distributions of the Various ^{116}Sb γ rays Obtained from the ^{116}Sn(p,nγ)^{116}Sb Reaction with E_p = 5.95, 6.25, 6.65, and 7.32 MeV.

Figure C-1. Gamma-ray angular distributions obtained with the proton energy at 5.95 Mev. The solid line represents the least sqares fit to $W(\theta)$ as explained in the text. The fit is normalized to 1 at 90°. The data in the lower right is normalized to the isotropic 93.7 keV gamma ray.

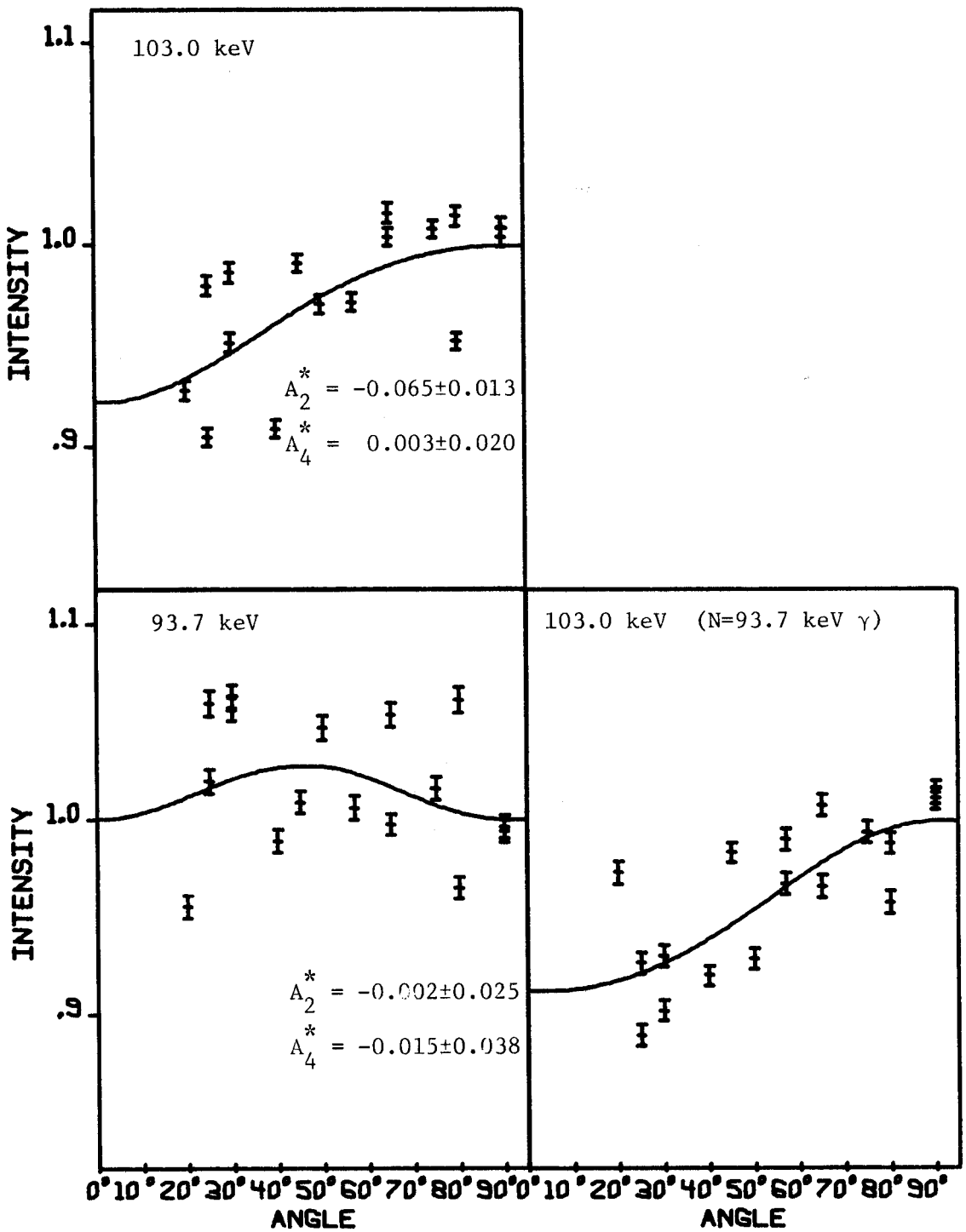
103.0 keV
1.1
1.0
.9
INTENSITY
$A_2^* = -0.065 \pm 0.013$
$A_4^* = 0.003 \pm 0.020$
93.7 keV
1.1
1.0
.9
INTENSITY
$A_2^* = -0.002 \pm 0.025$
$A_4^* = -0.015 \pm 0.038$
103.0 keV (N=93.7 keV γ)
0° 10° 20° 30° 40° 50° 60° 70° 80° 90°
ANGLE
0° 10° 20° 30° 40° 50° 60° 70° 80° 90°
ANGLE

Figure C-1.

Figure C-2. Gamma-ray angular distributions from the $^{116}Sn(p,n\gamma)^{116}Sb$ reaction at 6.25 MeV. The data are normalized to the isotropic 93.7 keV γ ray.

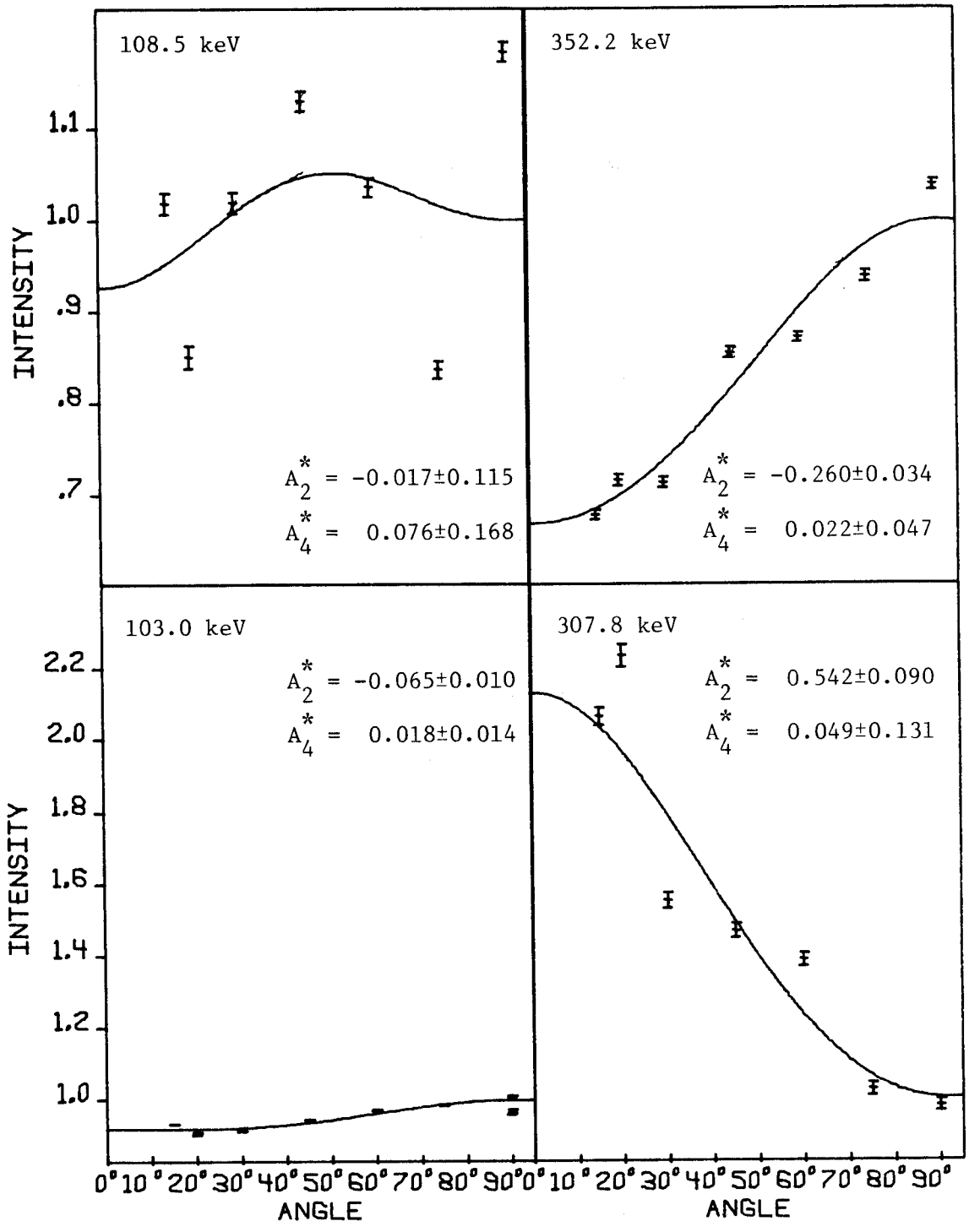
108.5 keV
352.2 keV
103.0 keV
307.8 keV
$A_2^* = -0.017 \pm 0.115$
$A_4^* = 0.076 \pm 0.168$
$A_2^* = -0.260 \pm 0.034$
$A_4^* = 0.022 \pm 0.047$
$A_2^* = -0.065 \pm 0.010$
$A_4^* = 0.018 \pm 0.014$
$A_2^* = 0.542 \pm 0.090$
$A_4^* = 0.049 \pm 0.131$
INTENSITY
INTENSITY
1.1
1.0
.9
.8
.7
2.2
2.0
1.8
1.6
1.4
1.2
1.0
0° 10° 20° 30° 40° 50° 60° 70° 80° 90°
0° 10° 20° 30° 40° 50° 60° 70° 80° 90°
ANGLE
ANGLE

Figure C-2.

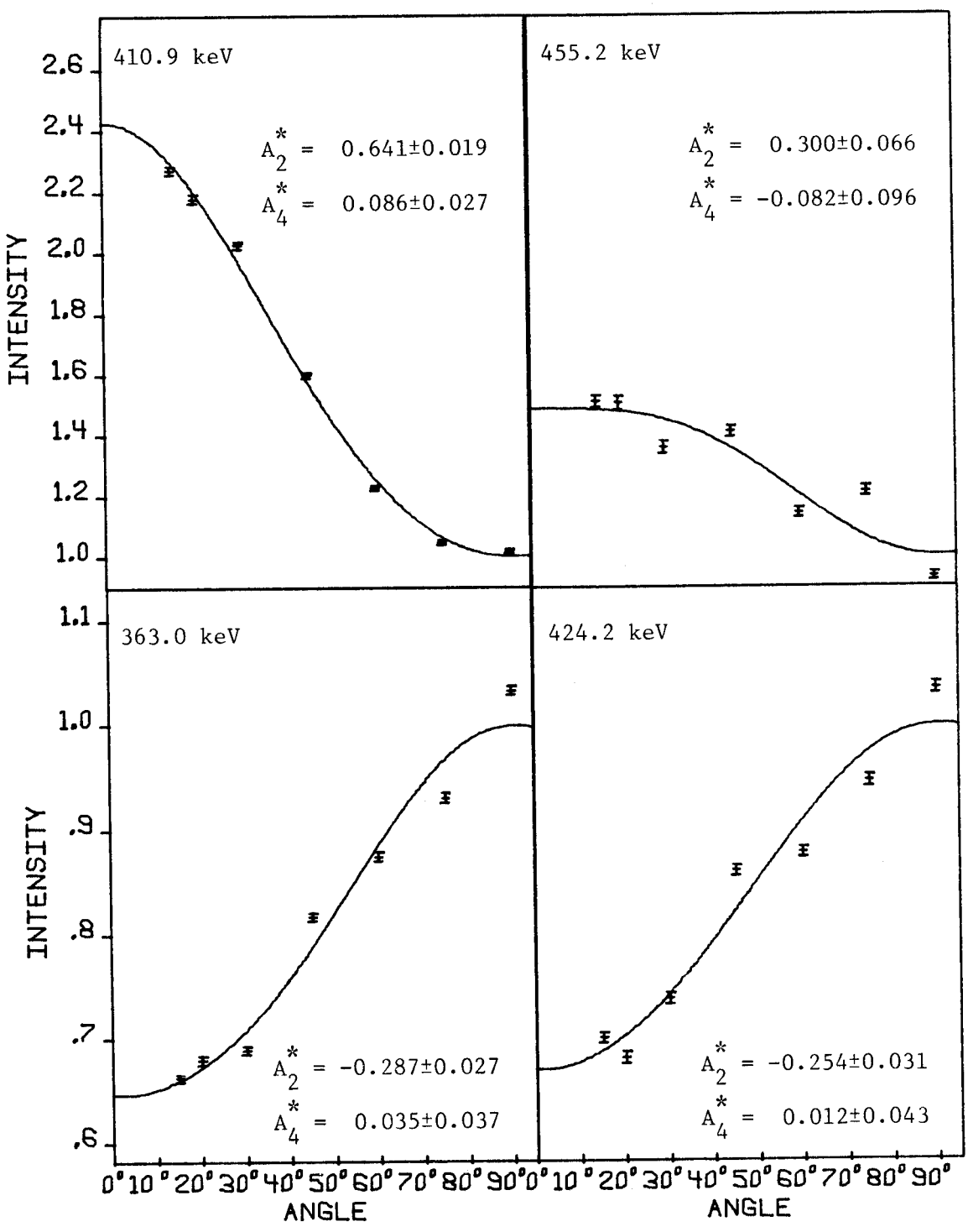

Figure C-2 continued.

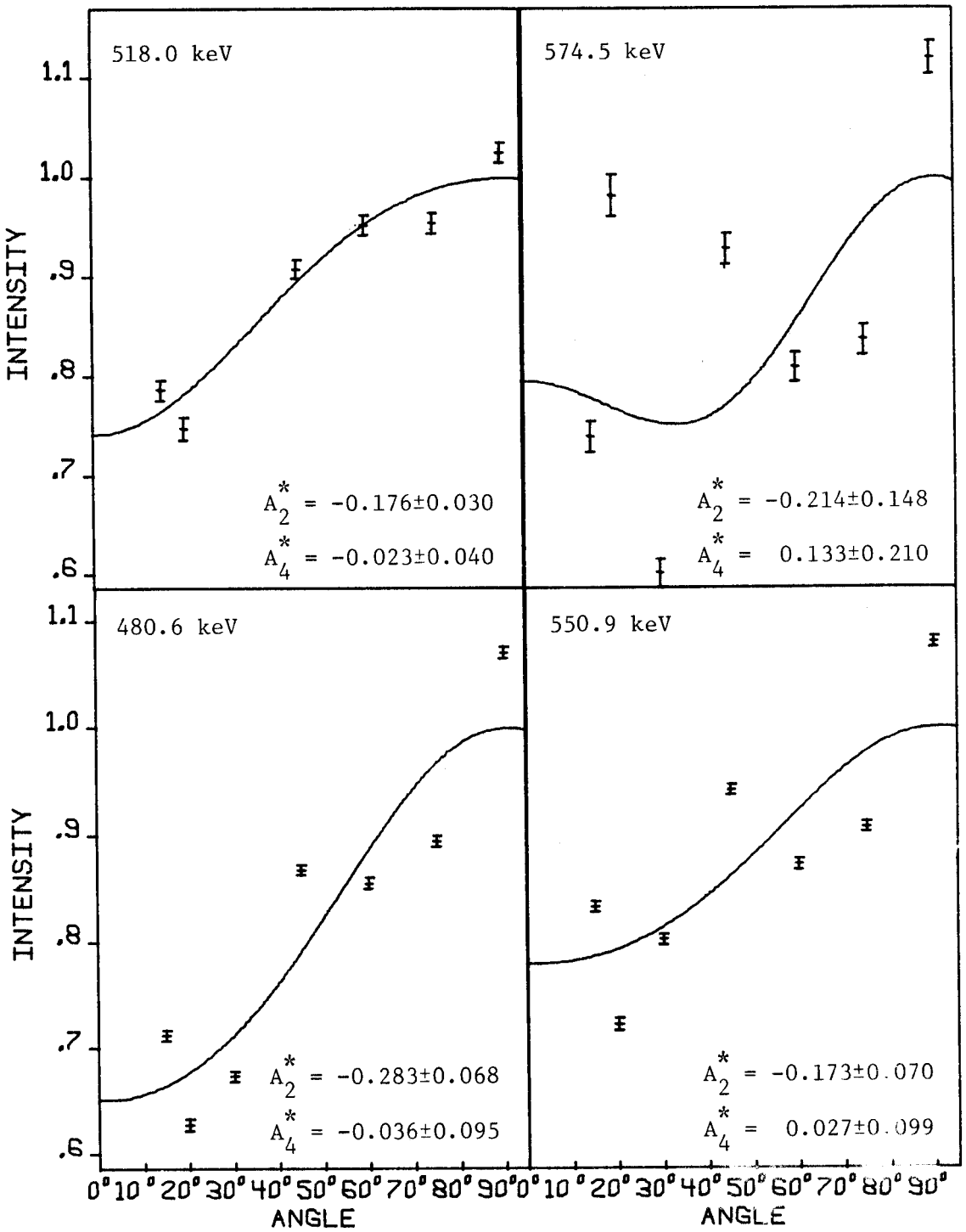

Figure C-2 continued.

Figure C-3. Gamma-ray angular distributions from the $^{116}Sn(p,n\gamma)^{116}Sb$ reaction at 6.65 MeV. The data are normalized to the isotropic 93.7 keV γ ray.

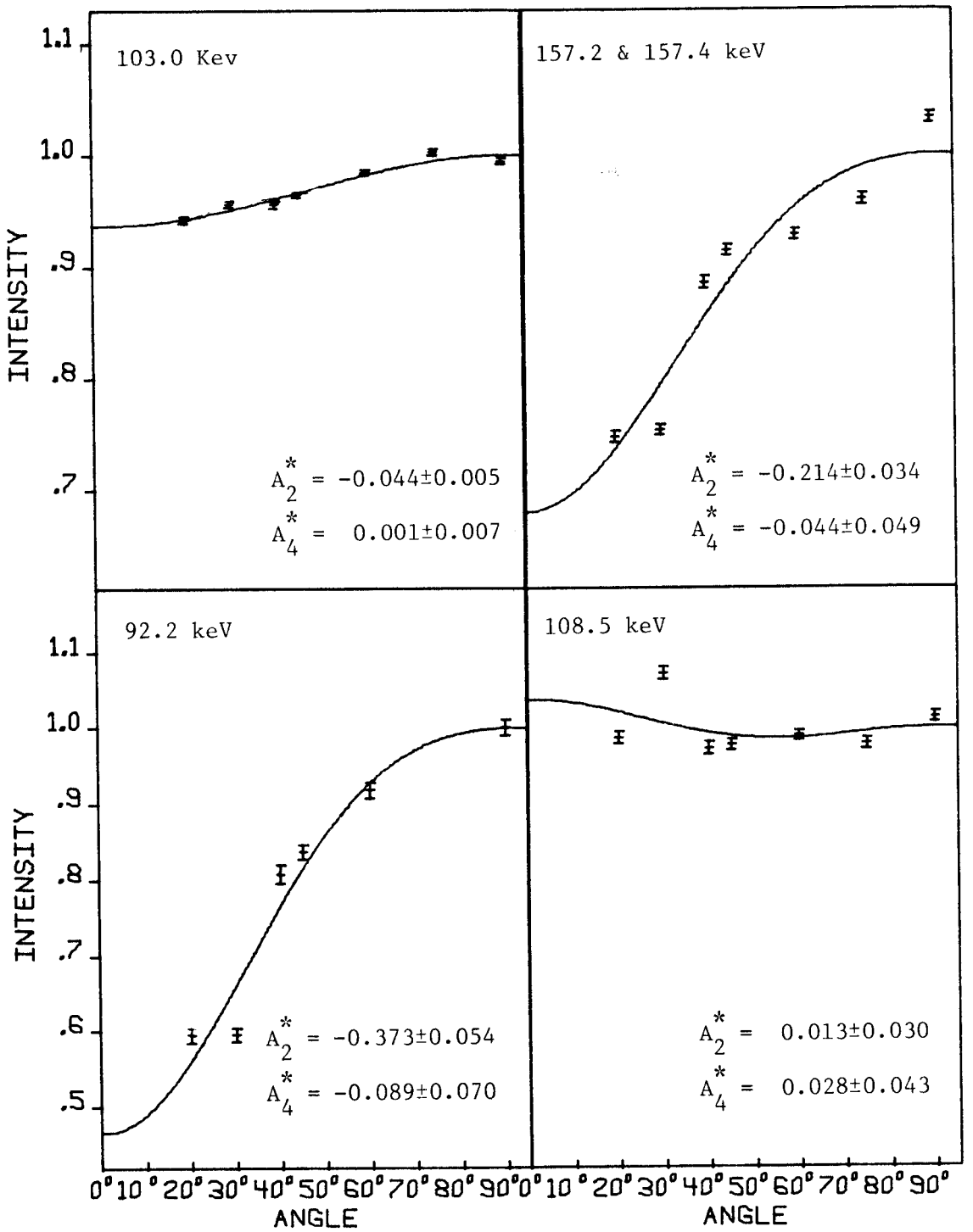
103.0 Kev
$A_2^* = -0.044 \pm 0.005$
$A_4^* = 0.001 \pm 0.007$
157.2 & 157.4 keV
$A_2^* = -0.214 \pm 0.034$
$A_4^* = -0.044 \pm 0.049$
92.2 keV
$A_2^* = -0.373 \pm 0.054$
$A_4^* = -0.089 \pm 0.070$
108.5 keV
$A_2^* = 0.013 \pm 0.030$
$A_4^* = 0.028 \pm 0.043$
INTENSITY
1.1
1.0
.9
.8
.7
.6
.5
0° 10° 20° 30° 40° 50° 60° 70° 80° 90°
ANGLE

Figure C-3.

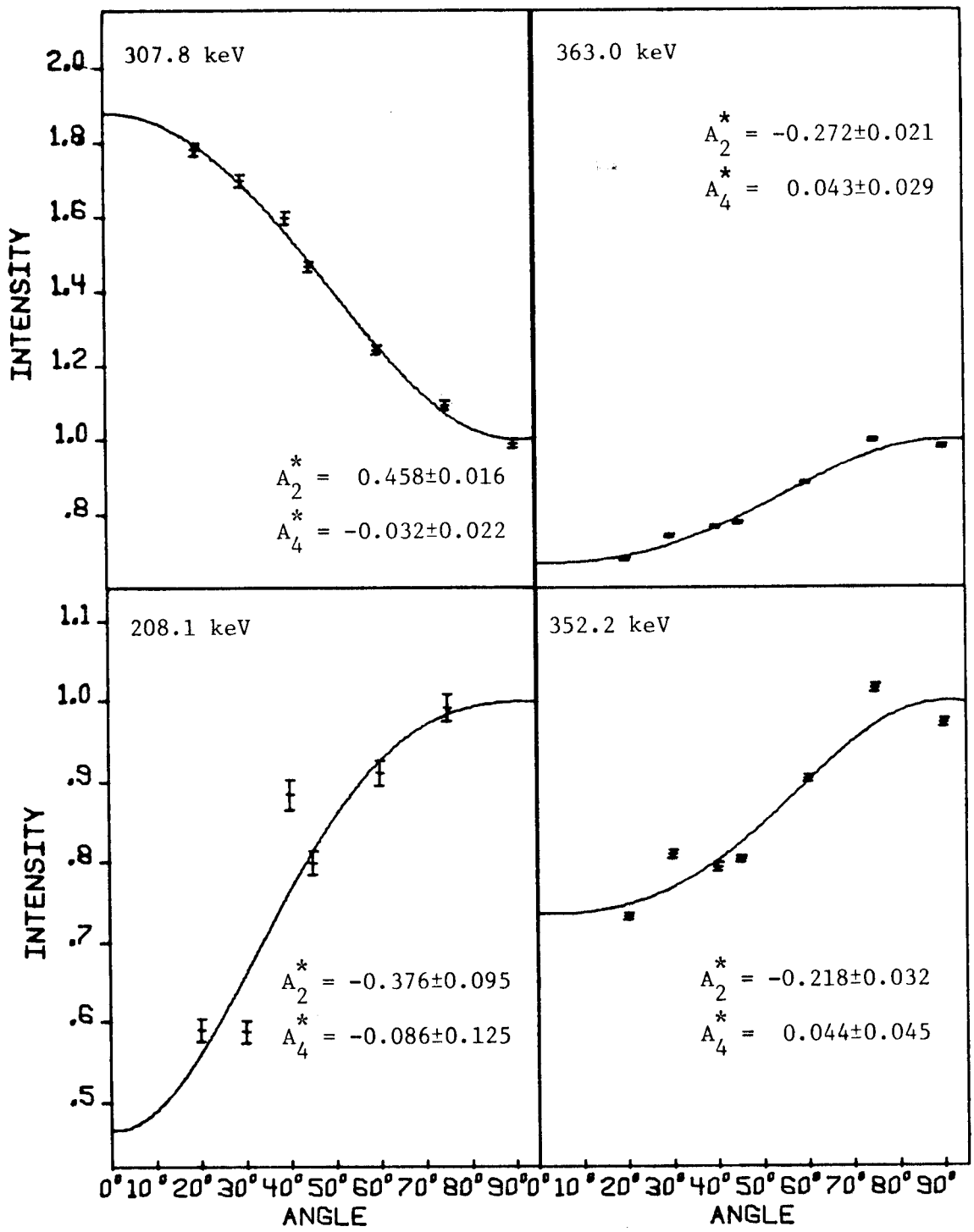

Figure C-3 continued.

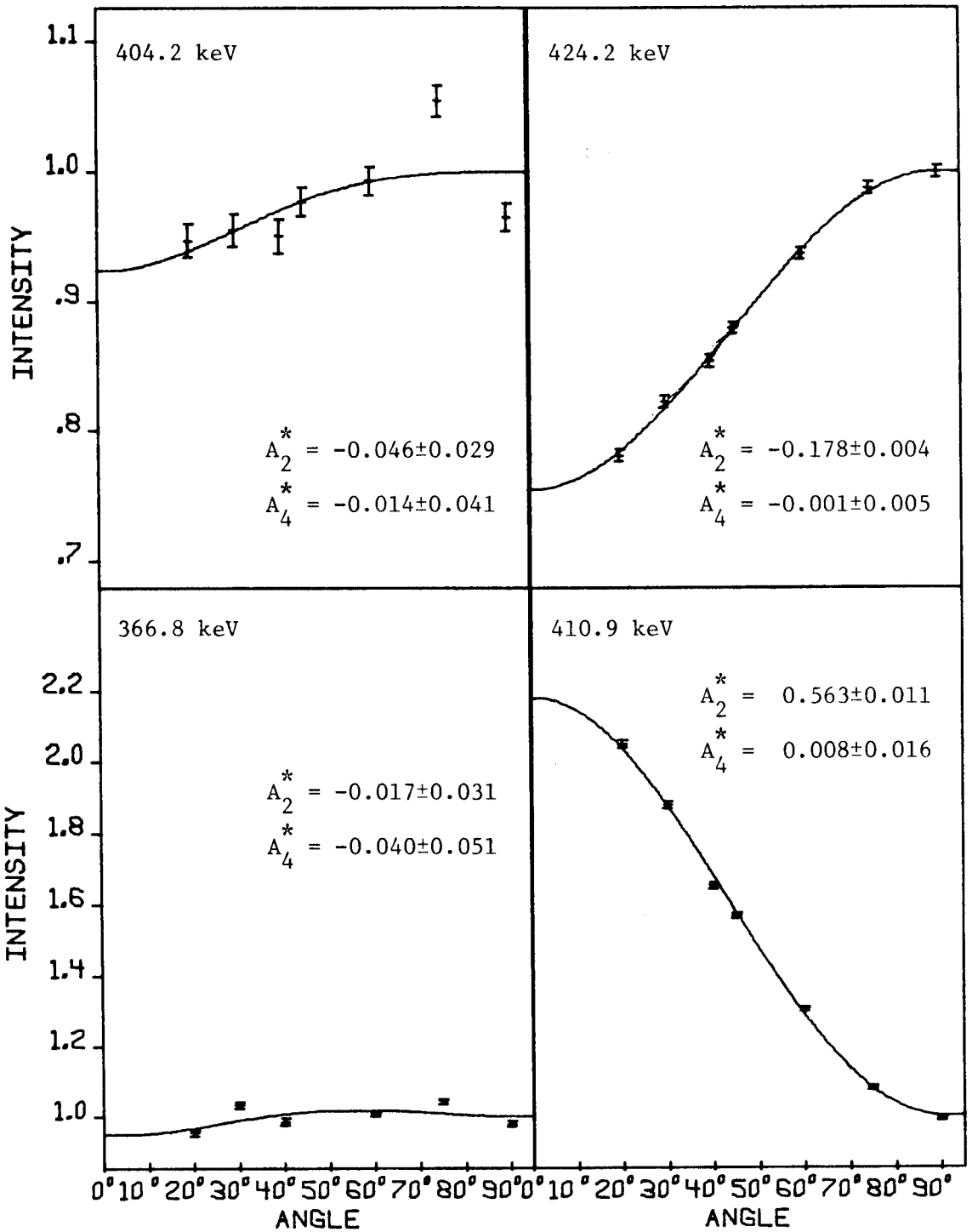

Figure C-3 continued.

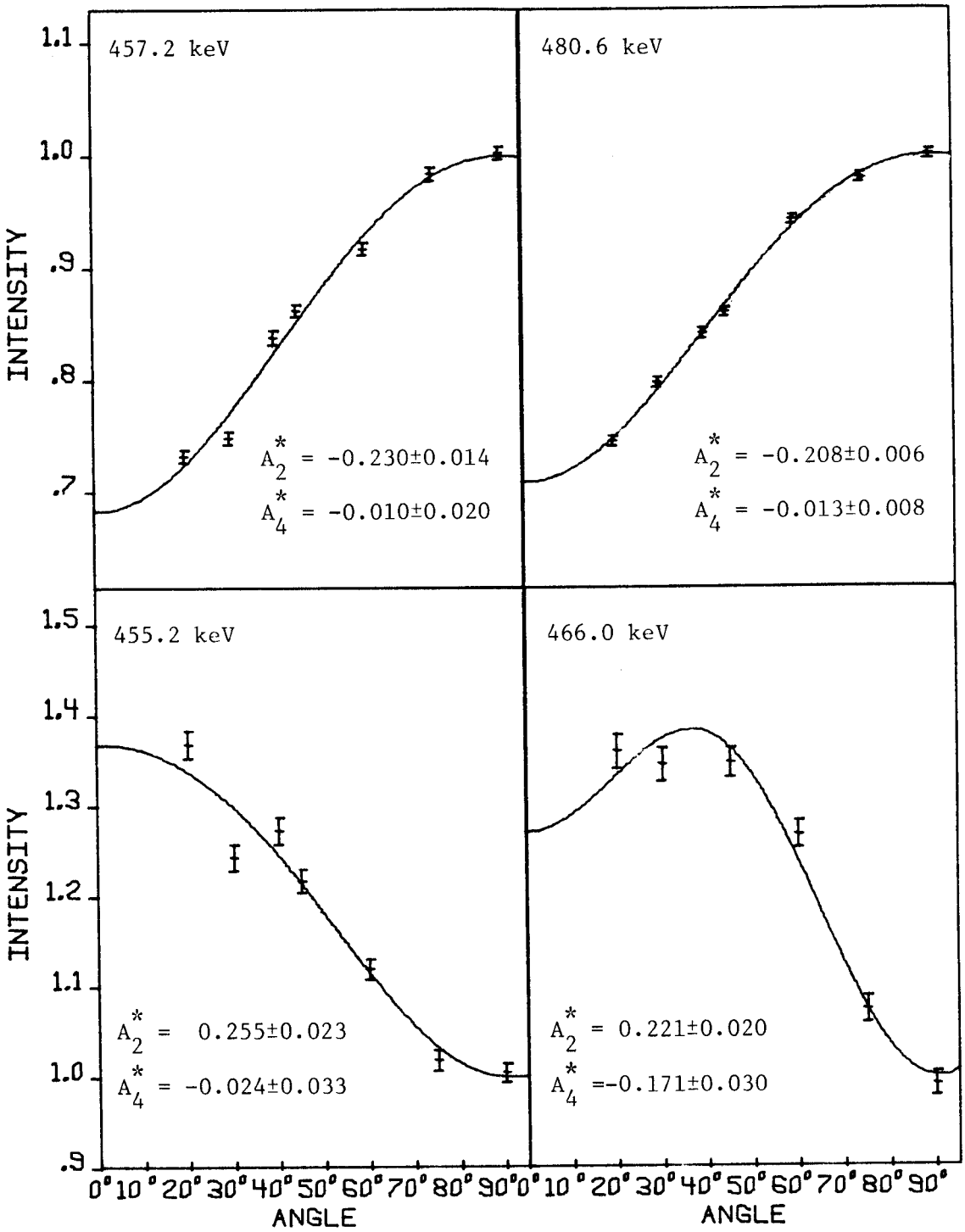

Figure C-3 continued.

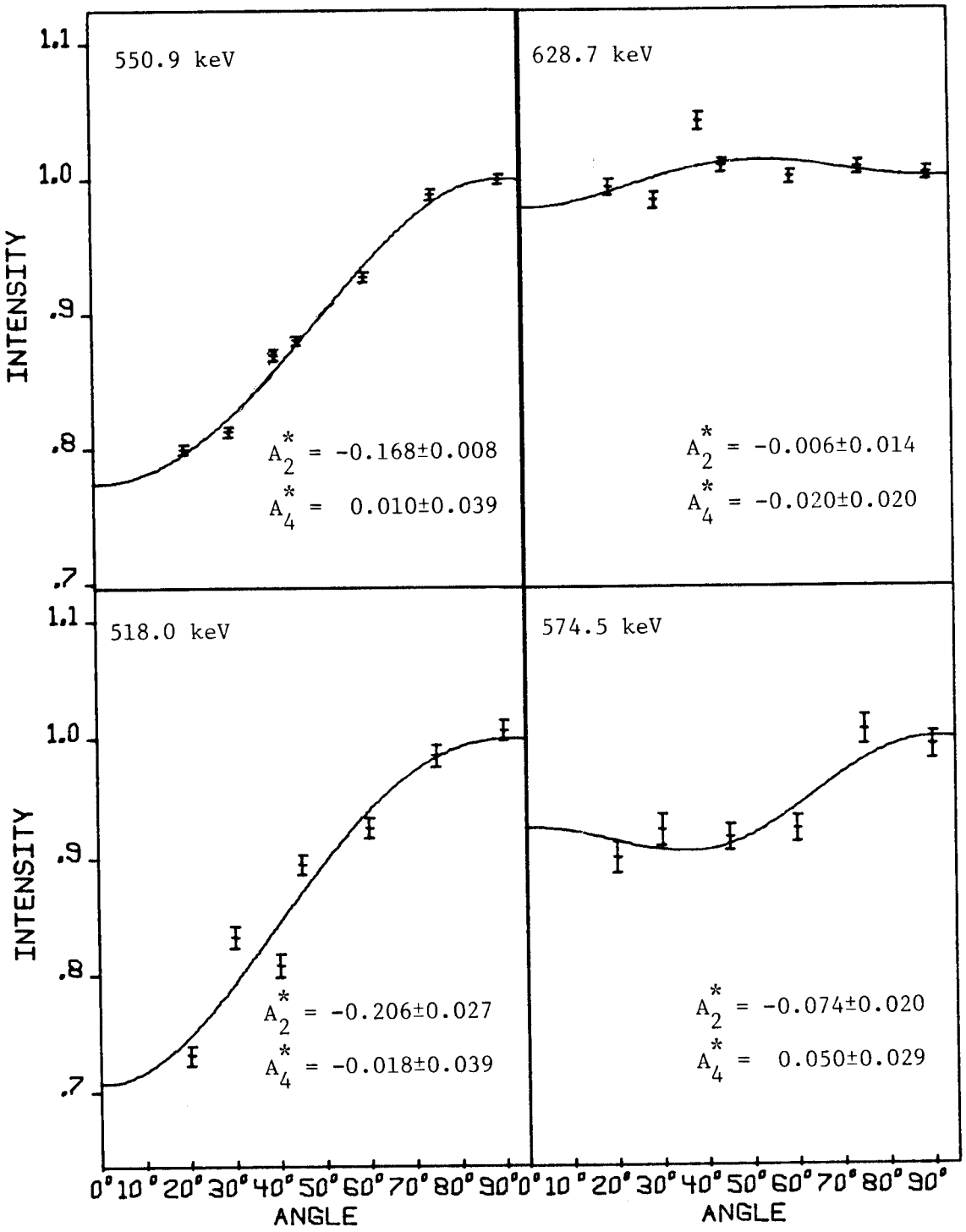

Figure C-3 continued.

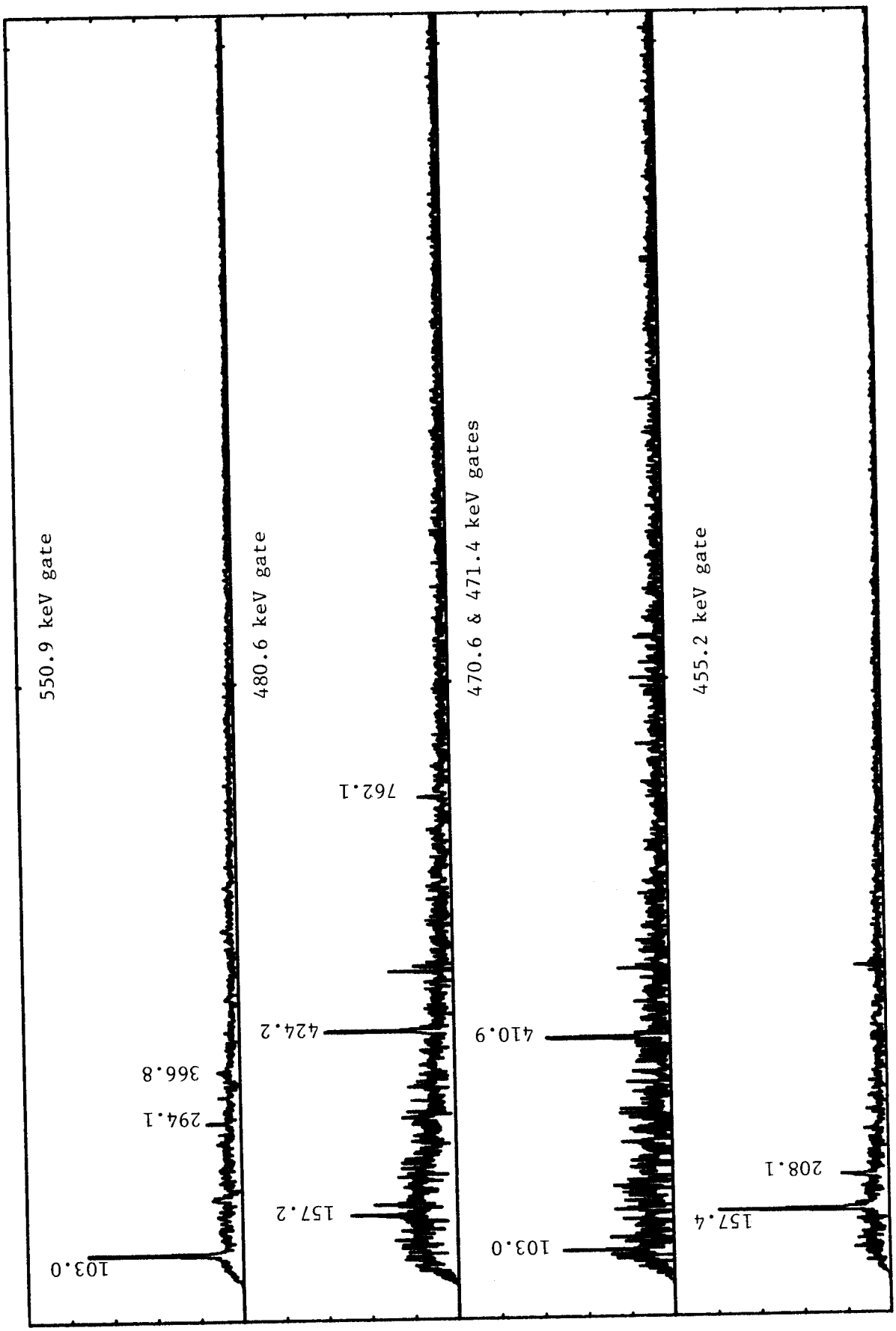

Figure B-2 continued.

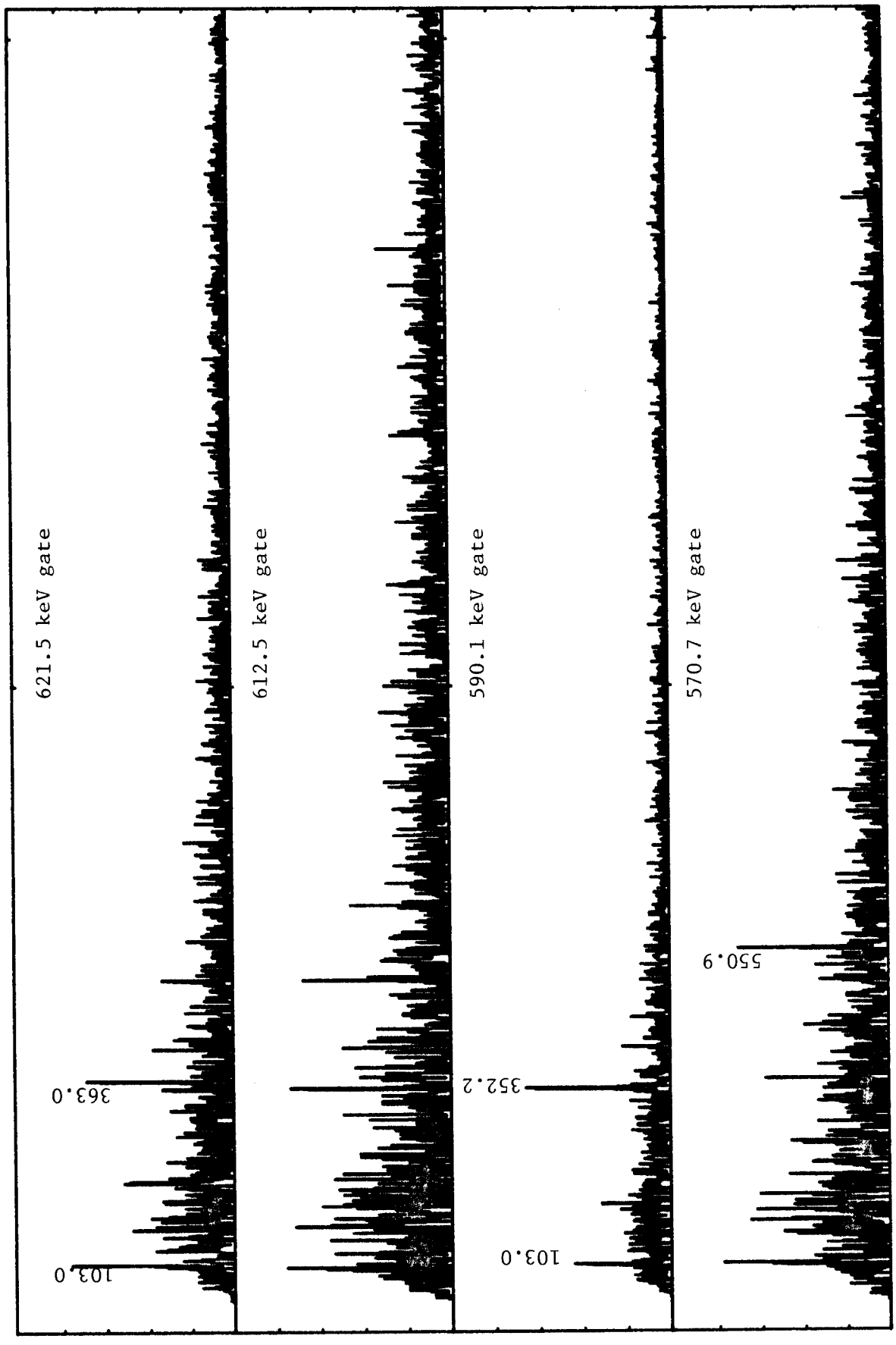

Figure B-2 continued.

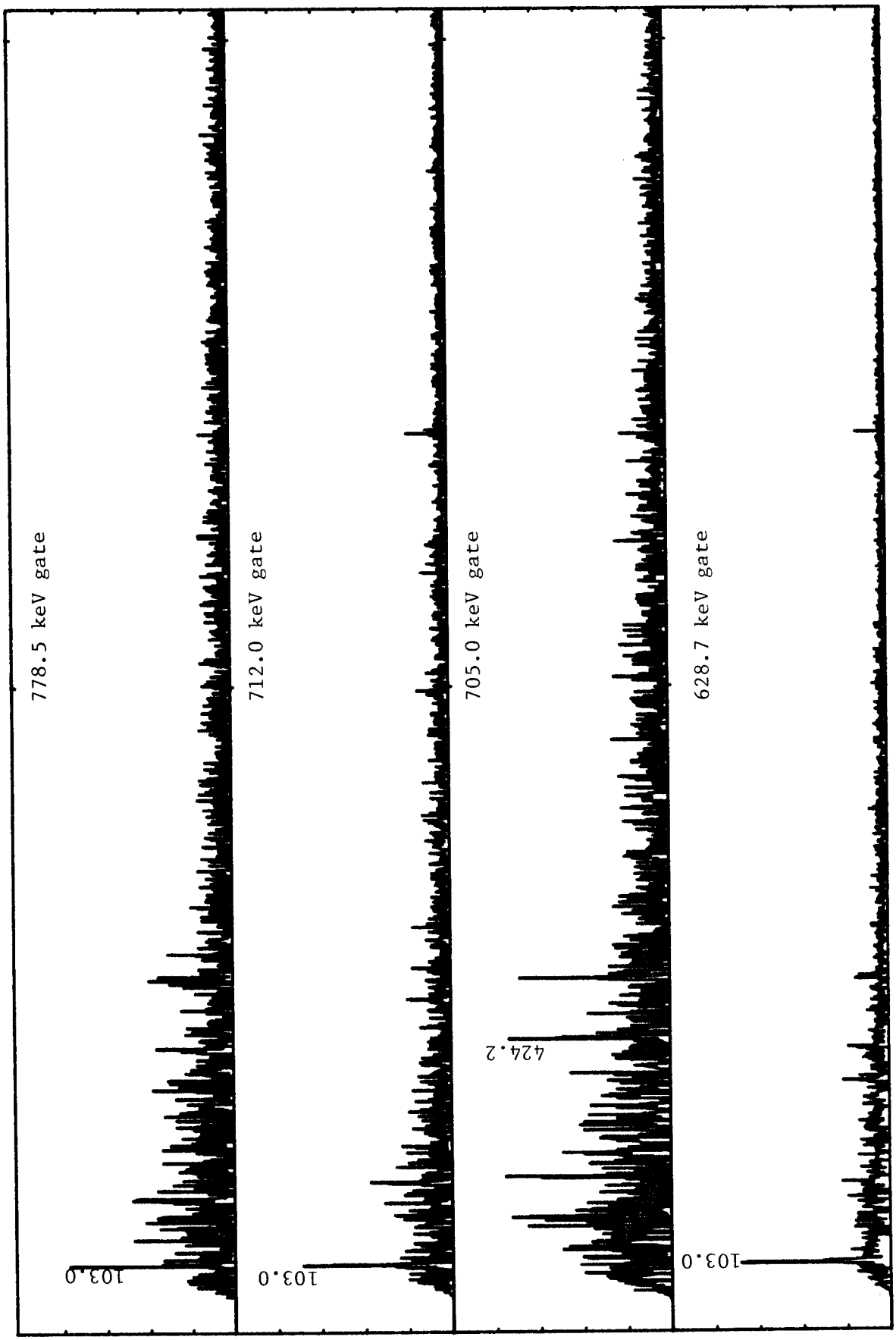

Figure B-2 continued.

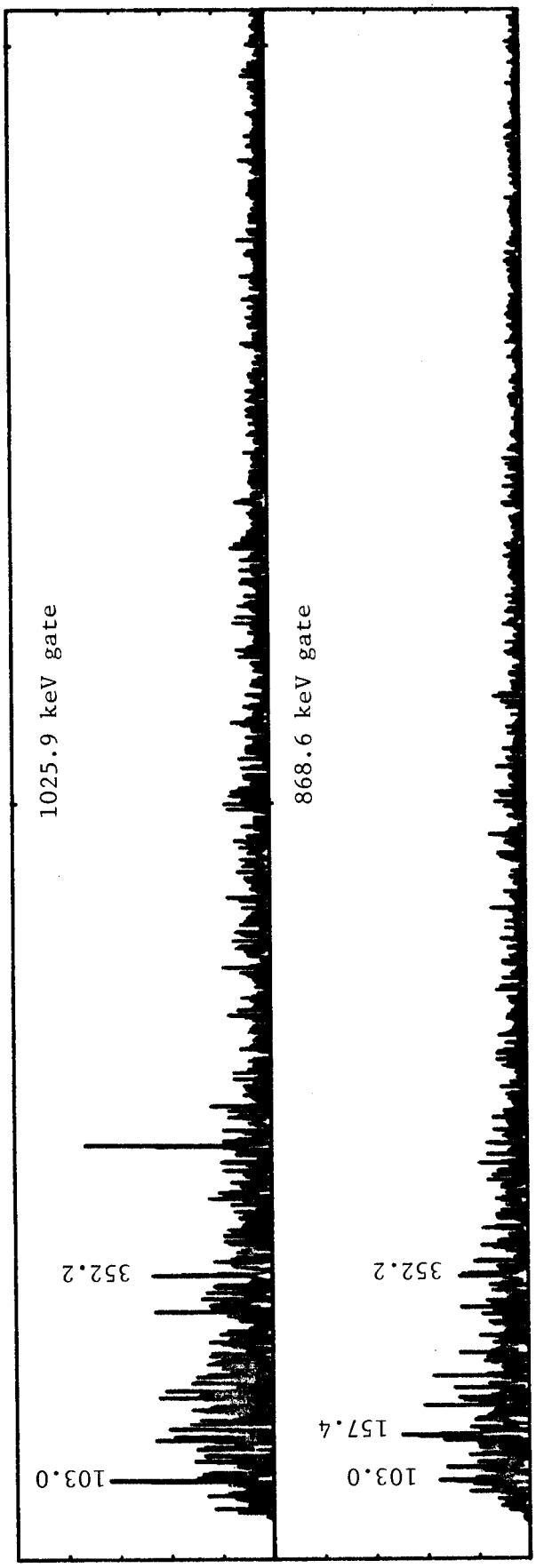

Figure B-2 continued.

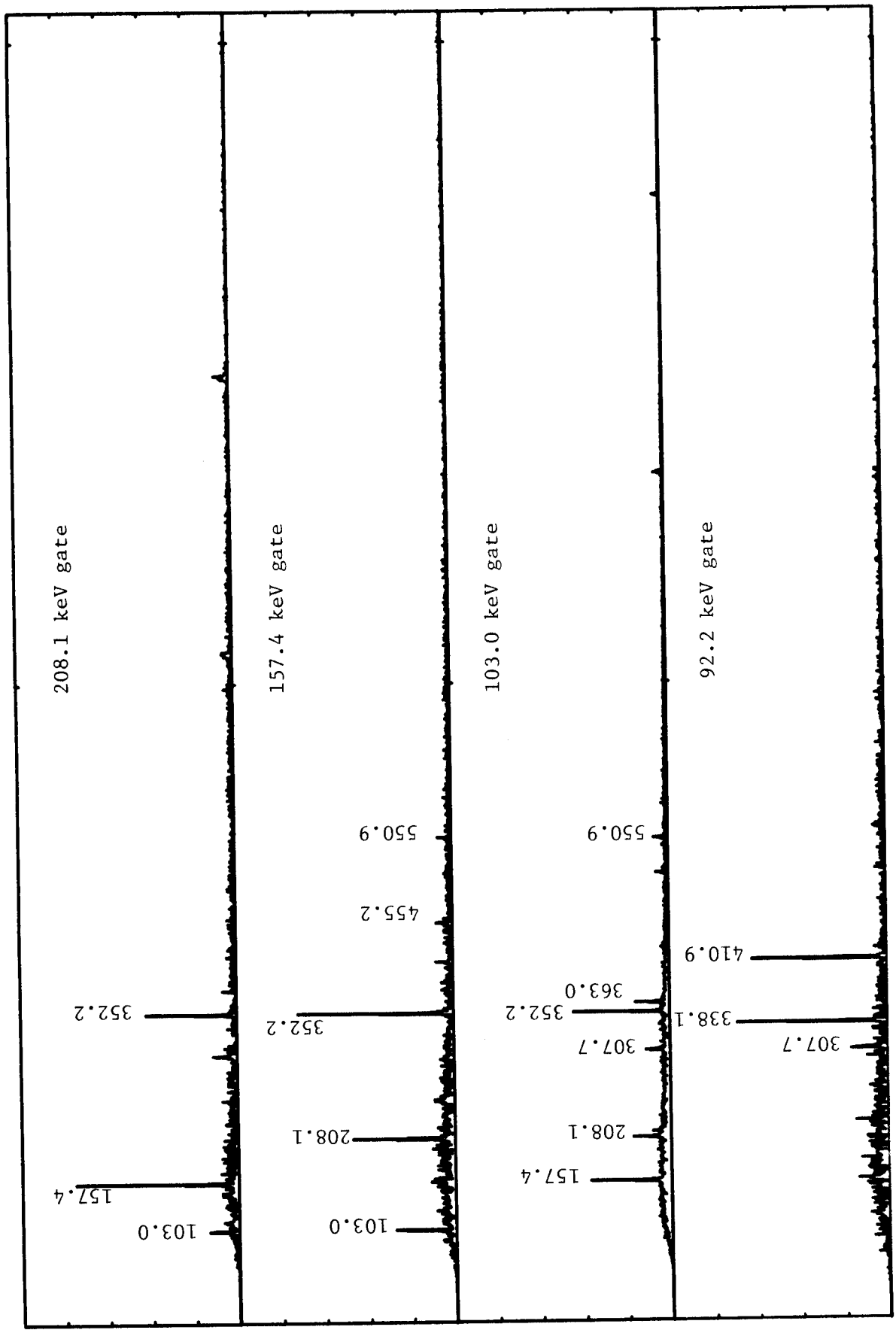
208.1 keV gate
103.0
157.4
352.2
157.4 keV gate
103.0
208.1
352.2
455.2
550.9
103.0 keV gate
157.4
208.1
307.7
352.2
363.0
550.9
92.2 keV gate
307.7
338.1
410.9

Figure B-3.

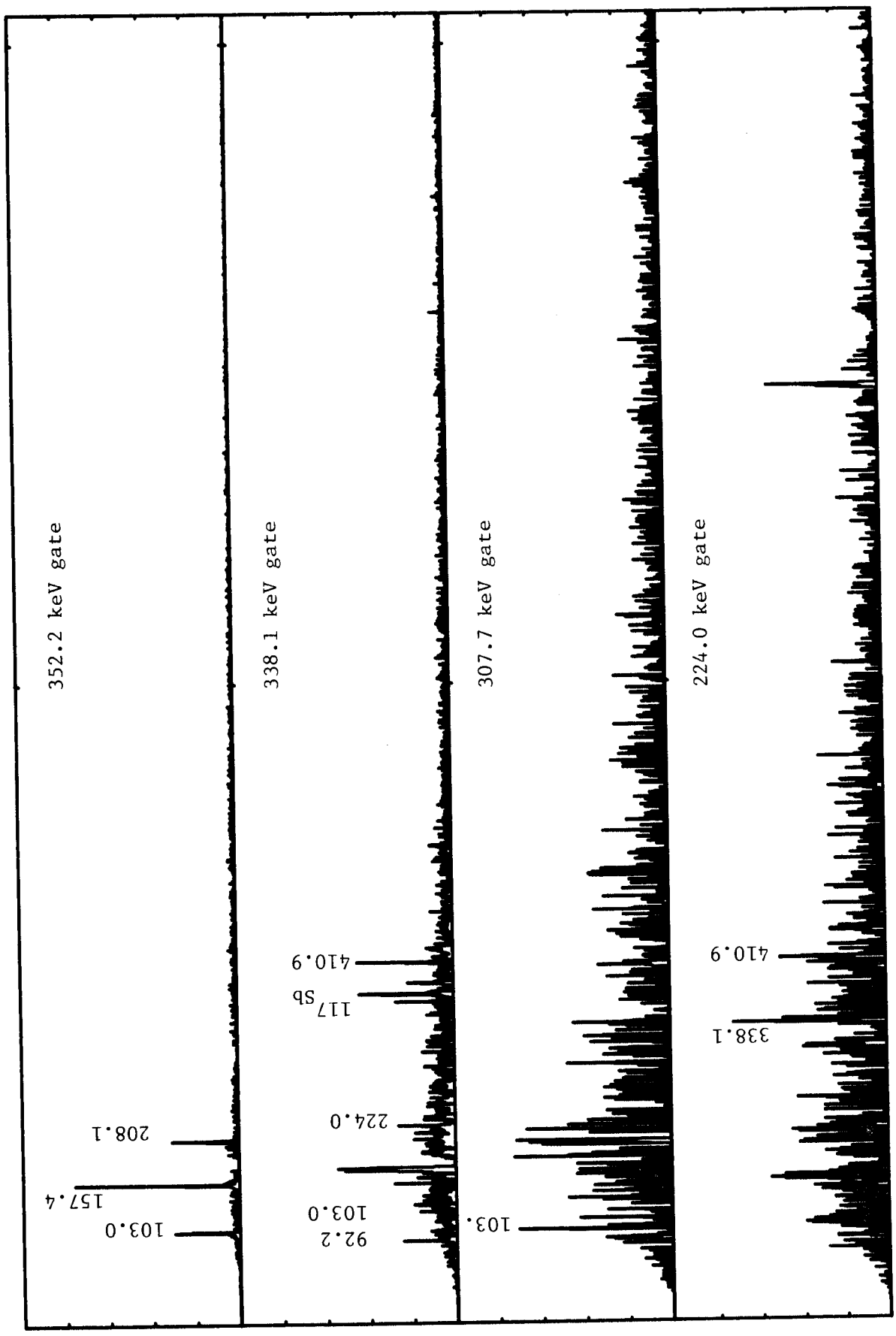

Figure B-3 continued.

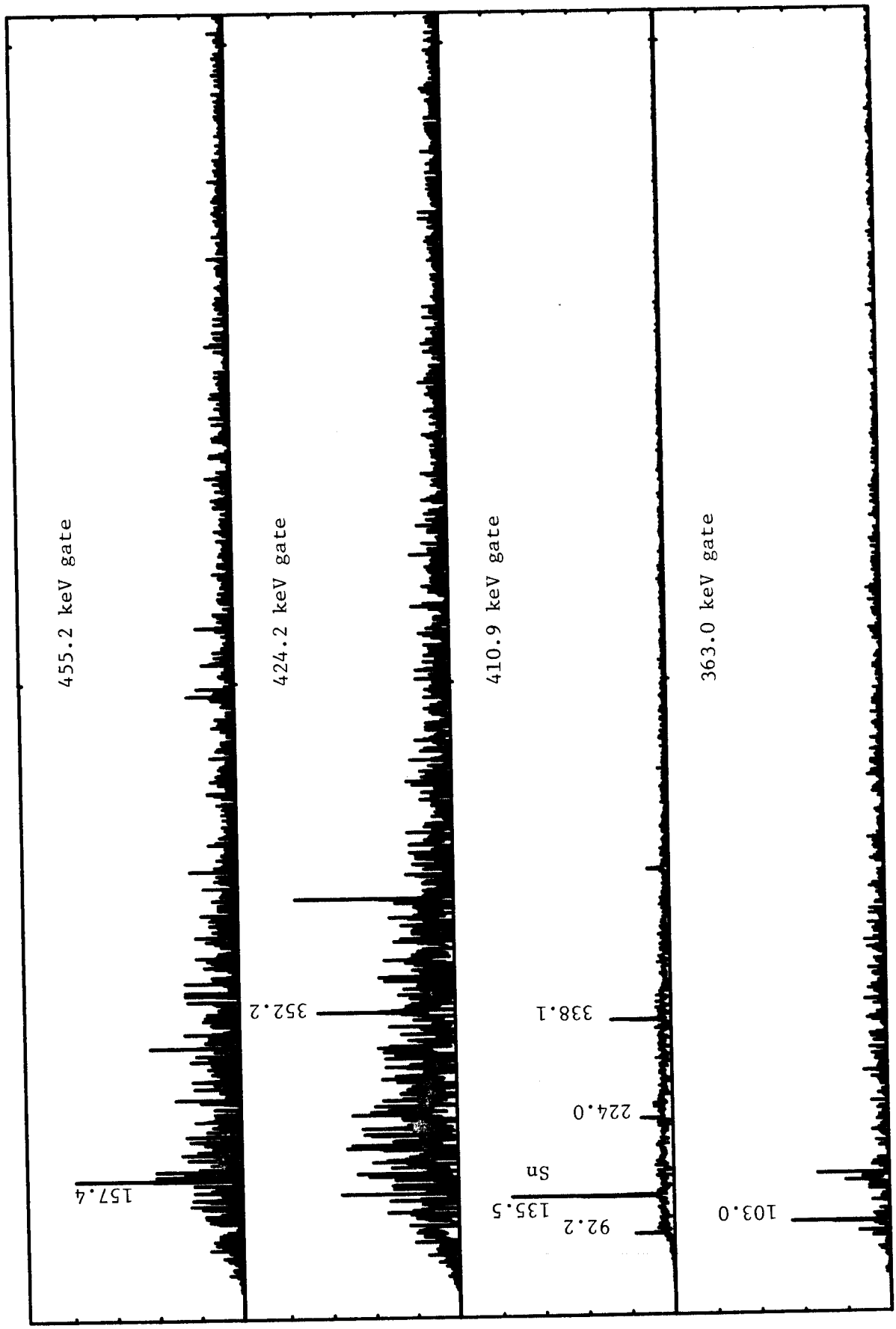

Figure B-3 continued.

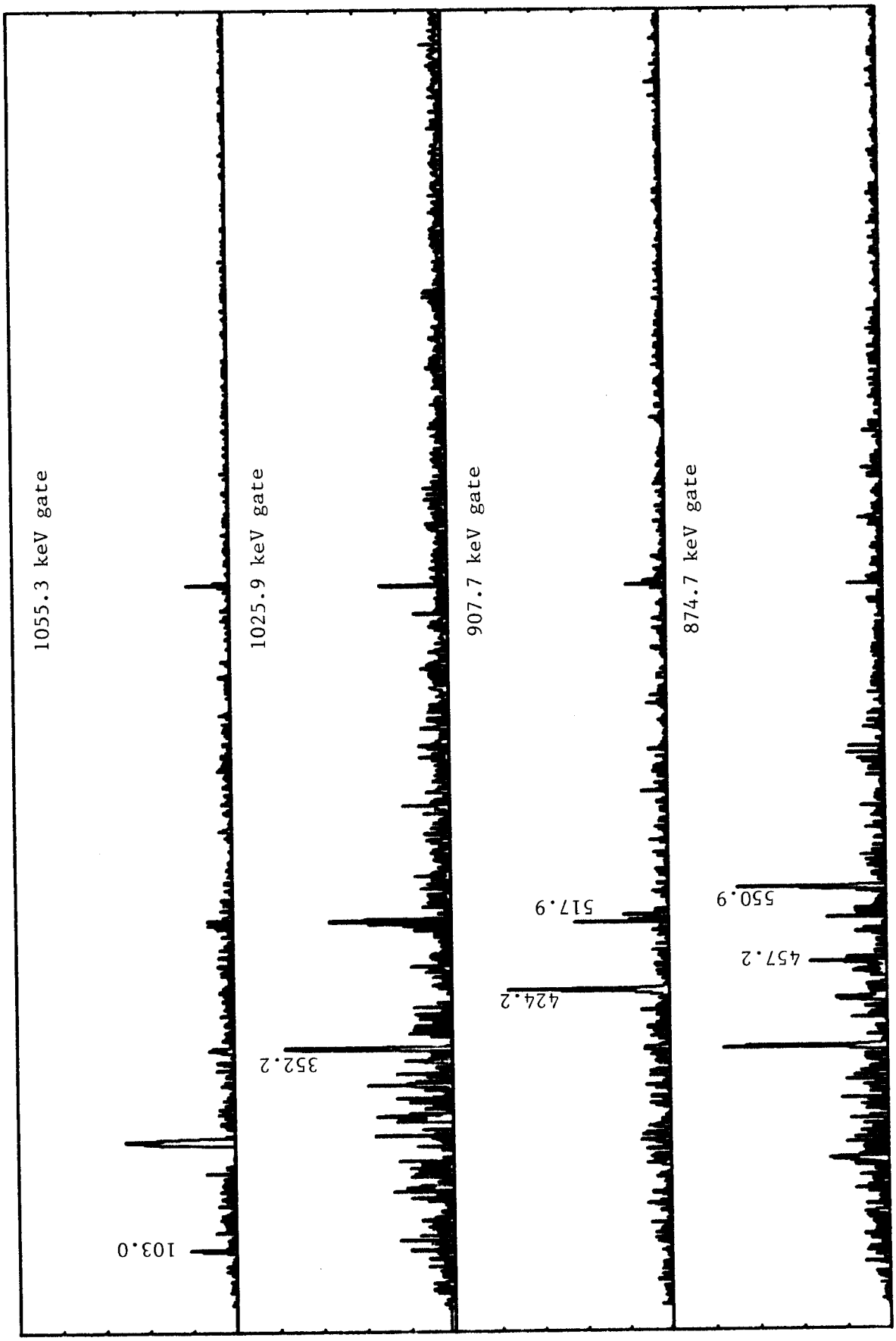

Figure B-1 continued.

Figure B-2. Integral coincidence and gated spectra form the in-beam $^{116}Sn(p,n\gamma-\gamma)^{116}Sb$ reaction at 11.75 MeV.

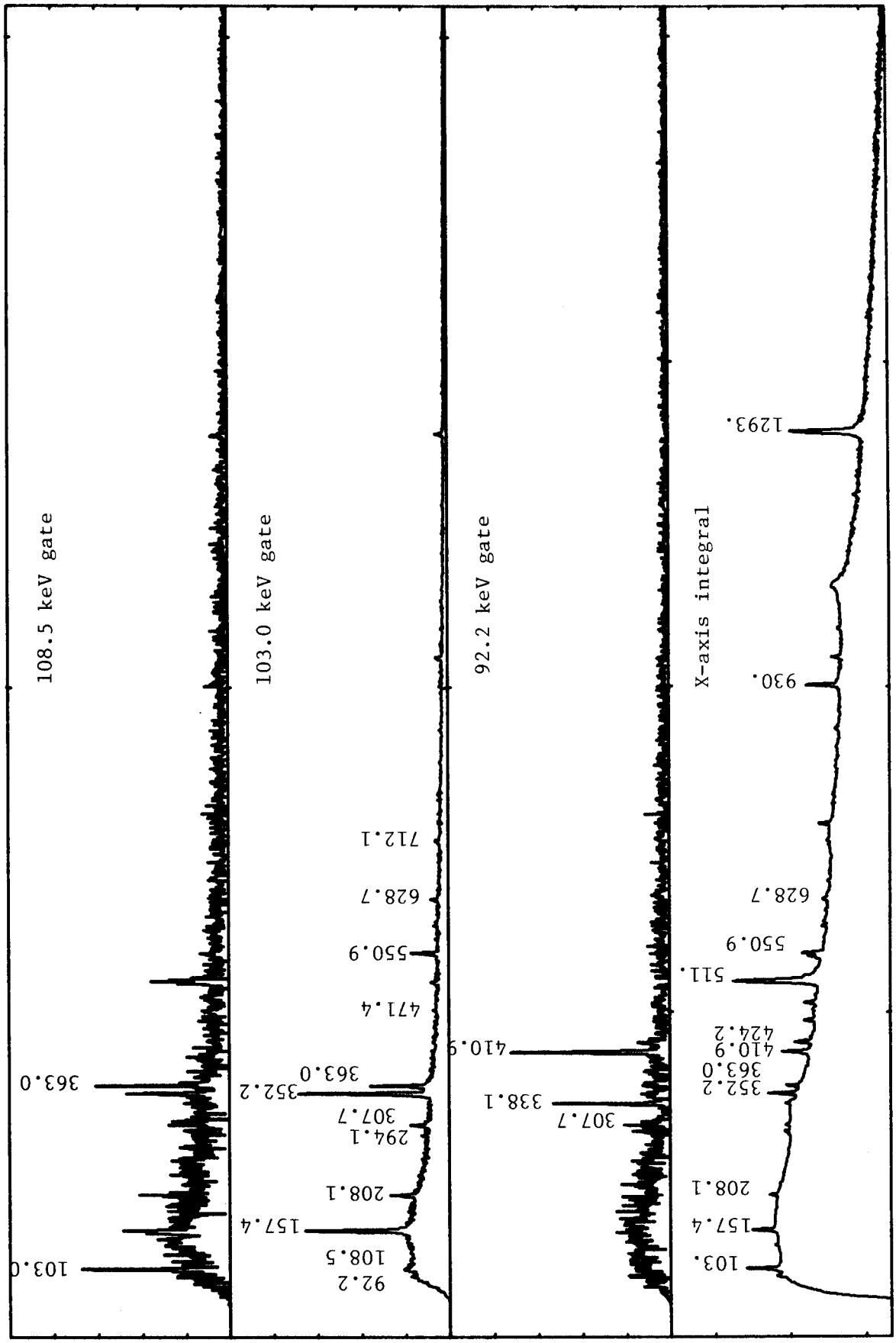
108.5 keV gate
103.0
363.0
103.0 keV gate
92.2
108.5
157.4
208.1
294.1
307.7
352.2
363.0
471.4
550.9
628.7
712.1
92.2 keV gate
307.7
338.1
410.9
X-axis integral
103.
157.4
208.1
352.2
363.0
410.9
424.2
511.
550.9
628.7
930.
1293.

Figure B-2.

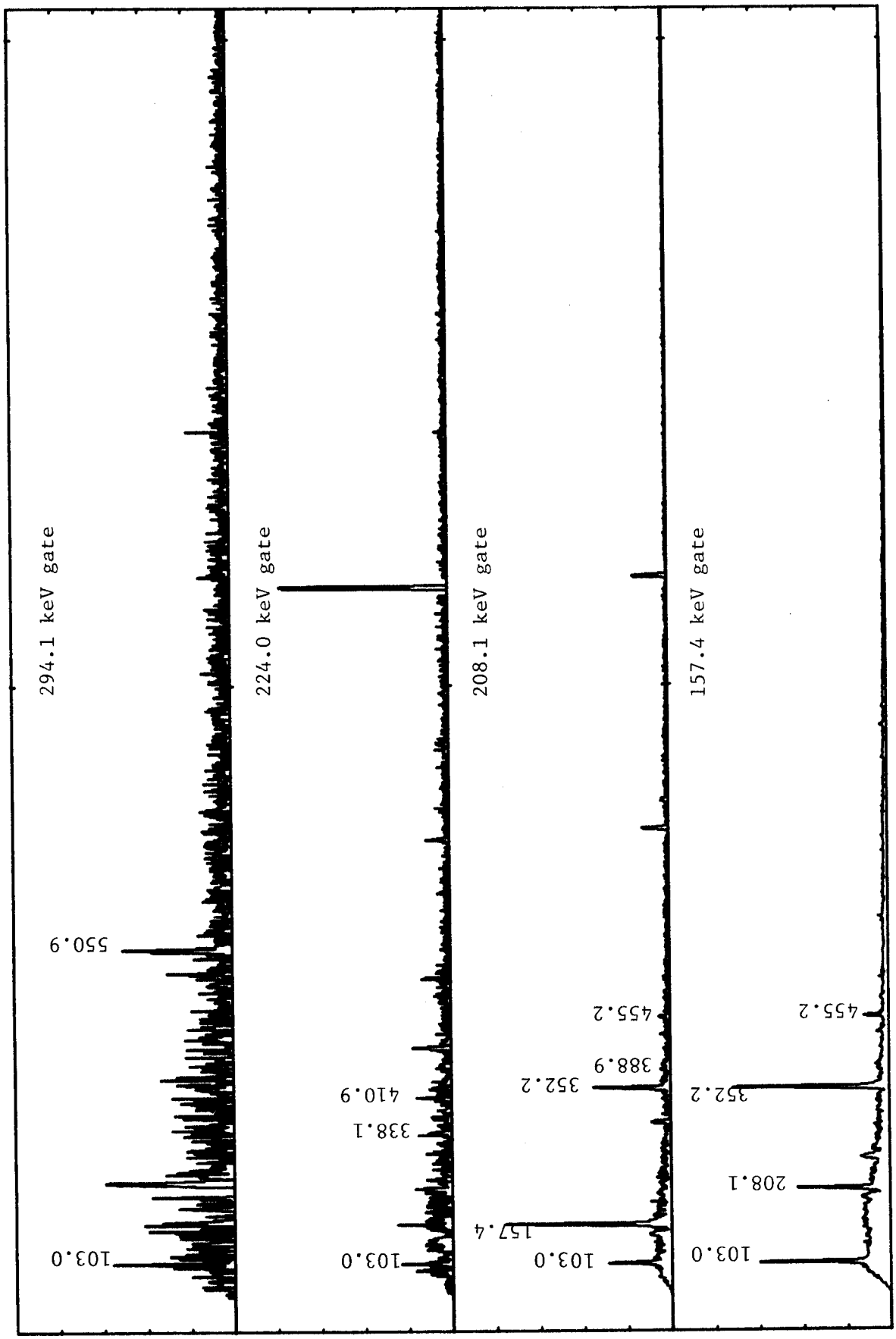

Figure B-2 continued.

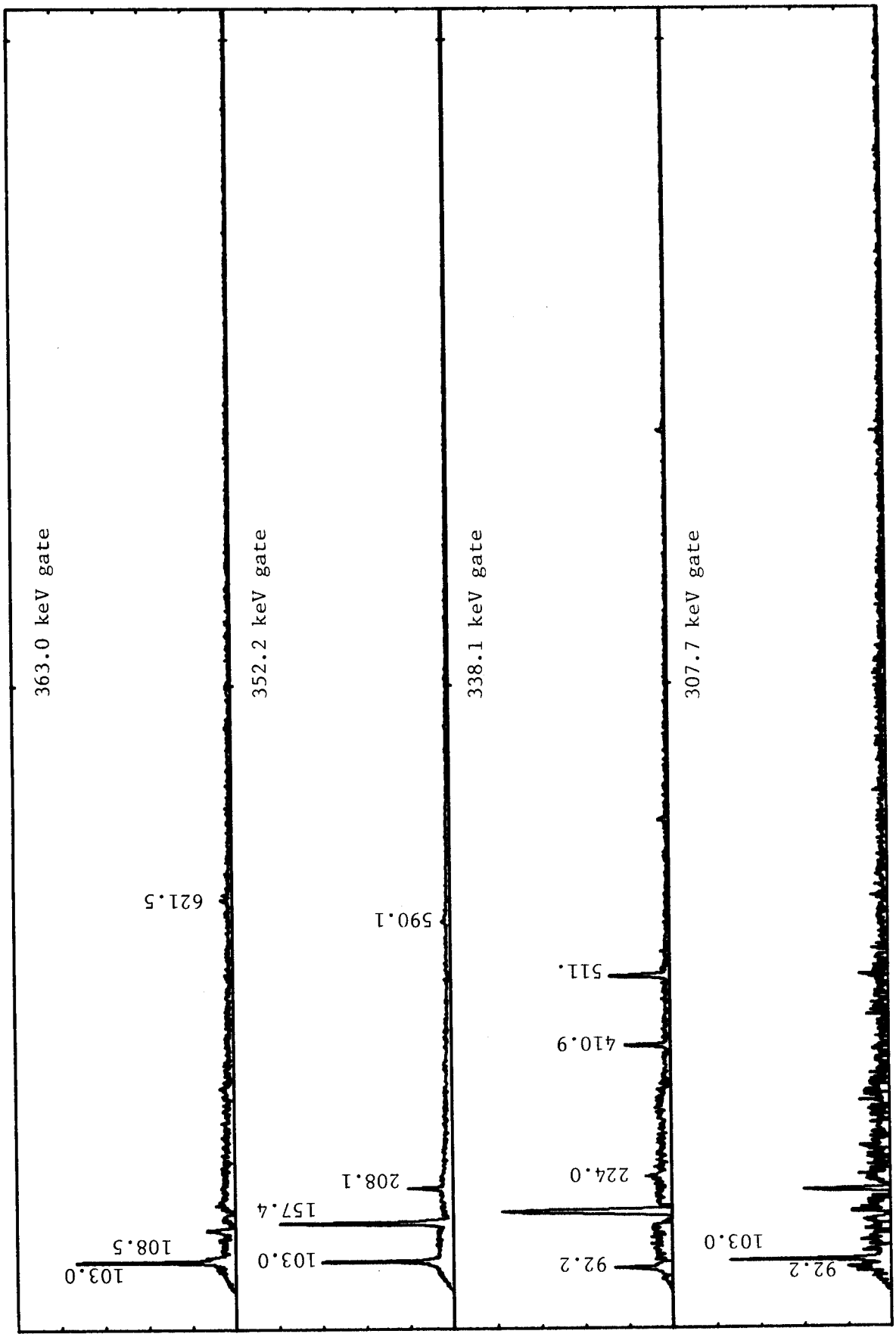

Figure B-2 continued.

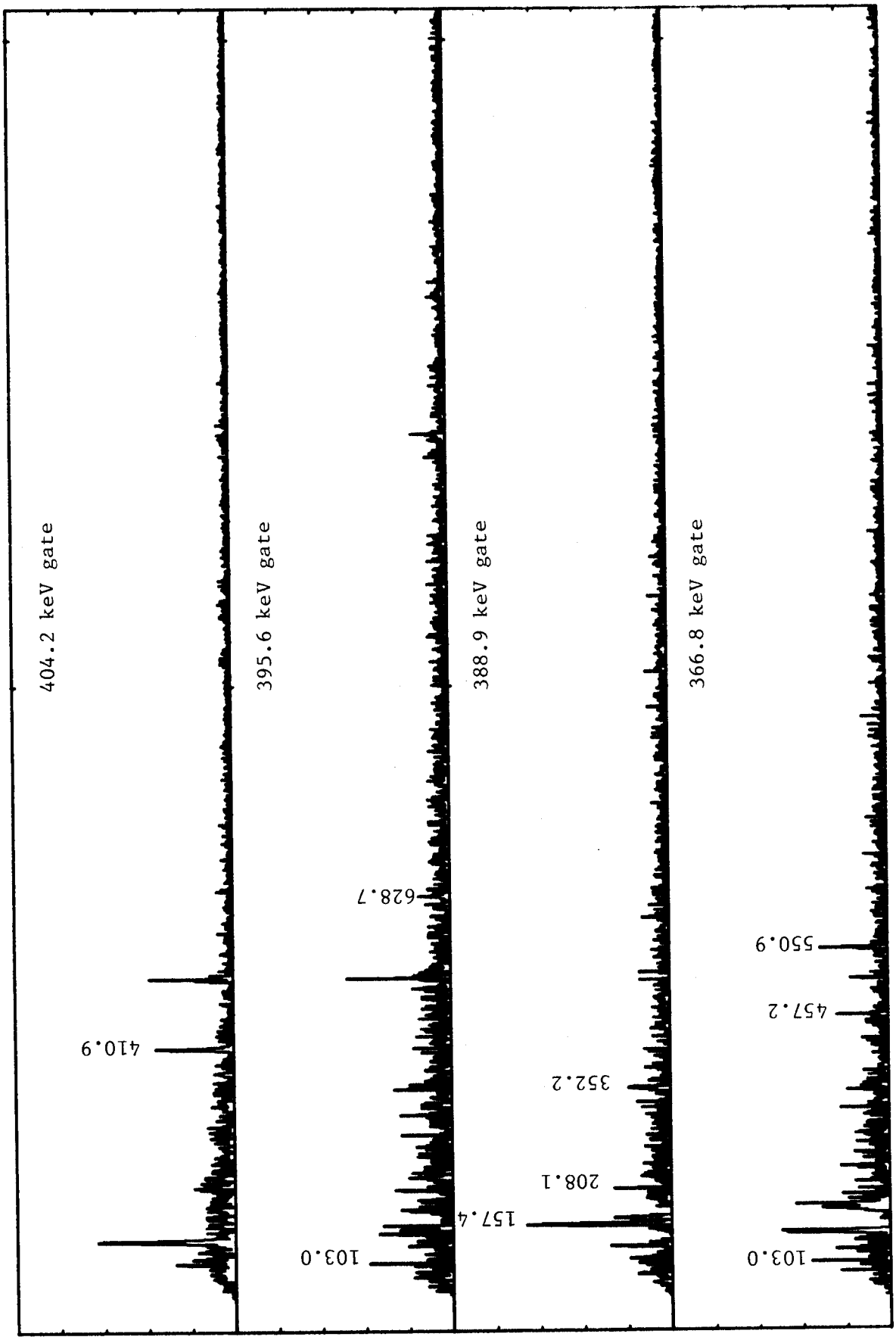

Figure B-2 continued.

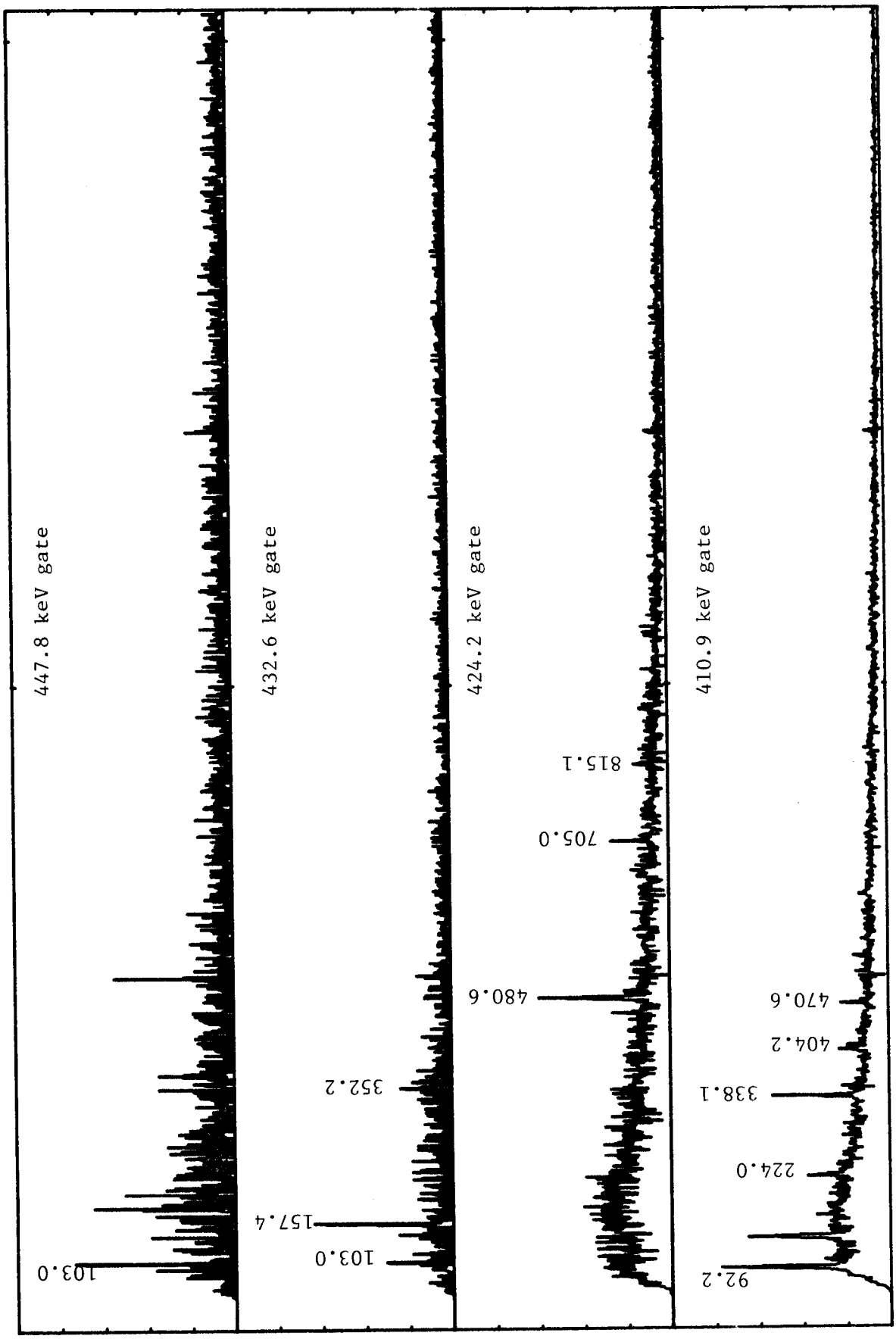

Figure B-2 continued.

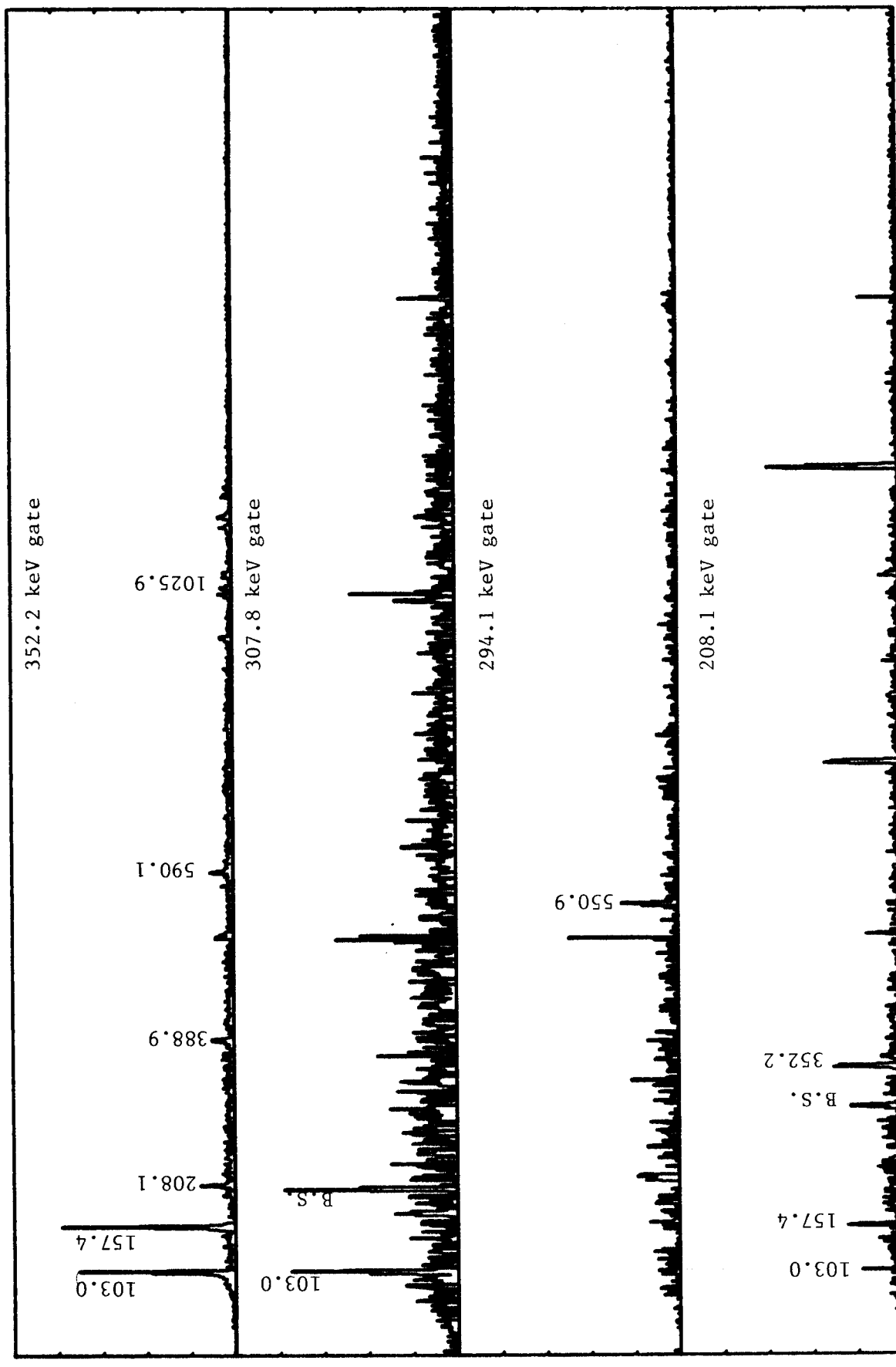

Figure B-1 continued.

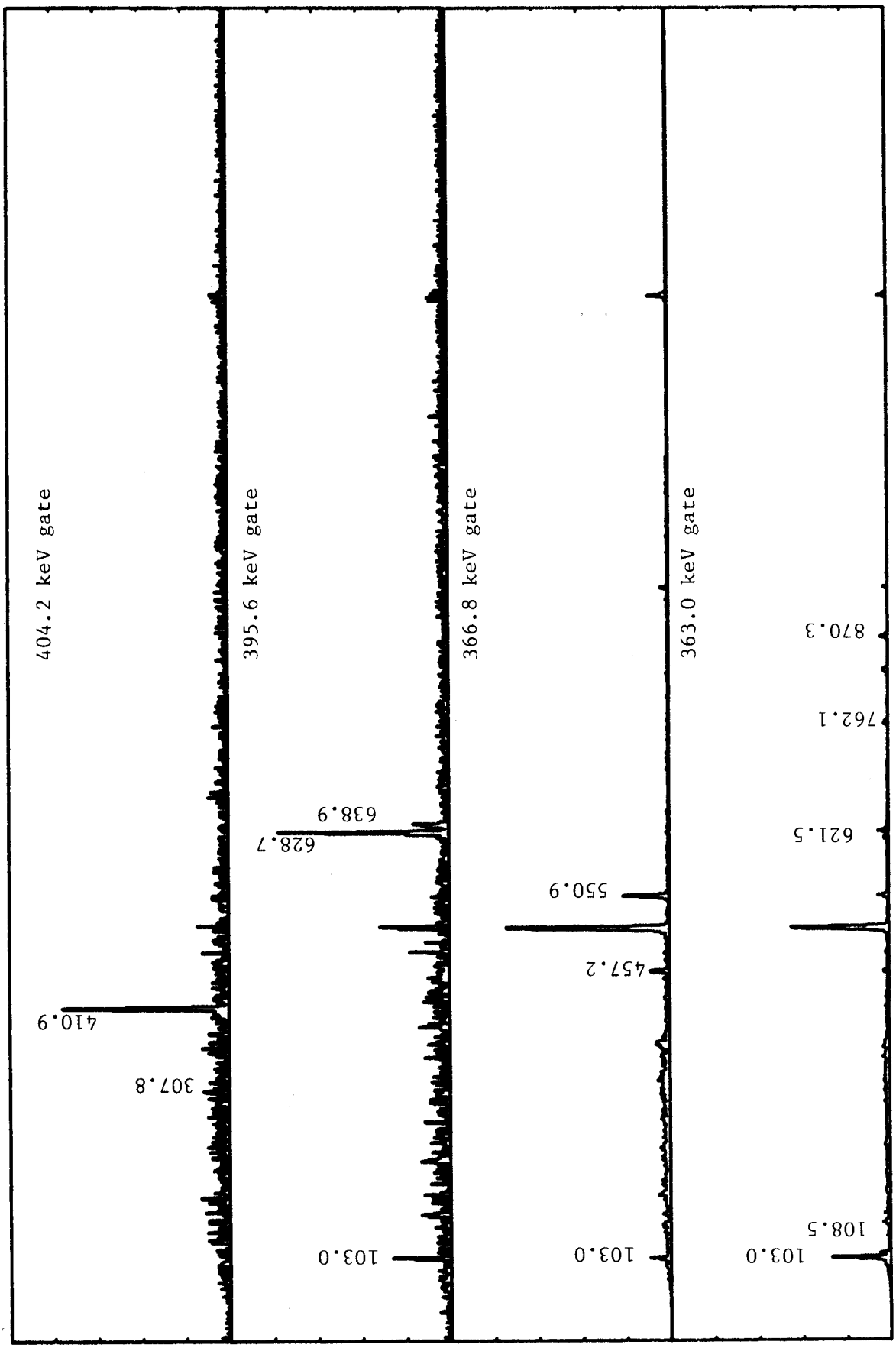

Figure B-1 continued.

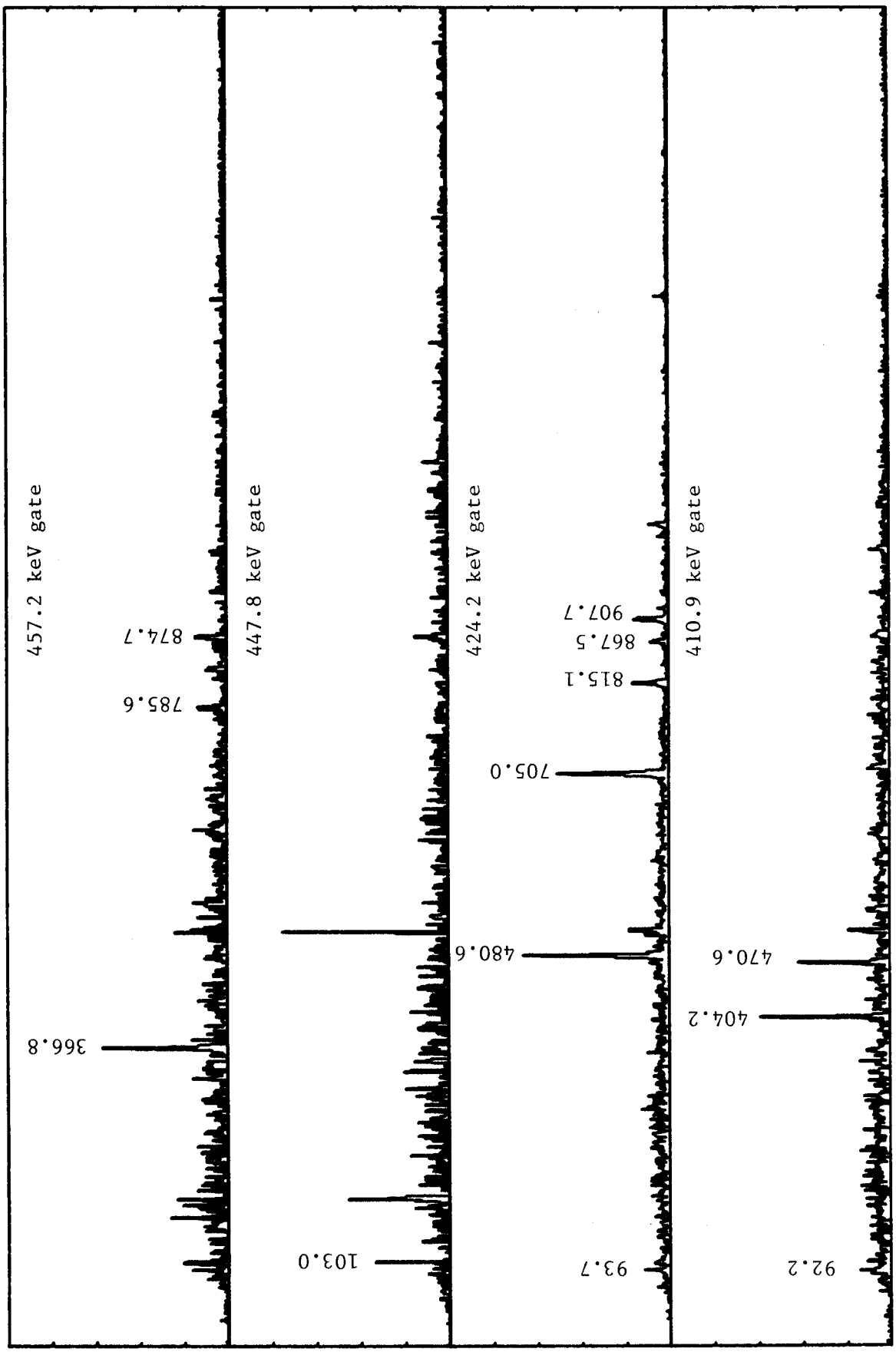

Figure B-1 continued.

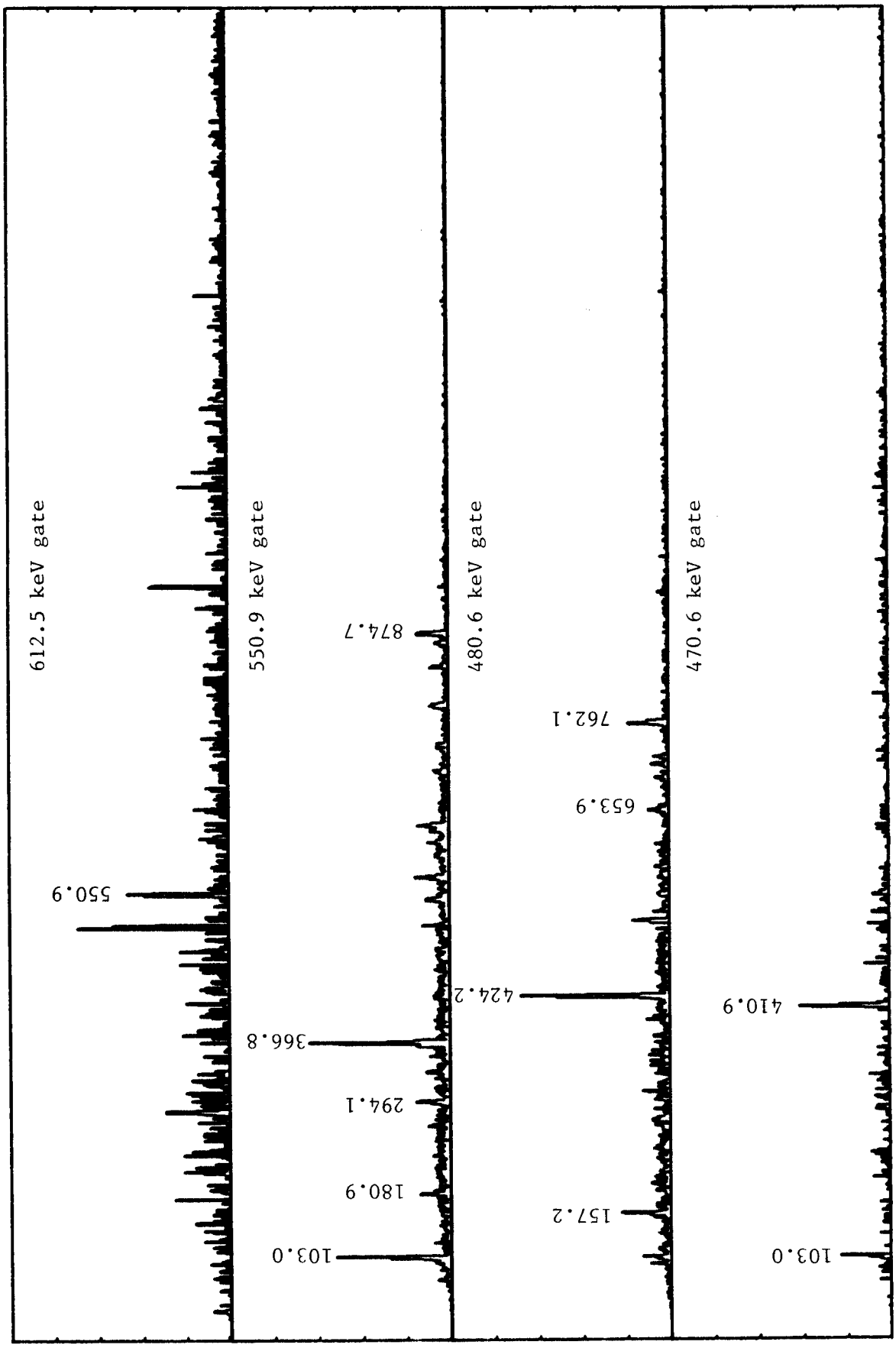

Figure B-1 continued.

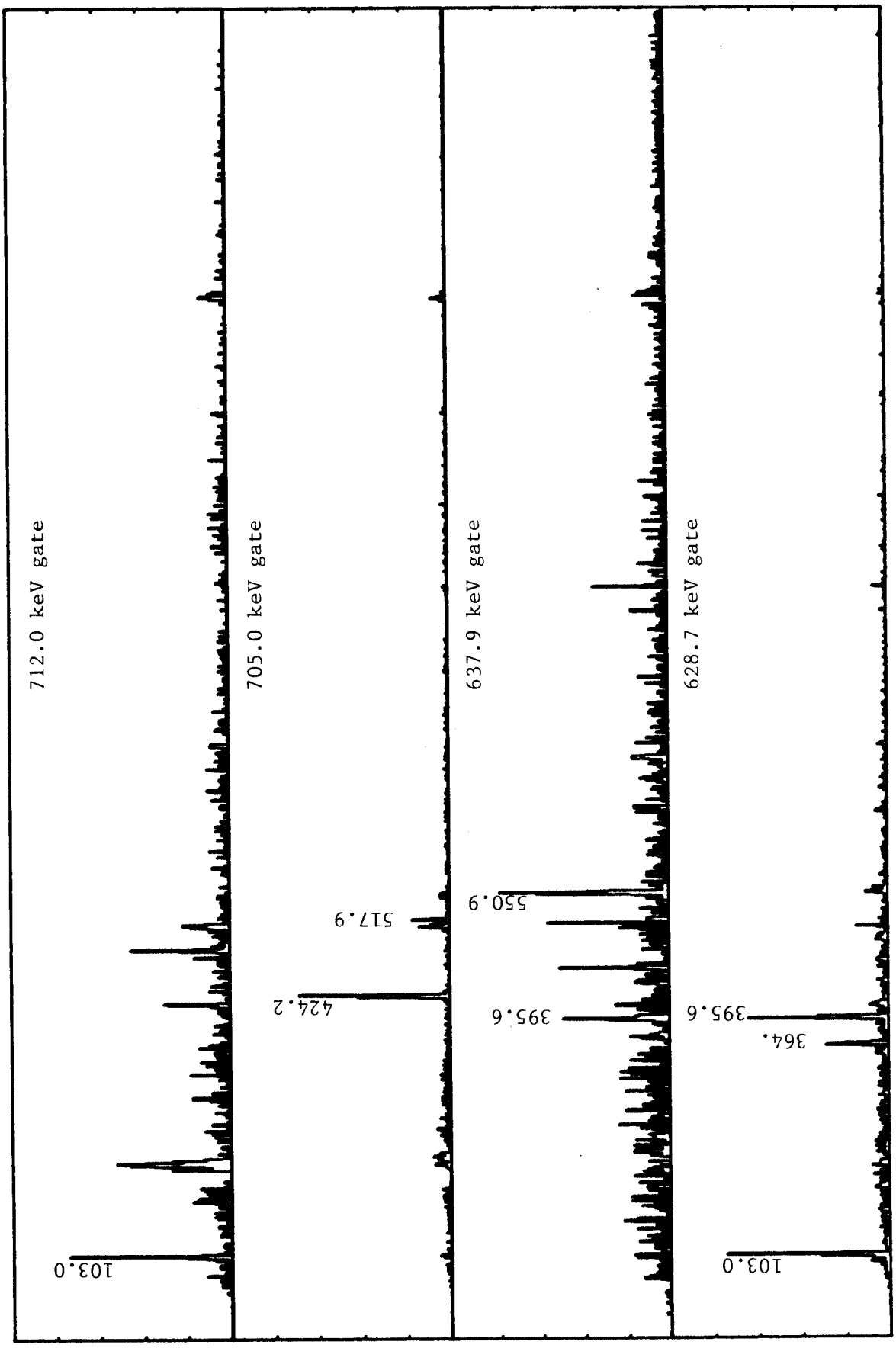

Figure B-1 continued.

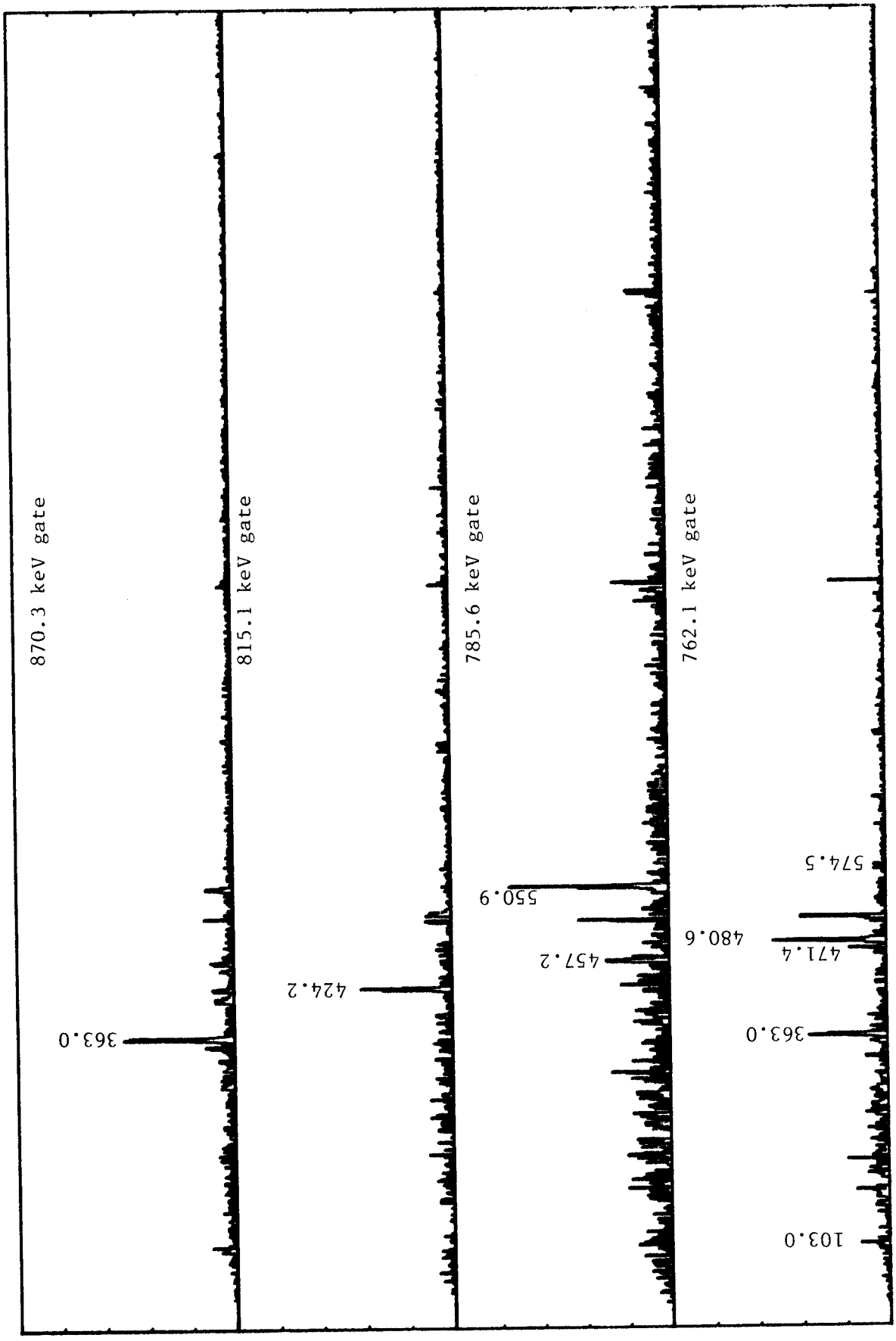

Figure B-1 continued.

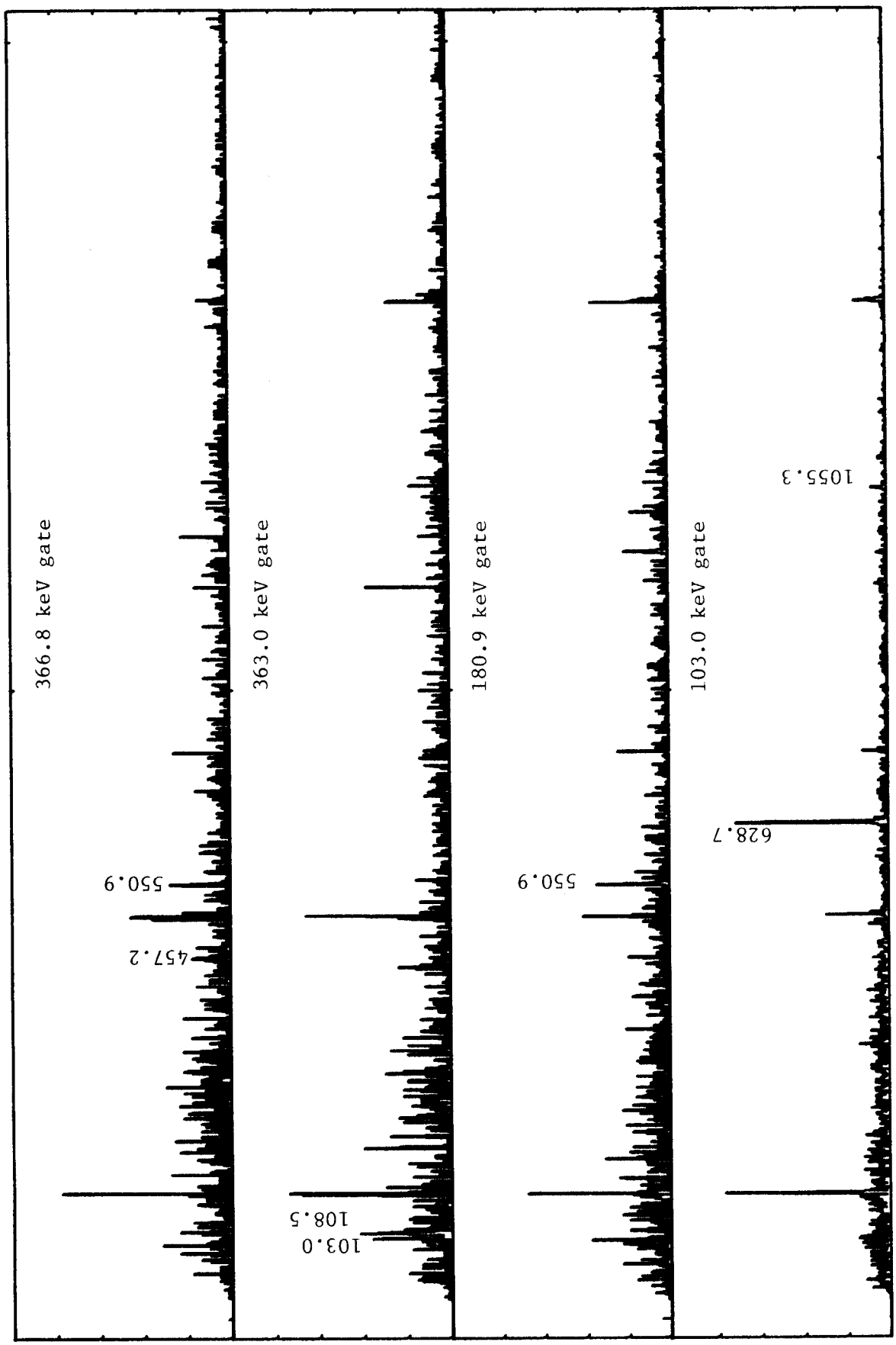

Figure A - continued.

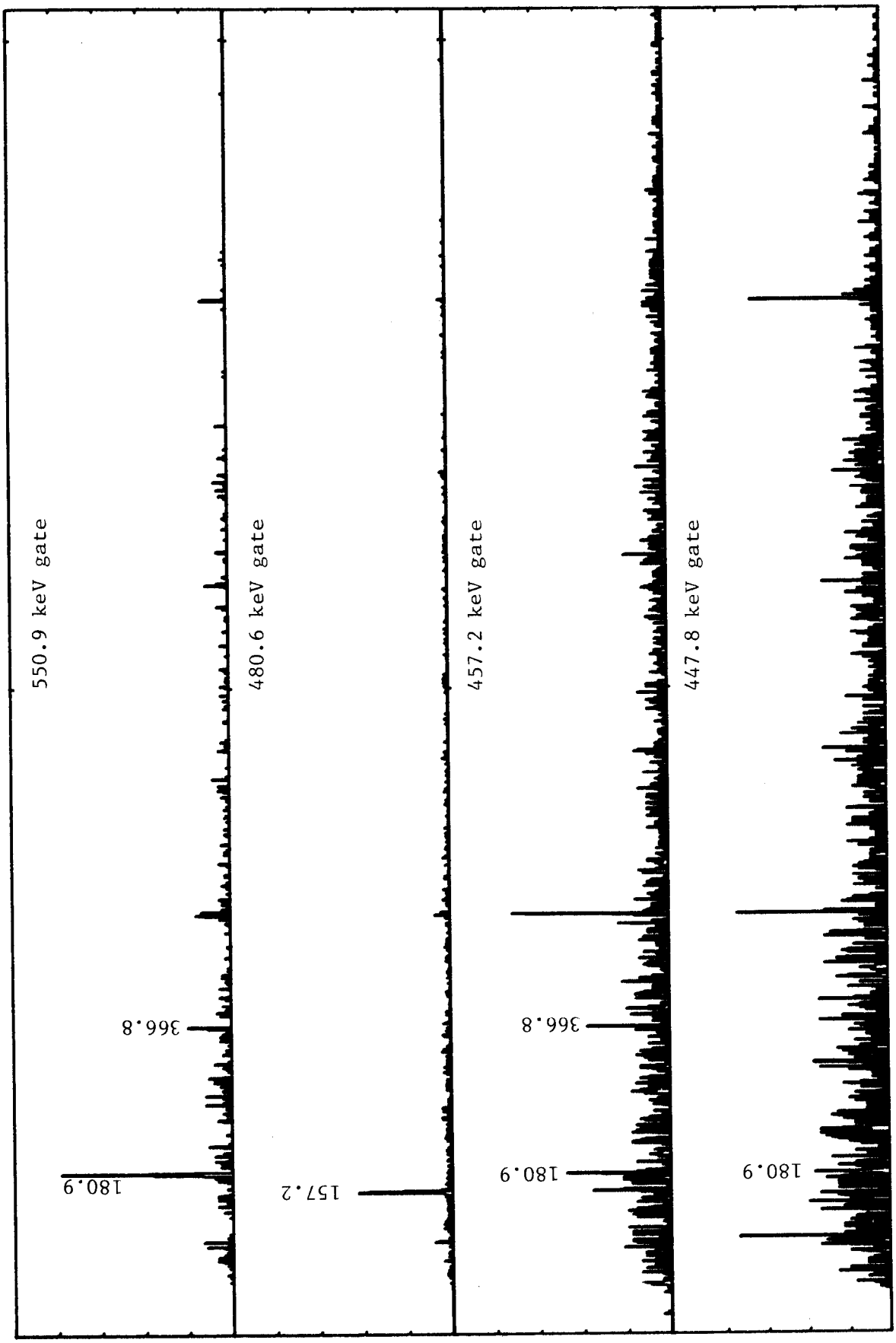

Figure A - continued.

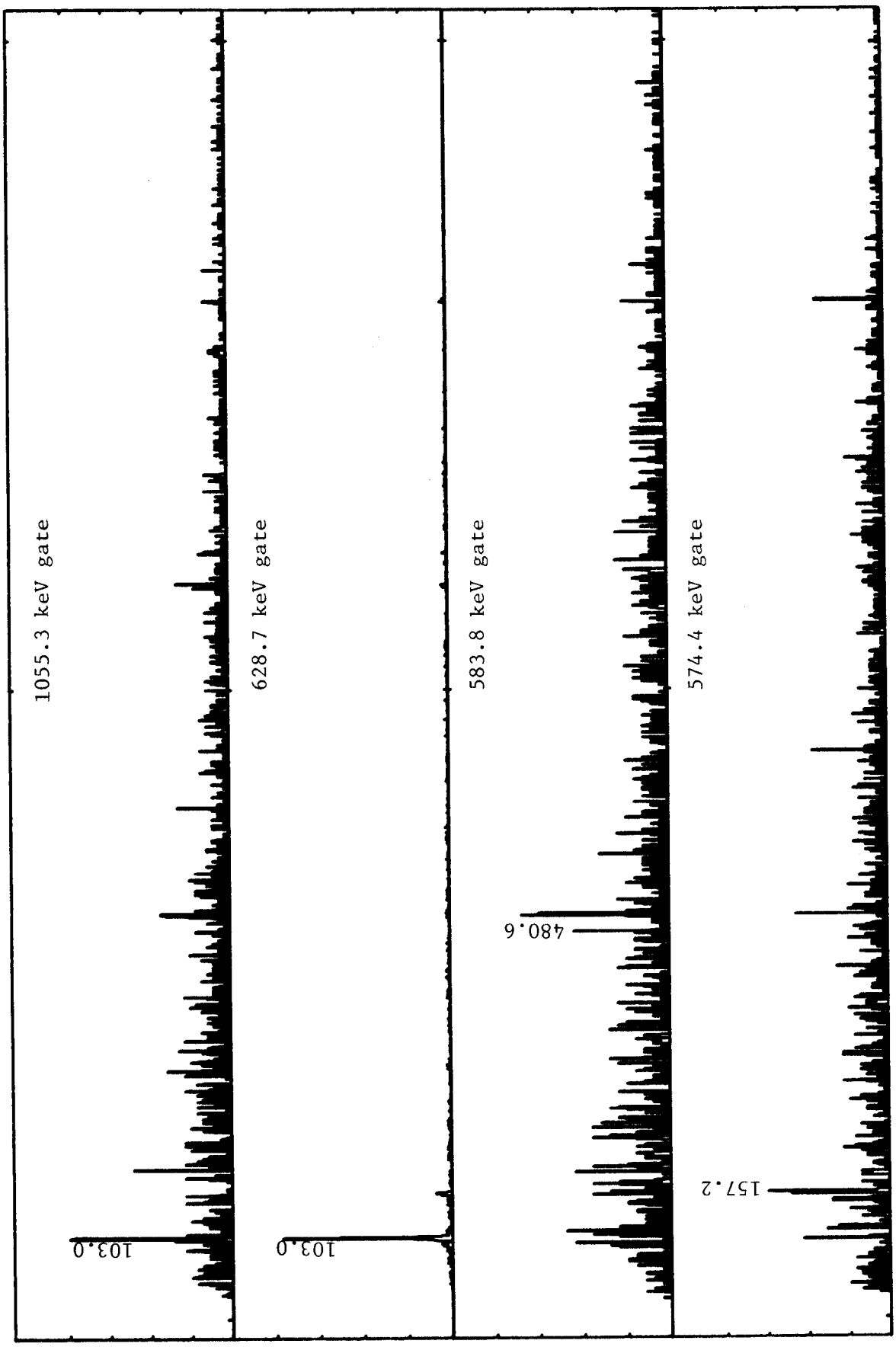

Figure A - continued.

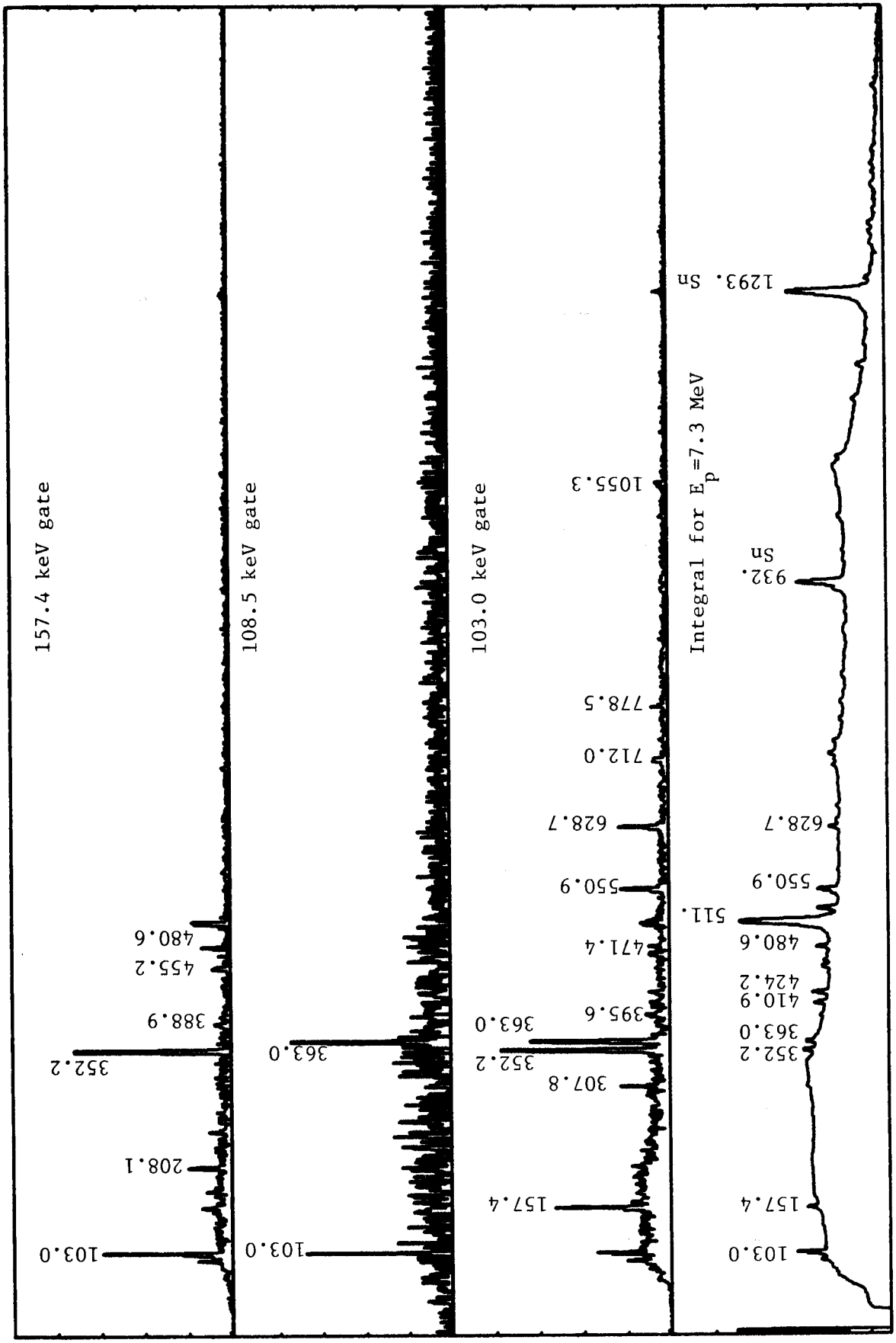
157.4 keV gate
103.0
208.1
352.2
388.9
455.2
480.6
108.5 keV gate
103.0
363.0
103.0 keV gate
157.4
307.8
352.2
363.0
395.6
471.4
550.9
628.7
712.0
778.5
1055.3
Integral for E_p=7.3 MeV
157.4
103.0
352.2
363.0
410.9
424.2
480.6
511.
550.9
628.7
932.
Sn
1293. Sn

Figure B-1 .

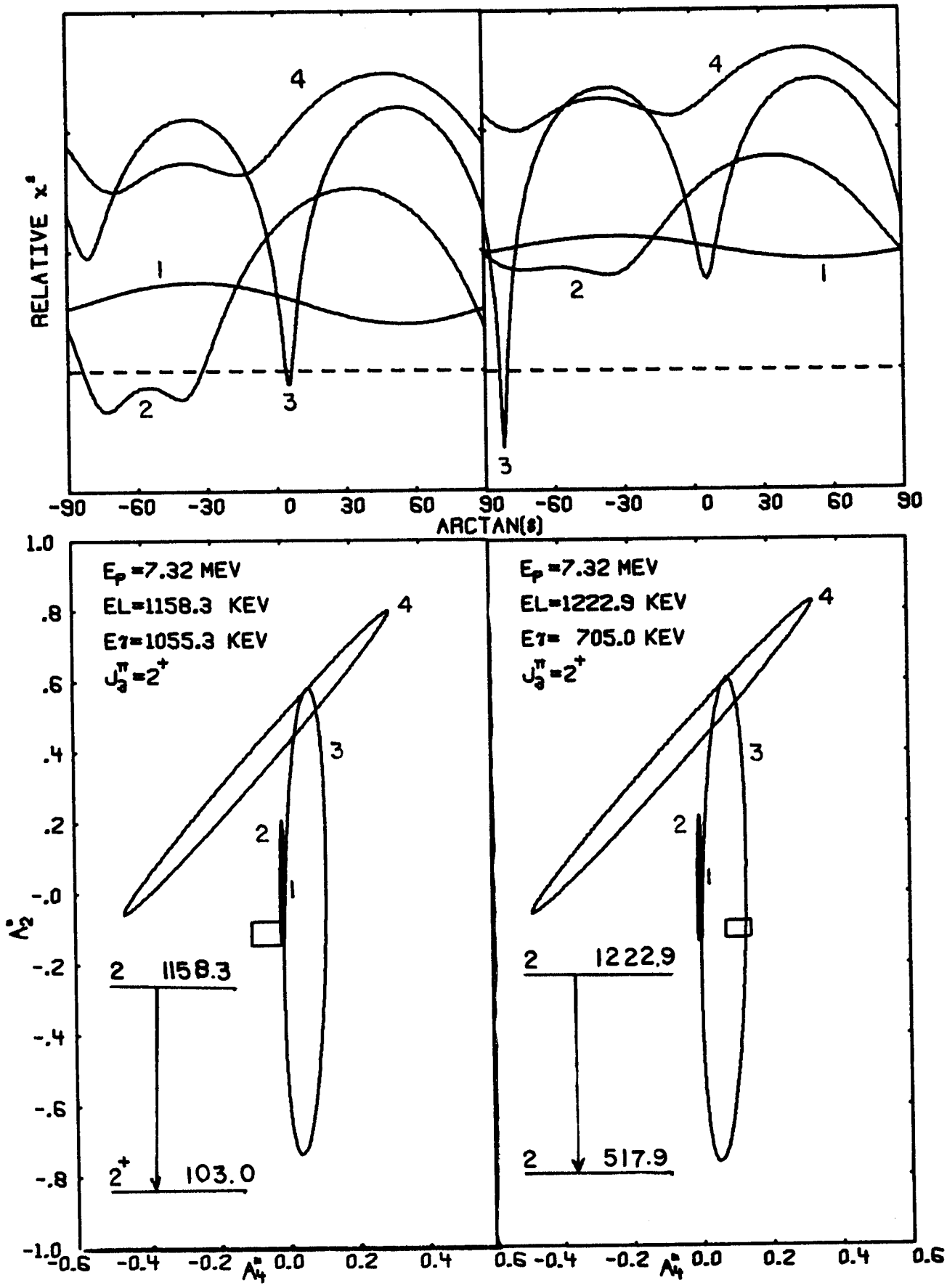

Chi square and delta ellipse plots for the 1055.3 and 705.0 keV gamma rays.

Figure VII-19.

VIII. SUMMARY AND CONCLUSIONS

The γ-ray decays of the excited states of ^{116}Sb below 1.5 MeV of excitation have been studied via the electron-capture decay of ^{116}Te and the in-beam ^{116}Sn(p,nγ)^{116}Sb reaction. Nineteen of the γ rays observed in the in-beam studies were also observed in the electron-capture decay. The Ge(Li)-Ge(Li) γ-γ coincidence technique used both on- and off-line was very useful in the placement of γ rays in the level scheme. Many weak γ rays were placed in the level scheme with the coincidence information which otherwise might not have been placed. Also, the coincidence information is very useful in the determination of which γ rays are doublets. There appear to be at least ten pairs of γ rays, some completely unresolvable, which are within one keV of the same energy. These unresolvable doublets caused many false starts in constructing the excited state level scheme.

The combined use of cross-section ratios and γ-ray angular distributions is an excellent method of determining unique spin assignments up to approximately one MeV of excitation. The γ-ray angular distributions are very useful for states with J = 1, 2, 3 and sometimes 4, as these states are fed strongly enough that very accurate measurements of their intensities may be made. Those states with $J \geq 3$ are well suited to cross-section ratio determination of their spins, as the relative differences between theoretical predictions are larger for these spins. Neither method can be used to determine the parity as the experimental errors are much larger than the required sensitivities needed to make parity determinations. There appears to be a breakdown in the ability of MANDY to handle relative cross-section ratios at

excitations above one MeV, as the experimental values are much less than predicted in this region. A possible explanation for these deviations is that above one MeV many levels exist which cannot be distinguished with our present methods and therefore these levels cannot be used explicitly as extra exit channels in MANDY, thereby causing the predictions for the observed states to be much too large.

Although the results reported here produce some new insights into the systematics of this region near the Z=50 closed shell, more information is needed before a good understanding of the behavior of the nuclei in this region can be obtained. The shell model structure of the states of ^{116}Sb cannot be inferred from the available data. With more data on this nucleus (e.g. internal conversion electron data) and systematics of the other Sb odd-odd nuclei the structure may become more evident.

REFERENCES

REFERENCES

1. D. O. Elliot et al., Phys. Rev. 5, 202 (1972).

2. W. B. Chaffee, Thesis, Michigan State University, 1974.

3. B. G. Diselev, V. R. Burmistrov, Yadern. Fiz., 8, 1057-62 (Dec. 1968).

4. O. Rahmouni Le Journal De Physique, 29, 550 (1968).

5. R. W. Fink, G. Anderson and J. Danstele, Arkiv. Fysik., 19, 323 (1961).

6. C. Ekstrom et al., Nucl. Phys. A226, 219-228 (1974).

7. W. Hauser, H. Feshbach, Phys. Rev., 87, 366 (1952).

8. E. Sheldon and D. M. Van Patter, Rev. Mod. Phys., 38, 143 (1966).

9. E. Sheldon and P. Ganterbeing, J. Appl. Math. Phys. (ZAMP) 18, 397.

10. E. Sheldon and R. M. Strang, Comp. Phys. Comm., 1, 35, (1969).

11. MANDY computer program written by E. Sheldon and D. M. Van Patter, Rev. Mod. Phys., Vol. 38, #1, Jan. 66.

12. K. L. Kosanke, et al., Annual Report, Michigan State University Cyclotron, page 45 (1970,71).

13. CS8N T. Sikkeland and D. Lebeck University of California, Berkeley.

14. Oak Ridge National Laboratory, 1972 Mass Compilation.

15. R. S. Hager and Seltzer, Nuclear data, Vol. 4, Numbers 1 & 2, Feb. 1968.

16. E. A. Auerbach, 'ABACUS-II', Brookhaven National Laboratory, Preprint BNL-6562.

17. F. Perey and B. Buck, Nucl. Phys. 32, 353 (1962).

18. O. Rahmouni, Compt. Rend., Ser. A & B 267: 736,8 (Oct. 7, 1968).

19. Edited by K. Siegbahn, Alpha-, Beta- and Gamma-ray Spectroscopy, Vol. 2, page 905, R. E. Bell.

20. GADFIT, computer code written by R. A. Warner, Michigan State University Cyclotron Laboratory, unpublished.

21. J. T. Routti and S. G. Prussin, Nucl. Instr. and Meth., 72, 125 (1969).

22. F. Perey, Direct Interaction and Nuclear Reaction Mechanisms, (Gordon and Breach, Science Publishers Inc., New York, 1963).

23. R. C. Greenwood et al., Nuclear Instruments and Methods, 77 (1970) 141, 158.

24. R. G. Helmer et al., Nuclear Instruments and Methods 96 (1971) 173,196.

25. J. B. Marion, Nuclear Data A4, 301-319 (1962).

26. R. J. Gehrke, et al., Idaho Nuclear Corporation, Idaho Falls, Idaho.

27. G. Berzins and D. Berry, private communication.

28. G. Berzins et al., Nucl. Phys. A104, 241,262 (1967).

29. R. Helmer, Phys. Rev., 155, 1263,4 (1967).

30. M. H. Brennan and A. M. Berstein, Phys. Rev., 120, Number 3, 927,33 (1960).

31. J. P. Schiffer, Annals of Physics, 66, 798,809 (1971).

APPENDICES

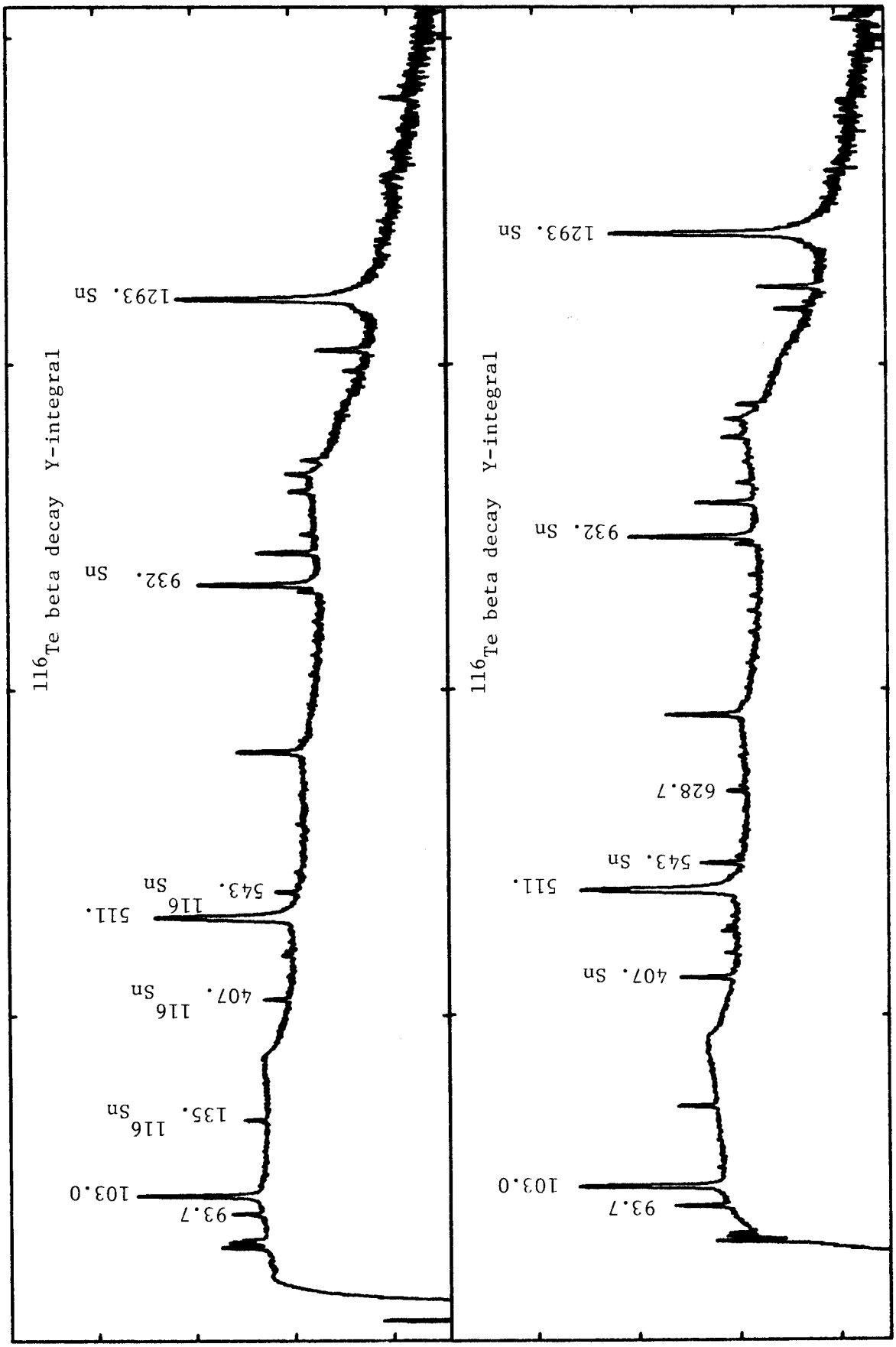
116Te beta decay Y-integral
1293. Sn
932. Sn
543. 116Sn
511.
407. 116Sn
135. 116Sn
103.0
93.7
116Te beta decay Y-integral
1293. Sn
932. Sn
628.7
543. Sn
511.
407. Sn
103.0
93.7

Figure A.

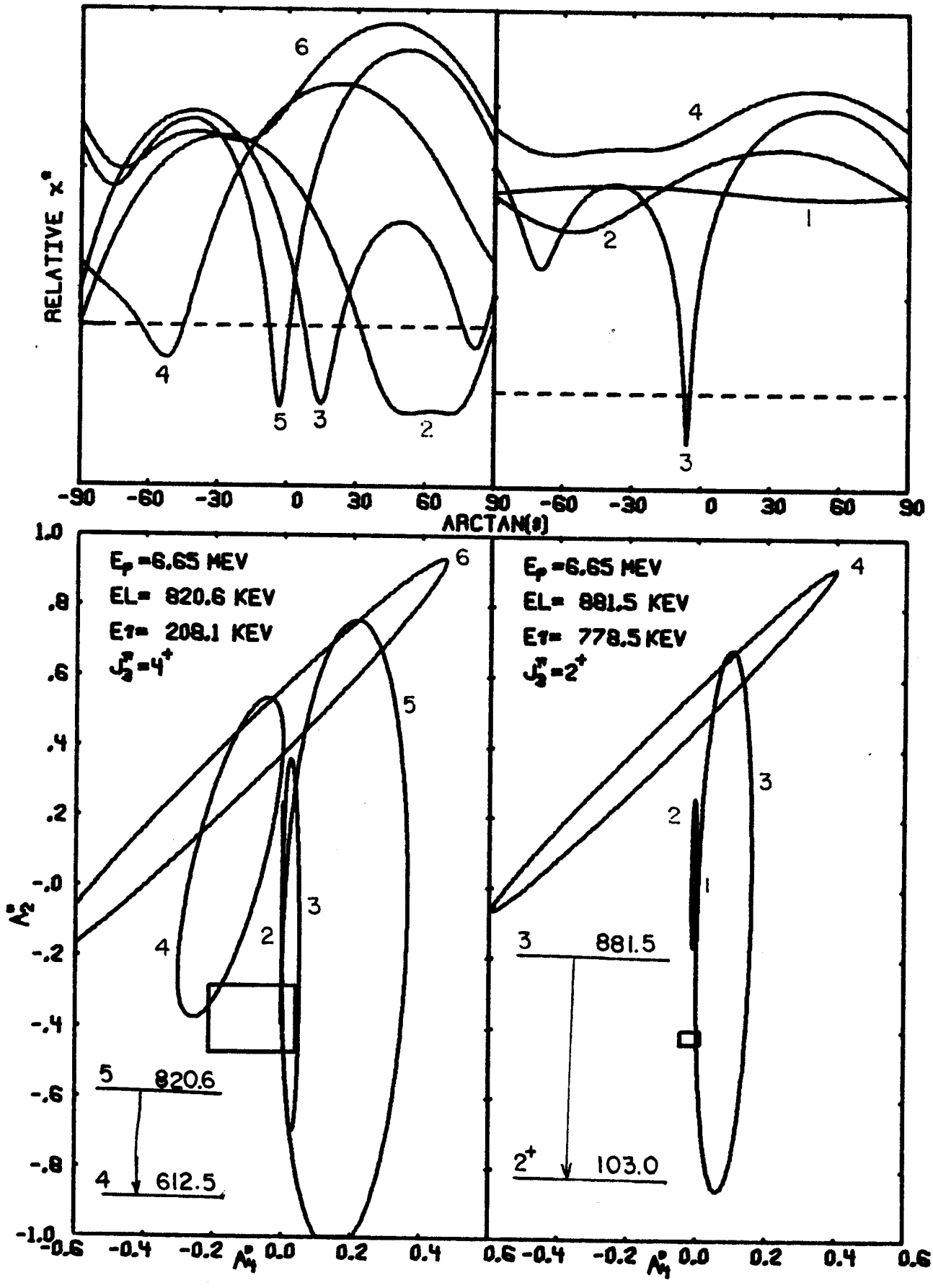

Chi square and delta ellipse plots for the 208.1 and 778.5 keV gamma rays.

Figure VII-15.

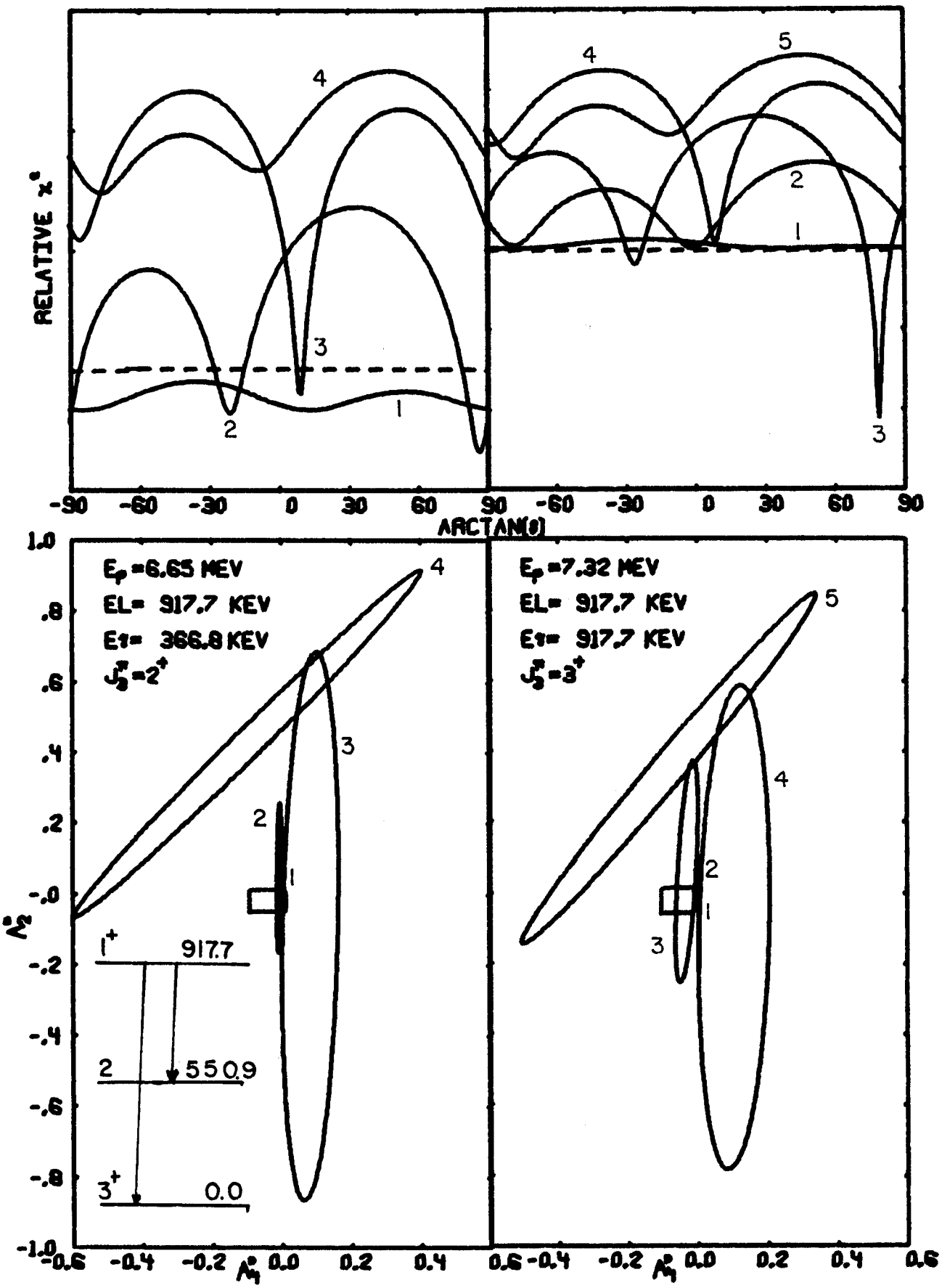

Chi square and delta ellipse plots for the 366.8 and 917.7 keV gamma rays.

Figure VII-16.

The excitation function data in Figure VII-14 show only that the cross section is too high for J = 3, and does not distinguish between J = 1 or 2.

S. E_x = 948.0 keV J = 4

The 294.1 keV γ-ray branch of the decay from the 948.0 keV level has a large negative A_2^* which allows an unambiguous choice of J = 4, as shown in Figure VII-17. Excitation function data indicate a spin of either 4 or 5.

T. Higher Excited States

Fifteen levels were placed using γ-γ coincidence data, at excitation energies ranging from 992. to 1481.1 keV. Although excitation function data and angular distribution data were collected at sufficient excitation energies to produce these states, only three states (1127.2, 1158.3, and 1222.9 keV) have analyzable angular distributions, and most fail to have sufficient data from the excitation function measurements to allow spin assignments to be made with any degree of confidence. These excitation function data are shown in Figure VII-18.

The 395.6 keV transition from the 1127.2 keV level has an analyzable angular distribution as shown in Figure VII-17, which indicates a spin of 2.

The 1158.3 keV level is observed to be fed in beta decay with a log ft of 5.4 which indicates an allowed transition with the spin and parity of the level being either 0^+ or 1^+. Only one of the

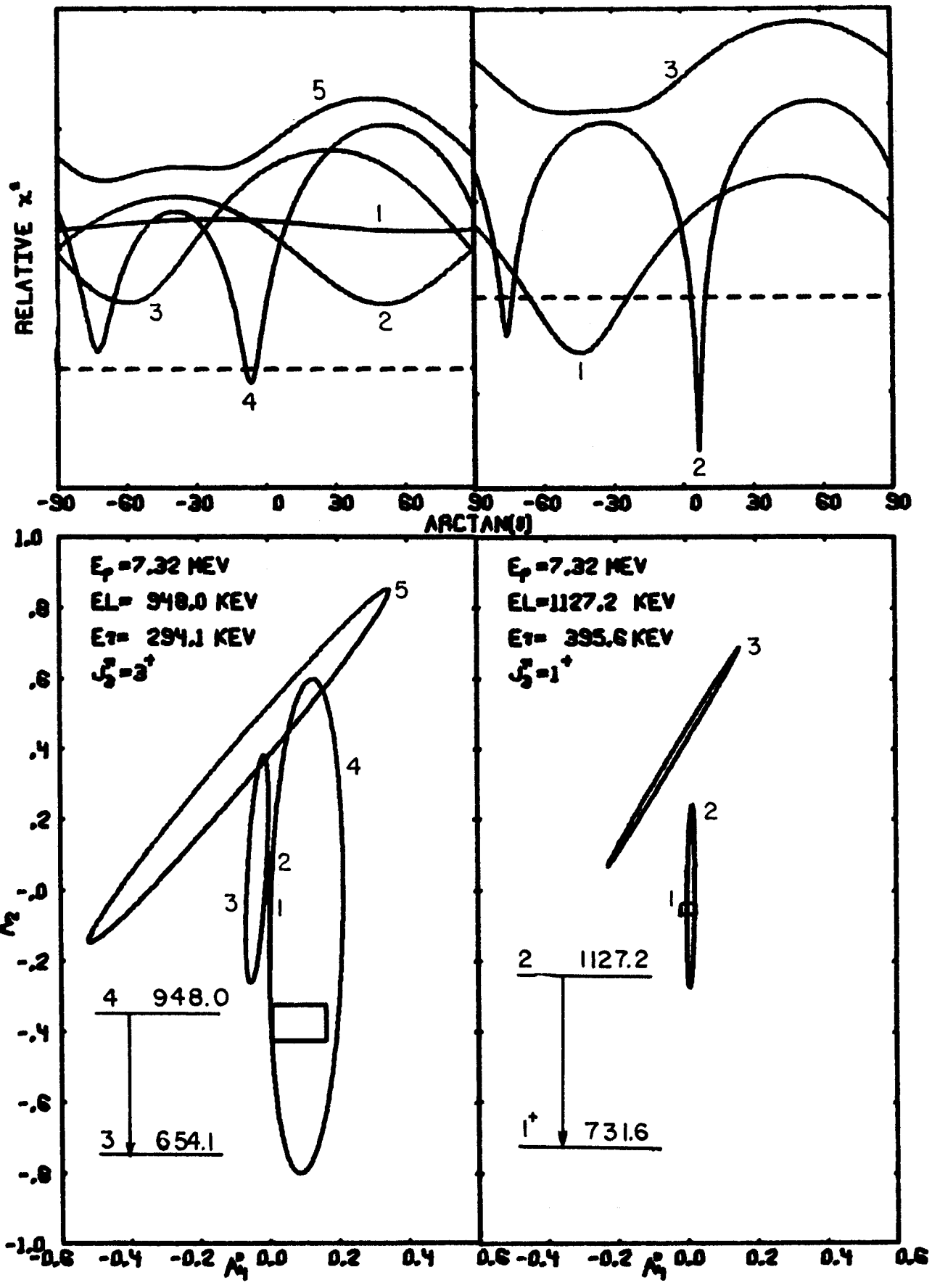

Chi square and delta ellipse plots for the 294.1 and 395.6 keV gamma rays.

Figure VII-17.

Figure VII-18

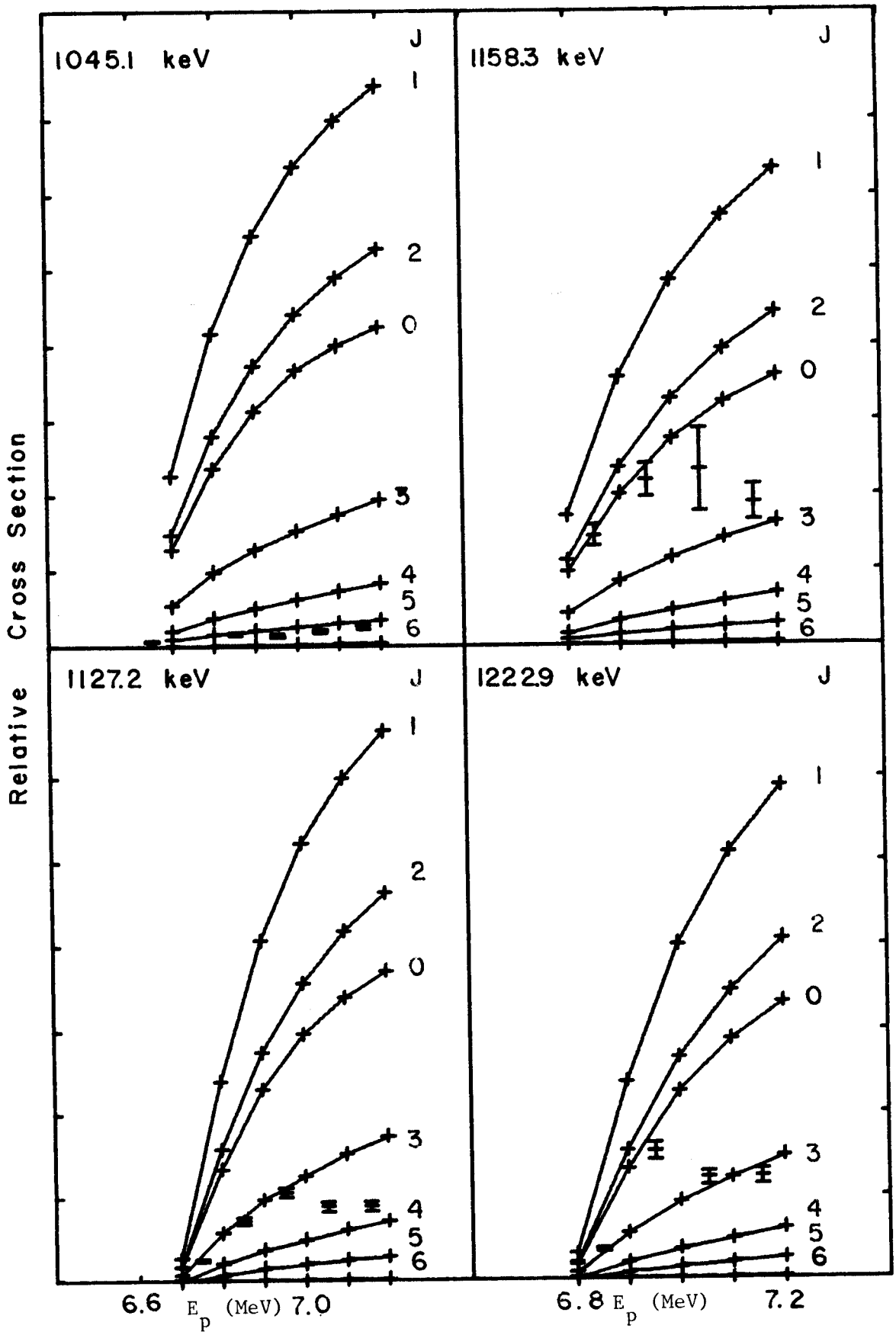

Excitation functions for the 1045.1, 1127.6, 1158.3, and 1222.9 **kev** levels.

three γ rays de-exciting the 1158.3 keV state (1055.3 keV) has an analyzable angular distribution as shown in Figure VII-19, which indicates that J = 1, 2, or 3 are all possible values for the spin. Since the angular distribution is not isotropic and the beta decay is allowed, an assignment of 1^+ is made to the 1158.3 keV level.

The angular distribution of the 705.0 keV gamma ray from the 1222.9 keV level, shown in Figure VII-19, indicates the most likely value for the spin is 3.

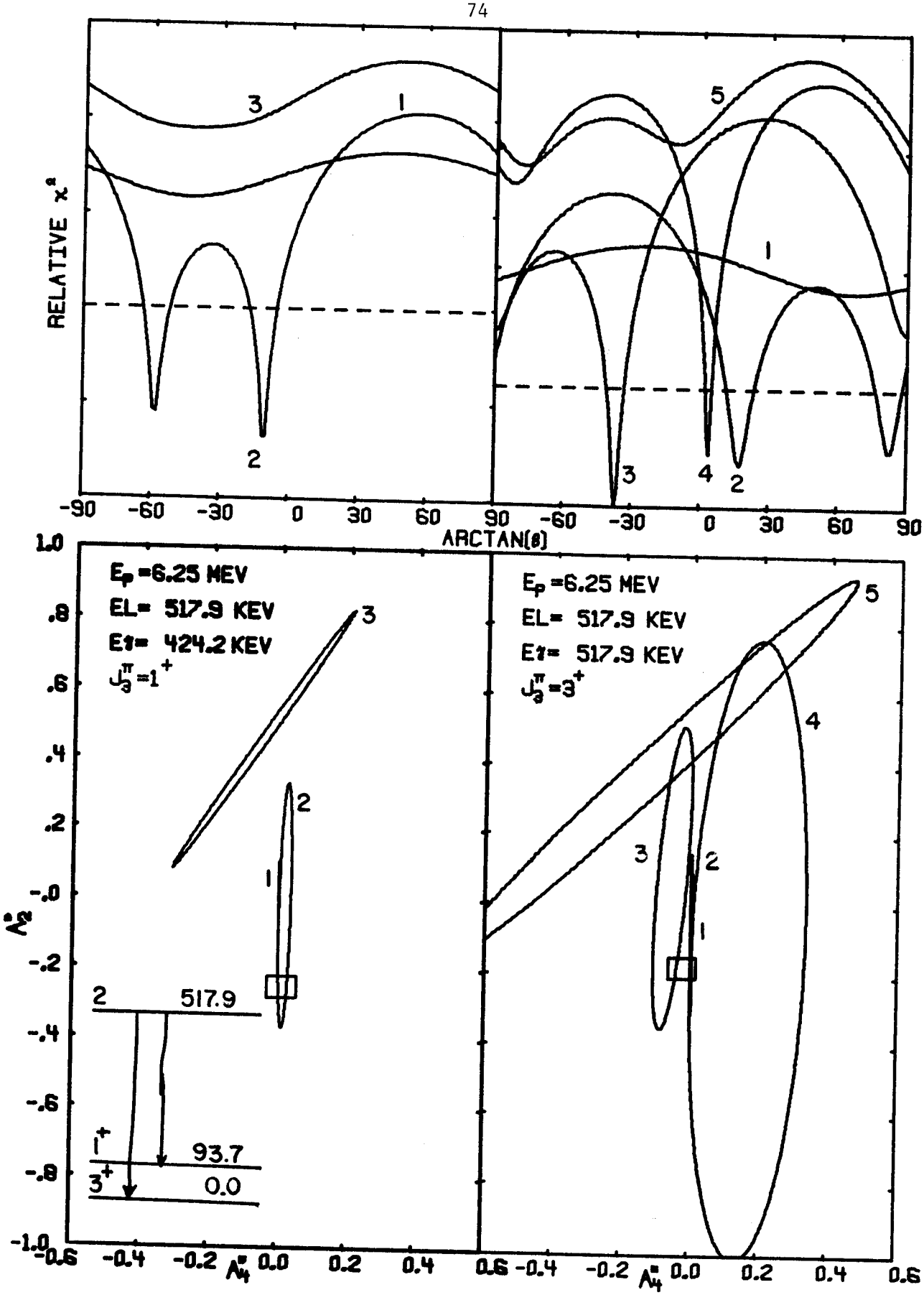

Chi square and delta ellipse plots for the 424.2 and 517.9 keV gamma rays.

Figure VII-7.

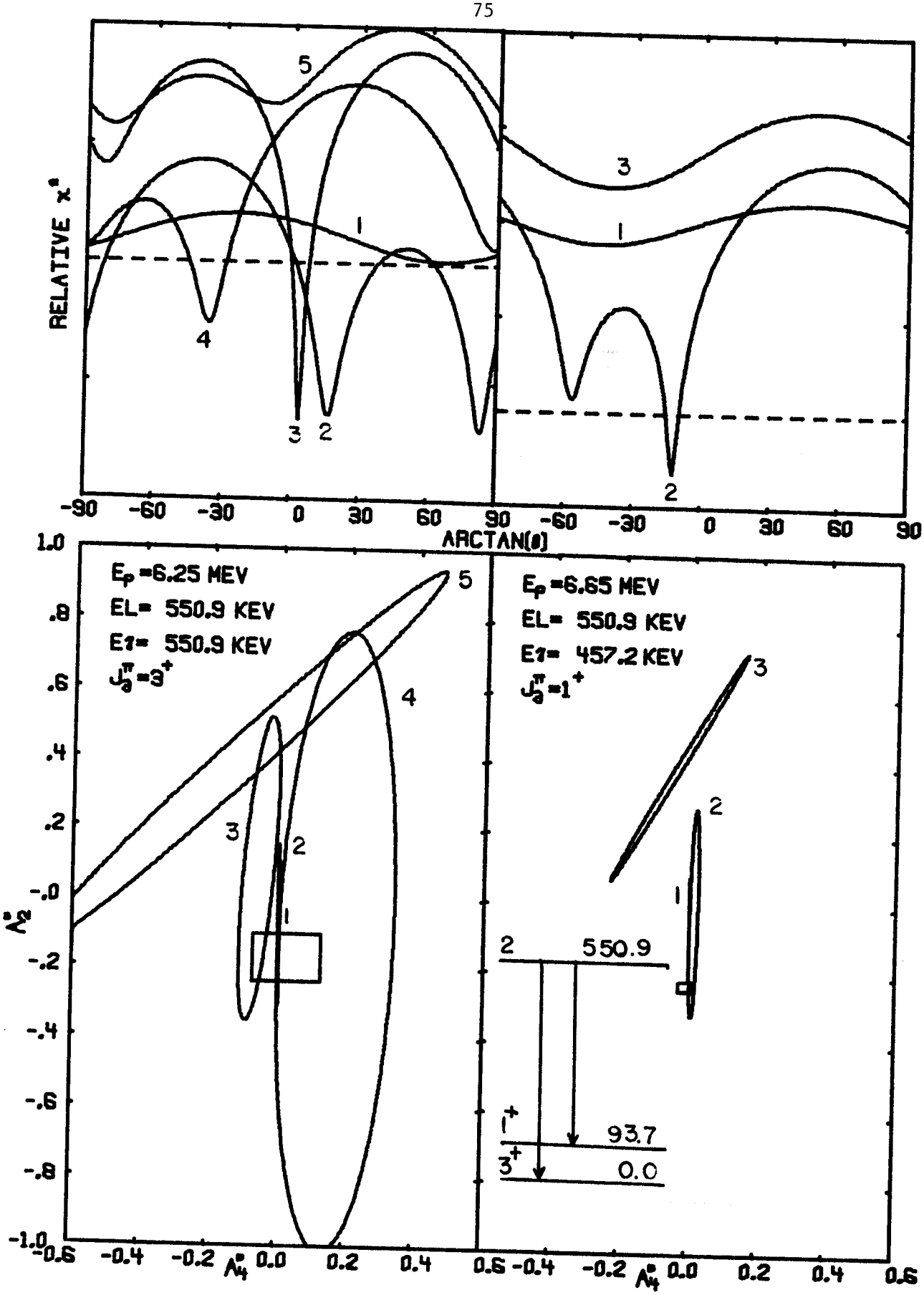

Chi square and delta ellipse plots for the 550.9 and 457.2 keV gamma rays.

Figure VII-8.

J. E_x = 574.4 keV J = 2

Only the 480.6 keV transition from the 574.4 keV level gives an unambiguous angular distribution as shown in Figure VII-9. The other three γ rays are too weak to be useful as shown in Figure VII-9 and Figure VII-10. The 480.6 keV γ ray has a fairly large negative A_2^* making the choice J = 2 most likely. Excitation data (Figure VII-6) also are a reasonable fit to J = 2. The depopulation of this state produces states with J = 1, 2, 3. The best choice for the spin of this state is 2.

K. E_x = 612.5 keV J = 4

The 612.5 keV state is depopulated via the 157.4 keV γ ray. Difficulties were encountered with nearby γ rays when fitting the data. Special care was taken to separate the 158.5 keV γ ray (from the decay of ^{117}Sb) from these data. The 157.2 keV γ ray from the 731.6 keV state could not be resolved and in the angular distribution measured at 6.65 MeV it contributed about 30% of the total intensity. The angular distribution measured, Figure VII-10, allows J = 2, 3, and 4 although it must be assumed that this measurement is perturbed somewhat by the 157.2 keV transition. The excitation function data, shown in Figure VII-11, which are corrected for the intensity of the 157.2 keV γ ray are a reasonably good fit to J = 4. On the basis of the excitation data and the angular distribution, we have made the assignment of J = 4.

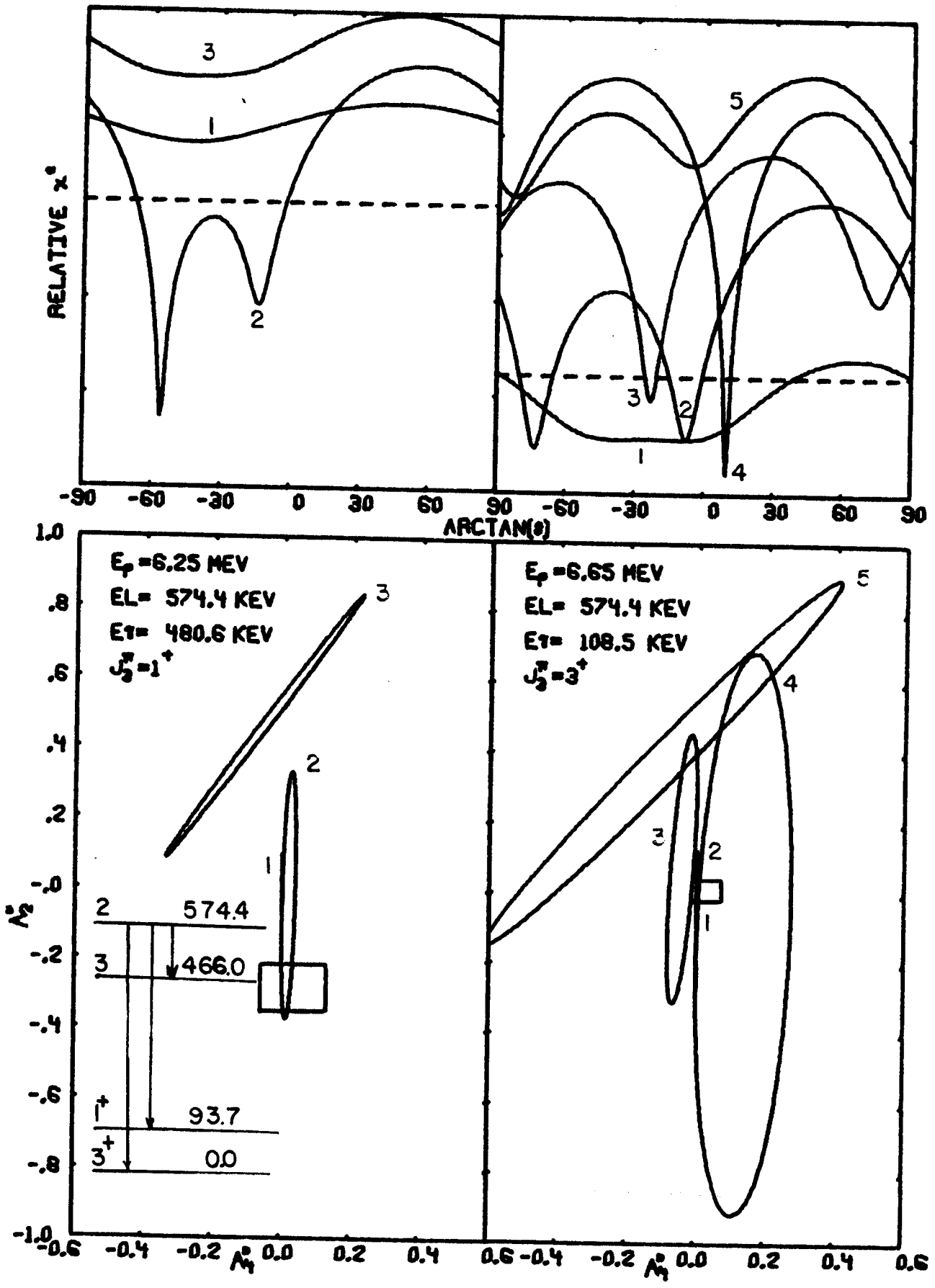

Chi square and delta ellipse plots for the 480.6 and 108.5 keV gamma rays.

Figure VII-9.

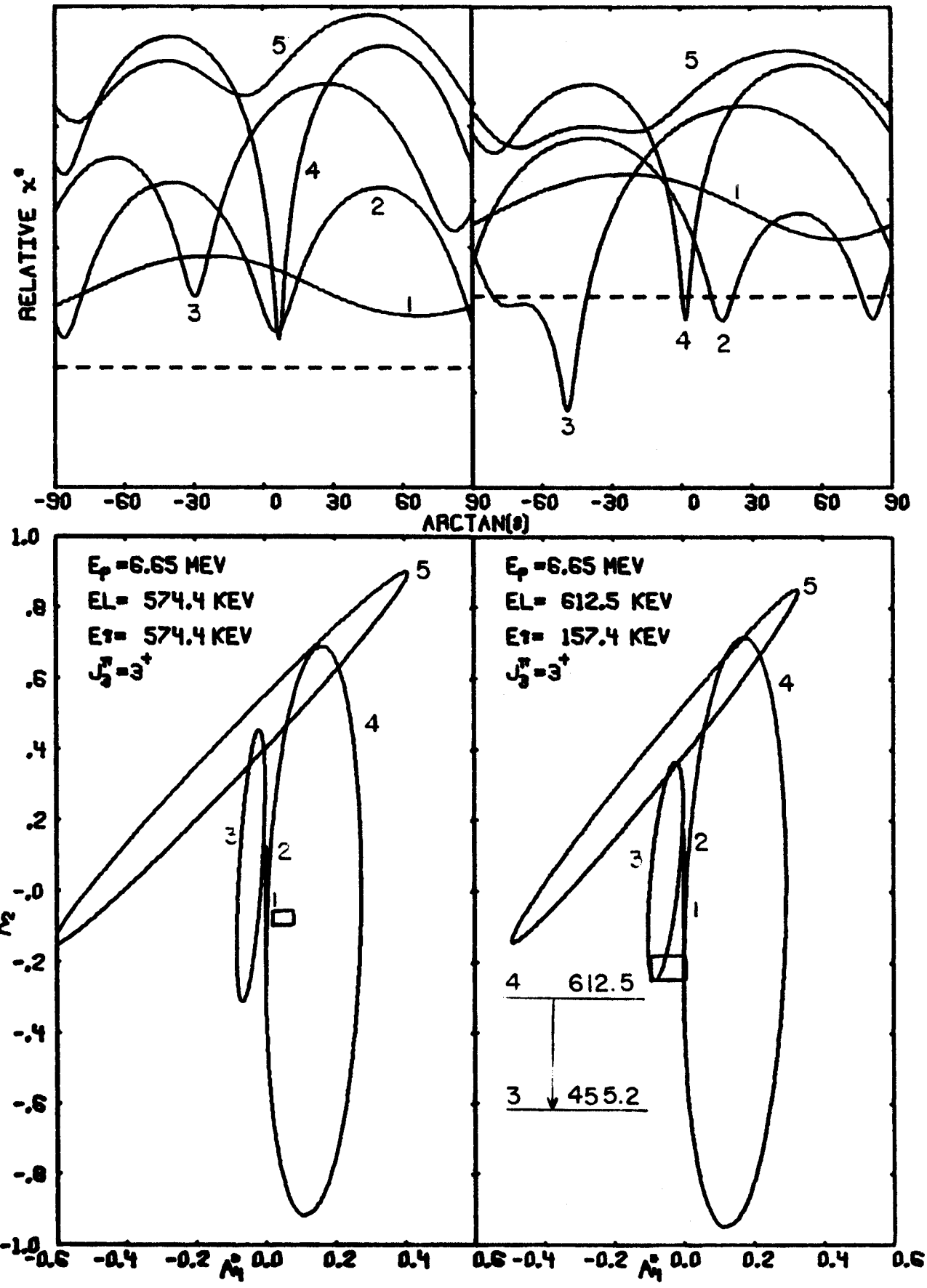

Chi square and delta ellipse plots for the 574.5 and 157.4 keV gamma rays.

Figure VII-10.

Figure VII-11

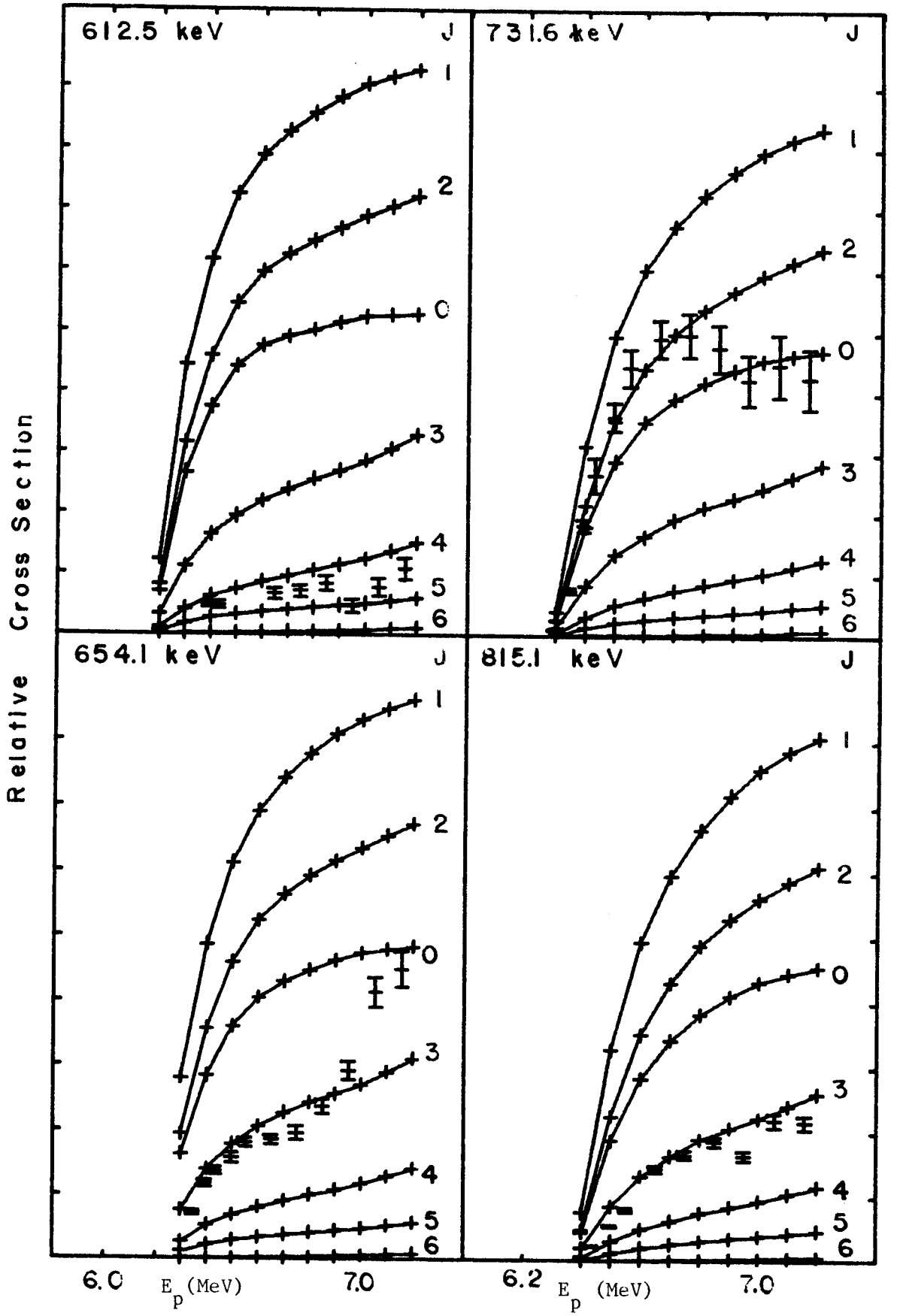

Excitation functions for the 612.5, 654.1, 731.6, and 815.1 keV levels.

L. E_x = 654.1 keV J = 3

For the 654.1 keV level the excitation data (Figure VII-11) give a good fit to J = 3. Neither the 653.9 or the 550.9 keV branch is able to give a good angular distribution as the 653.9 keV γ ray is much too weak, and the 550.9 keV γ ray is part of an unresolvable doublet. At an excitation of 1.0 MeV approximately 45% of the 550.9 keV doublet is produced by the decay of the 654.1 keV state.

M. E_x = 731.6 keV $J^\pi = 1^+$

The beta decay log ft of 5.5 indicates that this level probably has $J^\pi = 1^+$. As shown in Figure VII-12, the angular distribution measurements of the 628.7 and 637.9 keV γ rays are in agreement with this value. The 157.2 keV transition which constitutes 9% of the decay of this level, is part of an unresolved doublet. The intensity for the 157.2 γ ray was calculated from the intensities of the gamma rays which depopulate the 574.4 keV level in the beta decay studies.

N. E_x = 815.1 keV J = 3

The angular distributions of the 712.1 keV gamma ray shown in Figure VII-13 has a very good fit for a J = 3 assignment to the 815.1 keV state, while that for the 404.2 keV γ ray allows values of 2, 3, and 5 for the spin. The excitation function data, shown in Figure VII-11, clearly indicates J = 3. The minimum in χ^2 for J = 3 yield mixing ratios which indicate that both branches are nearly pure ($\tilde{=}$ 99.7%) M1 (E1).

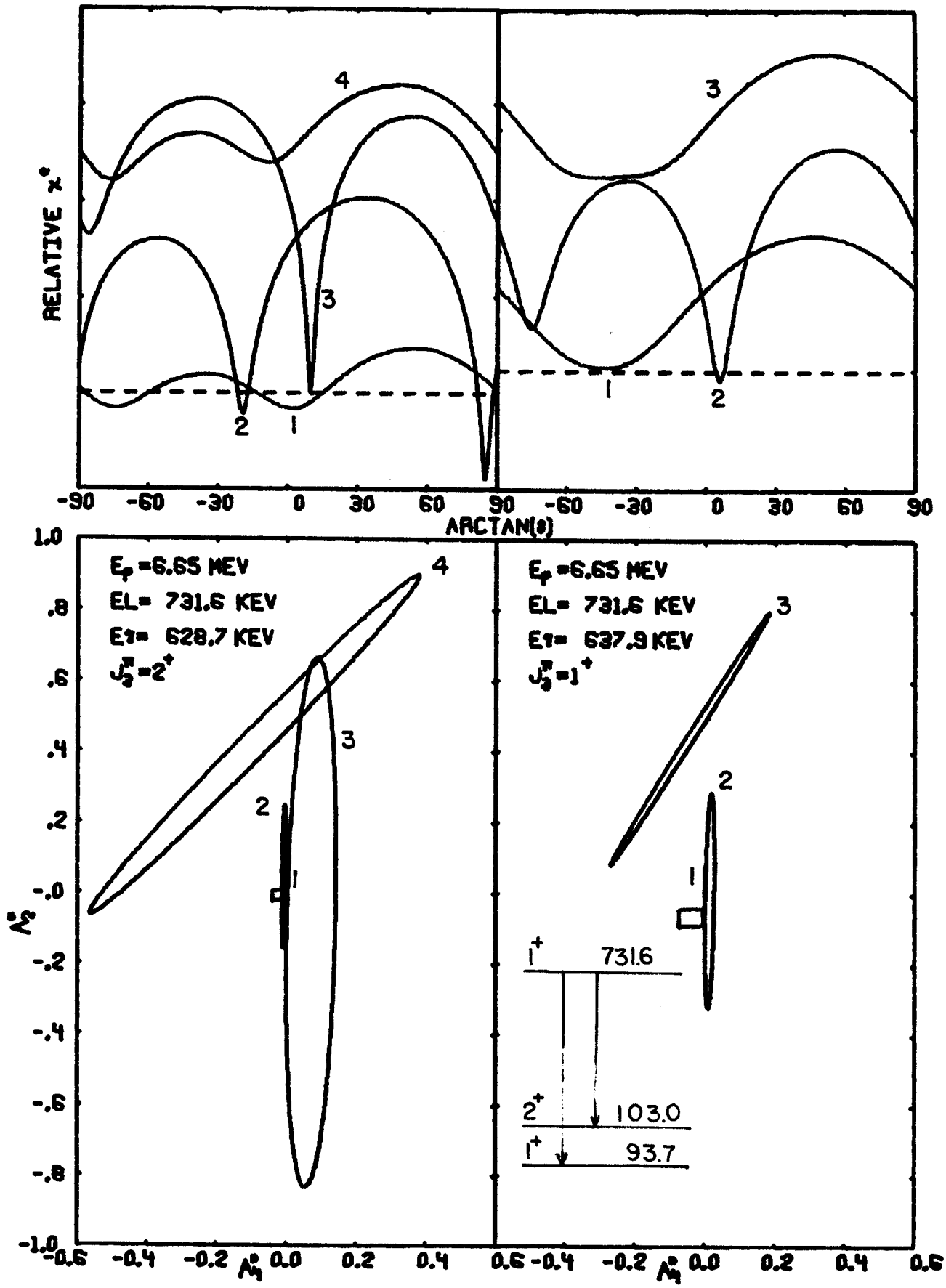

Chi square and delta ellipse plots for the 628.7 and 637.9 keV gamma rays.

Figure VII-12.

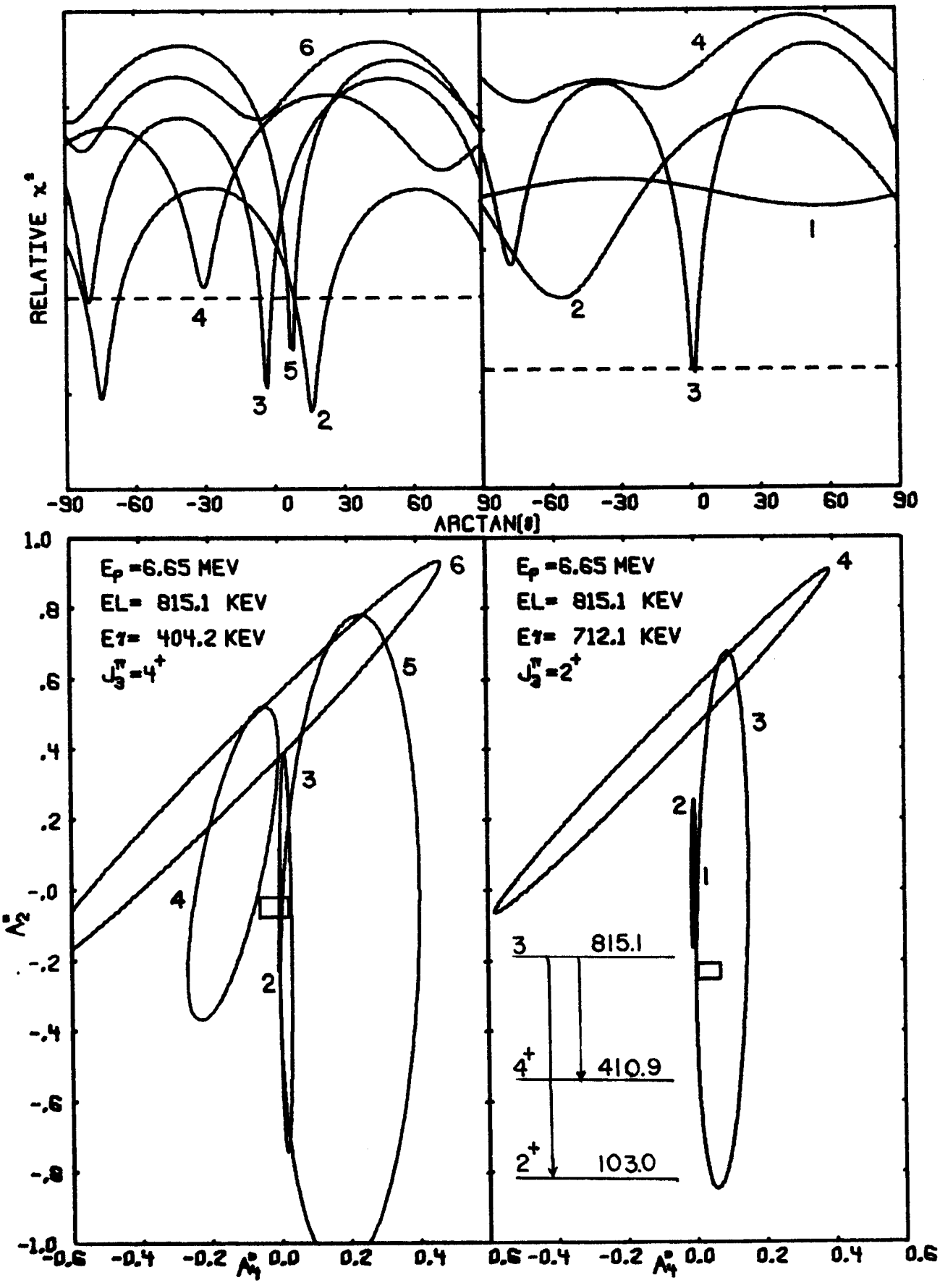

Chi square and delta ellipse plots for the 404.2 and 712.1 keV gamma rays.

Figure VII-13.

O. E_x = 820.6 keV J = 5

The angular distribution data are inconclusive for this level indicating equal likelihood of J = 2, 3, 4, or 5 as shown in Figure VII-15. Excitation function data in Figure VII-14 show a fit to the theory which is consistent with J = 5.

P. E_x = 841.1 keV J = (6)

The 841.1 keV level depopulates via a 338.1 keV transition which is very weak and which also has nearly the same energy as a contaminant γ ray from our lead beam stop. The intensity is much too low for measurement of angular distributions, however, the excitation function data, shown in Figure VII-14, indicates the spin may be 6.

Q. E_x = 881.5 keV J = 3

The angular distribution of the 778.5 keV γ ray shown in Figure VII-15 indicates that only the J = 3 for the 881.5 keV state is a good choice. The excitation function data tend to confirm this value as is shown in Figure VII-14.

R. E_x = 917.7 keV $J^{\pi} = 1^+$

The 917.7 keV level is observed to be fed in beta decay with a log ft of 6.3, which indicates an allowed or first forbidden transition. Since the angular distributions (Figure VII-16) are not isotropic and are in agreement with J = 1, an assignment of 1^+ is made to this level, as no shell model configurations exist for the 1^- possibility.

Figure VII-14

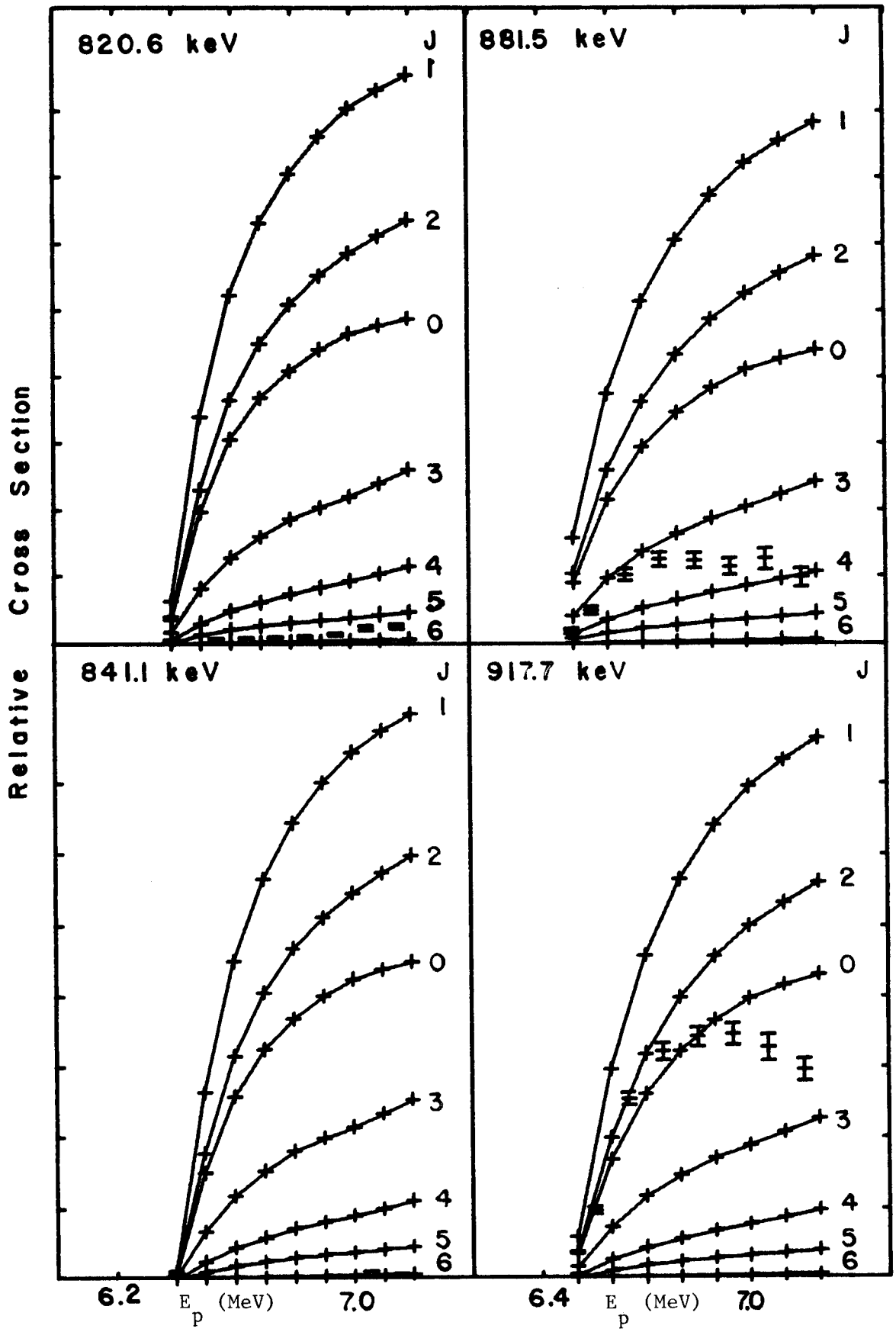

Excitation functions for the 820.6, 841.1, 881.5, and 917.7 keV levels.